Anna Shcherbacheva

AGENT-BASED MODELLING FOR EPIDEMIOLOGICAL APPLICATIONS

ACTA UNIVERSITATIS LAPPEENRANTAENSIS 844

Anna Shcherbacheva

AGENT-BASED MODELLING FOR EPIDEMIOLOGICAL APPLICATIONS

Thesis for the degree of Doctor of Science (Technology) to be presented with due permission for public examination and criticism in the Auditorium 1318 at Lappeenranta-Lahti University of Technology LUT, Lappeenranta, Finland on the 29th of March, 2019, at noon.

Acta Universitatis
Lappeenrantaensis 844

Supervisors Professor Heikki Haario
LUT School of Engineering Science
Lappeenranta-Lahti University of Technology LUT
Finland

Associate Professor in Applied Mathematics Tuomo Kauranne
LUT School of Engineering Science
Lappeenranta-Lahti University of Technology LUT
Finland

Reviewers Assistant Research Professor Erin L. Landguth
School of Public and Community Health Sciences
University of Montana
United States of America

Associate Professor Jonathan Keith
School of Mathematical Sciences
Monach University
Australia

Opponent Professor Kari Auranen
Faculty of Science and Engineering
Department of Mathematics and Statistics
University of Turku
Finland

ISBN 978-952-335-344-2
ISBN 978-952-335-345-9 (PDF)
ISSN-L 1456-4491
ISSN 1456-4491
Lappeenrannan teknillinen yliopisto
LUT University Press 2019

Abstract

Anna Shcherbacheva
Agent-based modelling for epidemiological applications
Lappeenranta 2019
112 pages
Acta Universitatis Lappeenrantaensis 844
Diss. Lappeenranta University of Technology
ISBN 978-952-335-344-2, ISBN 978-952-335-345-9 (PDF), ISSN-L 1456-4491, ISSN 1456-4491

Malaria is an infectious disease induced by protozoan parasite called *Plasmodium* and transmitted by *Anopheles* mosquitoes which still imposes a health threat to virtually half of the human populace and causes severe mortality, especially in sub-Saharan Africa.

The characteristics of malaria transmission depend on many relevant factors, such as socio-economic conditions, availability of control measures and local composition of mosquito species. Mathematical modelling of disease propagation is conducted to evaluate the impact of these factors and to ameliorate the lack of experimental data in this field.

In this thesis an agent-based model of short-range mosquito host-seeking behaviour in the presence of Long-Lasting Insecticidal Nets (LLINs) is introduced and further calibrated by the means of experimental data. The model is extended to quantify the overall impact of intervention strategies in community-level situations. As demonstrated in the present study, other optional factors can be included into the simulations, such as parasite ecology and socio-economic conditions. Model simulations are conducted for a short-term period of one day. Additionally, when coupled with regression models based on the simulation results under various conditions, the proposed approach allows transition from the *in situ* mechanisms of mosquito behaviour to commonly estimated characteristics of malaria transmission.

Keywords: Agent-Based Models, malaria transmission, mosquito host-seeking behaviour, vector control, LLINs, Markov Chain Monte Carlo and regression analysis

Acknowledgements

This study was carried out in the School of Engineering Science, division of Computational and Process Engineering at Lappeenranta University of Technology, Finland. First of all, I would like to thank the Academy of Finland for availing the funding sufficient for all duration of my studies. Otherwise, this undertaking would have been practically impossible.

Next, my gratitude comes to my supervisor, Professor Heikki Haario, for his endless patience, wisdom and profound guidance within the study process. In addition, I appreciate the inspiration for carrying out research that I have always received from his side.

Also I want to thank especially Miracle Amadi for collaboration and continuing working on the project related to the topic of my dissertation. I would like to thank my fellow graduate students, research technicians and collaborators who contributed to this work. I am really grateful to all of you.

In addition to that, I would like to thank all the members of the Simugroup in University of Helsinki, and especially Professor Hanna Vehkamäki, for their patient support of my PhD process and ultimate encouragement of the future endeavours.

Last, but not the least, I would like to express my hearty gratitude to my family for their endless support in many different situations and their inexhaustible love that they keep giving me. In particular, I am immensely grateful to my parents, who had helped and encouraged me throughout my life. Especially, thank you for persuading me to acquire the education, which was absolutely essential for this undertaking. Also, I am grateful to my father, who has always been providing me with the inspiring examples of what it takes to become and be a successful academician and to pursue an engineering career.

Special thanks goes to my husband Alexander, who stayed with me during all these years, supporting my personal development and explaining many useful ideas that were often relevant to my work.

Thank you all for keeping me going as I would never reach that far without all of you.

Anna Shcherbacheva
February 2019
Espoo, Finland

To my beloved husband, parents
and grandmothers.

Yours, Anna!

Contents

Nomenclature

2D	two-dimensional
3D	three-dimensional
ABM	Agent-based model (modelling)
ACD	Artemisinin-based combination therapy
CEA	Cost-effectiveness analysis
DRAM	Delayed rejection adaptive Metropolis algorithm
GIS	Geographical Integration System
GPU	Graphical Processing Unit
IRS	Insecticide-Residual Spraying
ITNs	Insecticide-Treated bed Nets
LLINs	Long-Lasting Insecticidal Nets
MCMC	Markov Chain Monte Carlo
ODE	Ordinary differential equation
SD	System Dynamics
SPP	Self-propelled particles
STEM	Science, Technology, Engineering and Mathematics
UML	Unified Modelling Language
WHO	World Health Organization

Glossary

Anthropophilic. Mosquito species that are characterized by the propensity to feed especially on humans. See pp. 38, 46, 57

Contact irritancy. A chemical action, which induces oriented movements of mosquito away from the source of the chemical after making contact with the impregnated surface. See pp. 25, 38, 42

Continuous-based approach. The agent-based framework where the environment is treated as a continuous 2D or 3D space. See p. 16

Detoxification. A metabolic process by which the toxic qualities of a poison or toxin are reduced by the body. See pp. 46–51, 67, 77, 78, 95

Emergence. The collective properties that result from the properties of the parts, the behaviour at a larger scale originating from the small-scale structure, behaviour and interactions. See pp. 15, 26, 31

Entomology. The discipline studying insects and their interactions with humans, environment, and other organisms. See pp. 32

Excito-repellency. The chemical action which induces the insects to move randomly which helps them to avoid the interactions with the chemicals caused by the insect's physical contact with insecticides on treated surfaces or with vapour particles spread in the air. See pp. 38, 46, 47, 50, 51, 77, 78, 81, 95

Exophily. An ecological characteristics of mosquitoe species to be independent of humans and their domestic environment. See p. 67

Grid-based approach. The agent-based framework where the environment is treated as a set of topologically connected cells. Each cell is associated with several state variables related to the environment of interest, such as the presence of valuable resources or local danger sites. See p. 16

Insecticide resistance. An inheritable change in the susceptibility of a vector population that is reflected in the systematic failure of a control measure to achieve the expected level of control when used according to the label guidelines for that vector species. See p. 67

Intervention strategies (or control measures). The methods that are applied in the context of malaria control in order to reduce the contacts of humans with malaria vector mosquitoes and to decrease mosquito populations. See pp. 21, 33, 34

Klinotaxis. The process of animal navigation in odour plume based on using the memories from the previous locations to navigate towards the increase of the odour concentration. See pp. 24, 38, 49, 83

Opportunistic. Mosquito species that are characterized by the propensity to feed on both humans and other animals, depending on physical availability. See pp. 38, 46, 57

Oviposition. A process of laying eggs. This term is used especially with insects. See p. 24

Parasite ecology. The discipline which studies the interactions between parasites, hosts, and their environments. See p. 21, 38, 81, 91, 96

Spatially explicit. Agent-based models that include 2D or 3D representation of the environment. See pp . 16, 96

Target proteins. The functional biomolecules that are influenced by the active compounds, such as chemicals. See pp. 48

Utility function. A function that is evaluated in the context of the agent-based modelling for quantifying the profit of decisions made by the agents. The evaluations are carried out at each step of the simulation for each of the agents individually.
See p. 15

Vector control . The method to restrict or eradicate animals (here collectively called "vectors") which transmit disease pathogens. See pp. 31, 33, 34

1 Introduction

1.1 Agent-based models

Agent-based models (ABMs) consist of autonomous entities (or agents) acting in accordance with a set of decision-making rules commonly implemented in computer simulation programs. Agents act and interact in pursuit of their individual benefits, e.g., survival, economic profit or reproduction.
Collective phenomena appear as a result of decision-making heuristics followed by the agents. As an outcome, the system often exhibits more complex behaviour than the agents acting individually. Origination of the complex patterns exhibited at the macro-level from simple micro-scale operations and interactions is a particular case of *emergence* phenomena often observed in physical, biological systems and social communities.
The concept of agent-based modelling was developed in 1940 and received an extensive spread only with substantial advances in computational capacities and improvement in software development environments in the 1990-s. In application to computer science the idea was exploited by von Neumann in 1971, who constructed a von Neumann self-replicating machine and introduced the concept of cellular automata.
Due to intuitive design and high generality, the scope of related disciplines is almost limitless. Given their flexibility, ABMs are extensively applied in such disciplines as biology and ecology, economy and sociology, artificial intelligence and cognitive science, and many other fields of STEM (Science, Technology, Engineering and Mathematics), where they are employed for simulating complex systems and generating emergent behaviour, (see Allan (2009), Macal (2016), Marvuglia et al. (2016), Abar et al. (2017)).
Particular advantages appear in applications when real experiments are impossible or inappropriate (e.g., due to ethical considerations). In such cases ABMs offer an analogue of physical, biological or chemical laboratory with possibility to isolate the system from external processes and concentrate on the impact of a single factor of interest.
Many applications were proposed in non-computational research areas. Among the representative examples, one can emphasize the social segregation model developed by Thomas Schelling T.C. (1971), the group of models describing opinion dynamics and opinion transmission mechanisms (Deffuant et al. (2002), Deffuant et al. (2004)), the models of supply chain optimization (Strader et al. (1998)) and industrial networks (Albino et al. (2003), Boero and Castellani (2004), Borrelli et al. (2005)).

1.1.1 Classification of the agents

The performance of each agent is commonly evaluated by a *utility function* linked to decisions taken by the agents. The actions corresponding to higher utility values are accepted with higher probability. By complexity of decision-making technique the agents are classified into four categories: reflexive agents, agents with internal states, goal-based and utility-based agents, (see Russell and Norvig (1995)). The latter two types of agents are capable of modifying their decision rules by learning and adaptation, usually implemented by the methods originating from artificial intelligence, such as neural networks

and evolutionary algorithms, (see Tang and Bennett (2010), Russell and Norvig (1995)).

1.1.2 Environments

ABMs often include an interactive environment, such as a geographic map or physical space, which typically contains attractions and obstacles, followed and surmounted by the agents. The environment can be represented utilizing a *continuous-based approach* or *grid-based approach*. In the former representation, the environment is treated as a set of topologically connected geometric features (e.g., lines, polygons and points), where size, shape and location of the items are described by continuous coordinates.
In the *grid-based approach*, the environment is divided into set of grid cells, where each element of the grid is divided into several state variables related to the environment of interest. Grid cells are connected using neighbourhood adjacency rules, such as von Neumann neighbourhood rule (4 neighbours), Moore neighbourhood rule (8 neighbours), or irregular neighbourhood rules, (see Gilbert and Troitzsch (2005), Tang and Bennett (2010)). In the present study, environment is treated by the means of a continuous representation.
Models in which the environment is represented as two- or three-dimensional landscape are referred to as *spatially explicit*. The interaction of the agent with the medium is illustrated in Figure 1.1.

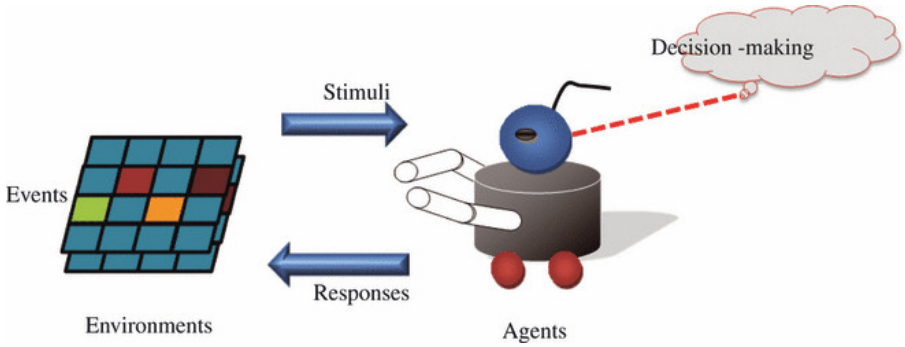

Figure 1.1: Illustration of an agent and its environment in an agent-based model adopted from Tang and Bennett (2010).

1.1.3 Modelling protocols and software tools

Simulation environments implementing the ABMs are commonly developed using object-oriented programming languages (e.g. Java, C++, Objective C, etc.), (see Tang and Bennett (2010)). Among the most common ready-made frameworks are NetLogo (`http://ccl.northwestern.edu/netlogo`) and Swarm (`http://www.swarm.org/`) developed in the mid-1990s, RePast (`http://repast.sourceforge.net`) and AnyLogic (`http://www.anylogic.com/`) appeared in 2000, and more recent template-based environment FLAME (`http://flame.ac.uk/`), with the latter extended to leverage the computing capacities of high performance GPU architectures. A convenient

graphical representation of agent and environment interaction is available in UML (Unified Modelling Language), (see Tang and Bennett (2010)). For an exhaustive overview of the software frameworks specifically designed for development of the ABMs, refer to Abar et al. (2017).
For the sake of computational efficacy, the model of mosquito host-seeking behaviour developed in this project was implemented by the means of CUDA tool-chain, with the parallel code embedded into a MEX executable, which is suitable for invocation from MATLAB environment. Parameter estimation in application to the above-mentioned model was performed using MATLAB toolbox, which provides an abundant collection of adaptive Markov Chain Monte Carlo methods, (see Haario et al. (2001) and Haario et al. (2006)). Toolbox description, together with the list of related articles and the examples of usage are available on the web page `http://helios.fmi.fi/~lainema/`. The combination of the optimized GPU implementation and the MCMC methods facilitated efficient sampling of model parameters. Given the flexibility and efficiency of parameter identification provided by the MCMC toolbox, the author decided to stick with her own low-level CUDA-based implementation of the model instead of opting for one of the commonly used software frameworks specifically designed for the ABM simulations. Further details are described in Section 2.4.

1.2 ABM versus continuous modelling approach

In classical formulation, the systems consisting of a large number of microscopic units (such as, particles in physics, traders in the market or animal swarms in ecology) are modelled through the evolution of macroscopic quantities that characterize the aggregate state of the system, (see Turchin (2003)). Specifically, the dynamics of macroscopic mean fields is commonly given as a set of algebraic and/or integro-differential equations, which is known as the *Eulerian approach*. In an alternative *Lagrangian approach*, the dynamics for each of the population members is specified individually, given by a set of heuristic rules. These rules can be formulated either via the algorithm which represents the decision tree with probabilistic choices (as in Gueron et al. (1996), Muiños-Landin et al. (2018)), or as a system of stochastic differential equations, (see, e.g., Morale et al. (2005), Burger et al. (2007) and Harris and Blackwell (2013)). In the present work, mathematical modelling of the animal movement is conducted, including animal herding and mosquito flight in response to the external stimuli, i.e., the plume of carbon dioxide originating from the hosts, following the agent-based methodology.
Generally, the swarm dynamics is driven by the global attraction force, that stimulates the spatial orientation of agents towards the target site. Additionally, in the case of interactive behaviour, animal-agents are influenced by the long-range aggregate force that maintains the cohesive movement of the swarm, and the short-range repulsive force which ensures that the animals do not collide. Following the *Eulerian methodology*, spatio-temporal evolution of the population density f is modelled by the means of the diffusion-convection-

reaction equation:

$$\frac{\partial f}{\partial t} = \frac{\partial}{\partial x}\left(D(f)\frac{\partial f}{\partial x}\right) - \frac{\partial}{\partial x}\Big(V(f)f\Big) + B(f), \tag{1.1}$$

where the first term on the right-hand side represents Brownian motion with the rate of diffusion given by $D(f)$, the second term introduces advection that occurs with velocity $V(f)$ which is conditioned on the density f. Here, the last term is optional and determines the local inflow and/or outflow of the population members. Refer to Nagai and Mimura (1983), Mogilner and Edelstein-Keshet (1999), Murray (2002), Milewski and Yang (2008), Bedrossian and Rodríguez (2014) as the illustrations of this approach.
In the above formulation, the advection component typically incorporates the attraction and repulsion processes, which means, that the direction and speed of motion is conditioned on the local population density and its local spatial variations. As the sensory abilities of animals are typically restricted in space, the interactions between the group members commonly occur not further than at a certain finite distance. This distance-dependent strength of the interaction can be introduced as a convolution:

$$V(f) = K * f = \int_{\mathbb{R}^3} K(x - x')f(x', t)dx'; \tag{1.2}$$

where the value of the kernel $K(x-x')$ is associated with the force of interaction per unit density, given that the animals are separated by the distance $x - x'$, (see Edelstein-Keshet et al. (1998), Mogilner and Edelstein-Keshet (1999)).
In the ABM framework, cohesion and repulsion are modelled by the means of *velocity alignment* utilized in so-called kinetic approach (Fetecau et al. (2016)) and self-propelled particle (SPP) modelling, (see Buhl et al. (2006), Strombom (2011) and Mann (2011)). Time-continuous version of the velocity alignment model is based on the equations, postulating the dynamics of position x_i and velocity v_i of each of the individuals:

$$\begin{aligned} \frac{dx_i}{dt} &= v_i, \quad i = 1, \dots, N, t > 0 \\ \frac{dv_i}{dt} &= \frac{1}{\rho_i(x)}\sum_{j=1}^{N}\psi(x_i - x_j)(v_i - v_j) - \frac{1}{N}\sum_{j\neq i}\nabla K(x_i - x_j), \end{aligned} \tag{1.3}$$

where N denotes the number of agents, the first term on the right-hand side of Equation 1.3 stands for *velocity alignment* force, with distance-dependent communication function ψ; $\rho_i(x)$ is the scaling function, which in the simplest case reduces to the number of interacting agents; $\nabla K(x_i - x_j)$ determines a short-range repulsion, which is similar to the above-discussed continuous case.
The similar alignment model with temporal discretization, originating from the Viscek type of models (see Czirók and Vicsek (2007)) is based on the trade off between individ-

ual movement direction and coherence with the swarm

$$\begin{aligned} x_i(n+1) &= x_i(n) + v_i(t), \quad i = 1, \ldots, N \\ v_i(n+1) &= \alpha v_i(n) + (1-\alpha) G(\langle v(n) \rangle_i) + \xi_i, \end{aligned} \tag{1.4}$$

governed by the coefficient $0 < \alpha < 1$. Herewith, the function $G(\cdot)$ determines the adjustment of a particle velocity to the velocities of its neighbours, $\langle v(n) \rangle_i$ stands for the averaged velocity of the individuals within the interaction range, excluding the i-th agent, ξ_i is a stochastic term, (see Buhl et al. (2006)).
In the present work the motion is treated by the means of the *accept-reject procedure*. In the case of non-interactive agents, this modelling approach was elaborated to reproduce the experimental data. After developing sufficient parametrization, the model is calibrated as discussed in detail in Section 2. Additionally, a toy-case example is given on modelling interactive agents with the goal to preliminarily illustrate the usage of the ABM approach. In this situation, *position alignment* is applied, with the swarming implemented by following the statistical data assimilation algorithm known as *Kalman filter* (see Kalman (1960)), where the *Kalman gain* coefficient determines the relative weight that the individual assigns to its own position and to that of its neighbours in deciding its position change. This mechanism is employed to introduce the cohesion effect in a similar fashion as the velocity alignment discussed above.

1.2.1 From continuous to ABM

In commonly used compartmental modelling, microscopic entities are classified into several compartments (or state variables), with certain rates specifying possible transitions between the existing states. This formulation leads to the assumption about homogeneity of microscopic units within a single compartment. Additionally, the number of compartments is always finite by definition.
Unlike the continuous modelling paradigm, the ABM approach features heterogeneous properties within the population of agents, which can be treated as an infinite number of compartments or states. Generally, the System Dynamics (SD) models cover only a subset of the models that can be implemented following the ABM paradigm. The task of transforming ABM into continuous model counterpart is more cumbersome and not generally feasible, (see Macal (2010)).
In general, the transition from the continuous to the ABM approach originates from numerical integration of the continuous equations. Often, the equations are not tractable analytically due to their complex non-linear structure. In application to the system of ordinary differential equations of the form

$$\frac{dx}{dt} = f(x,t) \tag{1.5}$$

the numerical integration can be carried out by discretizating the system, e.g., applying the simplest *Euler method* which results in the difference equations written as follows:

$$x(t + \delta\tau) \approx x(t) + \delta\tau f(x(t), t). \tag{1.6}$$

This approach results in a temporal stepping $\delta\tau$, where the time step chosen for propagation should be suitably selected to maintain the structural dynamics of the system.
For example, consider the simplest population dynamics model and the the set of probabilistic rules developed to construct the equivalent ABM, (see Shcherbacheva et al. (2018)). This model describes time evolution of the population density x decreasing with a decay rate μ, which can be expressed by the following equation:

$$\frac{dx}{dt} = -\mu x, \quad x(0) = x_0, \tag{1.7}$$

where x_0 is the initial population number at the beginning of the simulation. The model can be reformulated by discretizing the equations in time, i.e., by transforming the ODE into the difference equation:

$$x(t + \Delta t) \approx x(t)(1 - \mu\Delta t). \tag{1.8}$$

Intuitively, the simplest reformulation of this continuous model in the form of its agent-based counterpart can be achieved by forming the set of probabilistic rules for agents, with probabilities of events arising from the corresponding transition rates between the compartments.
In particular, when considering the population members, one can represent the probability of death attributed to each of the individual agents per unit time Δt as the decay rate multiplied by the time step:

$$p_{\text{death}} = \mu\Delta t, \tag{1.9}$$

where Δt is small enough, so that $\mu\Delta t << 1$.
Alternatively, a continuous model given by Equation 1.9 can be treated by the means of constructing a discrete event simulation as in the classical *Gillespie algorithm*, which is based on the Monte-Carlo sampling from distribution, (see Gillespie (1976) and Gillespie (2007)). In these simulations the events arrive at random time instances, following the exponentially distributed timing $\exp(-\lambda t)$, where λ stands for the occurrence frequency of the events. Unlike in the agent-based approach, in Gillespie algorithm the entities of the system are not tracked individually. Instead, the number of entities in each of the compartments is recounted after every successive arrival of the random event. However, in both cases the processes are stochastic, and the outputs are to be averaged over multiple repetitions to ensure statistical reliability of the quantities of interest. As an example of malaria transmission model based on discrete event simulation, see McKenzie et al. (1999).

1.2.2 From ABM to continuous approach

A known drawback of continuous modelling in epidemiological applications is the lack of experimental data indispensable for model calibration. However, the field measurements quantifying the impact of *intervention strategies* do exist, (e.g., see Kitau et al. (2012)). In that light, a hybrid approach is developed which facilitates the transition from ABM to continuous modelling. Initially, the ABM is developed in this work for the case of mosquito host-seeking behaviour inside of the hut, with a human sleeping under the bed net. The model is subsequently extended to the household-level, with multiple individuals sleeping under the same roof, and to community-level, where several households are randomly positioned inside of the experimental domain.
At the first stage, the basic hut-level model is calibrated by the means of the experimental data from Kitau et al. (2012). This calibration produces the parameter values attributed to the *in situ* mosquito behaviour in response to the human attraction and the Long-Lasting Insecticidal Nets (LLINs). Next, the household- and community-scale simulations are conducted, where the mosquito-to-human contact rates and mosquito mortality are calculated depending on the level of population coverage with the impregnated nets. Here, the level of coverage is defined as a percentage of population protected with the LLINs. Furthermore, the response surfaces are fitted to the ABM responses: the contact and mortality rates. The resulting coefficients given by the fitted response surfaces can be utilized when integrating the ODE-based model of malaria transmission, as they give the values of the key parameters, which enables to extend the ABM simulations carried out over a 'snapshot' time period of one night to continuous time interval. The schematic representation of the link between the ABM of *in situ* mosquito behaviour and the ODE-based modelling of disease propagation is outlined in Figure 1.2. However, the transition to ODE models is outside the scope of the present work and will be treated elsewhere.
The basic model of host-seeking behaviour in the hut and the underlying parametrization is introduced, and the calibration of the model is examined in Section 2. Next, the community-level simulations are developed and discussed, including the experimental design, which can be extended to incorporate several other meaningful factors, apart from the partial population coverage, such as the impact of socio-economic variables and *parasite ecology*. These examples are introduced and further examined in Section 3.

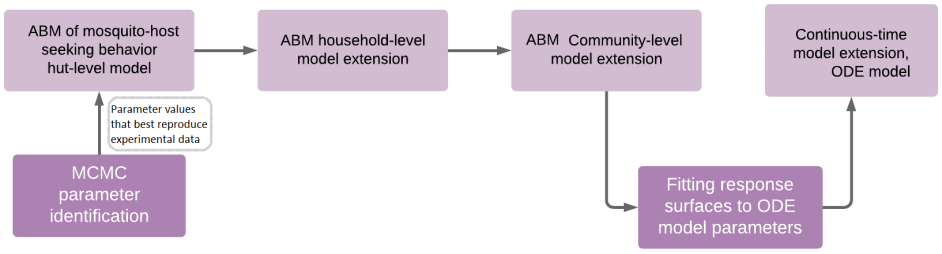

Figure 1.2: Schematic representation of transition from the ABM of mosquito host-seeking behaviour to the continuous modelling of malaria transmission.

1.3 Agent-based models of animal movement

A number of phenomena of interest in landscape ecology and biogeography, such as dynamics of the species, disease spread, animal migration, plant dispersal, spatial genetic variation among populations and gene flow are primarily associated with animal movement across heterogeneous landscapes, (see Turner (1989), Forman (1995), Quammen (1996), MacDonald (2003), Bowler and Benton (2005), Stucki et al. (2017), Day et al. (2018), Forester et al. (2018)). Investigating the cause-and-effect relationships governing animal movement significantly improves conceptual understanding of the processes underlying the aforementioned phenomena, (refer to Schick et al. (2008), Tang and Bennett (2010)). The ABM approach offers explicit representation of the interactions between the individuals and their environment and among the individuals.
Animal movement has been frequently studied with the ABM due to the possibility to include a realistic influence of the environment, such as integration of the Geographical Information System (GIS) and the individual-level telemetry data, as demonstrated by the works of Hooten et al. (2010), Patterson et al. (2008), Tang (2008), and Brown et al. (2005).
The ABM methodology has been applied to simulate the spatial dynamics of large variety of animal species, such as birds (Reuter and Breckling (1999)), fish (e.g., stream fish, tropical and pelagic fish; see Huse et al. (1999), Dagorn et al. (2000), Hölker and Breckling (2005), Railsback et al. (2006), Day et al. (2018)), insects (e.g. flies and mosquitoes; see Arrignon and et al. (2007), Shaman (2007), Linard et al. (2009)), large herbivores (e.g. bison, elk, and sheep; see Turner et al. (1994), Dumont and Hill (2001),Morales et al. (2005), Bennett and Tang (2006) and Creech et al. (2017)), large carnivores (e.g. tiger, bear and panther; see Comiskey and et al. (1997), Sean et al. (2001), Thatte et al. (2017) and Kristensen et al. (2018)), and large omnivores (e.g. primates; see Hemelrijk (1999) and Sellers et al. (2007)). See Table 1.1 for a summary.
Typically, animal-agents perceive information from surrounding environment with multiple sensors and orient in 2D or 3D landscape in response to the external and internal factors.
A usual ABM of animal movement normally includes the following essential components: environment, external state, internal state, motion capacities, and navigation capacities, (see Nathan (2008)). More detailed explanations of the typical ABM ingredients follow below, in the introductory part.

1.3.1 Modelling internal state of the animal

The ABM approach is especially suitable for modelling internal physiological and psychological states of the animals. Among physiological states of the animals, one can list the energetic state related to energy consumption and utilization, body mass and body size. Psychological states are strongly bound with physiological condition of the animal, and include, among many others, short- and long-term memory, cognitive capacities, learning and various goals (associated with, e.g., mating, resource allocation, reproduction and territory establishment) pursued by the animal, (see Shettleworth (2001)).

Categories	Citations	Agents	Environment
Birds	Reuter and Breckling (1999), Wolff (1994)	Robin (*Erithacus rubecula*), and wood storks	Food resources (fish, or arthropods), temperature, and water depth
Fish	Dagorn et al. (2000), Hölker and Breckling (2005) Huse et al. (1999), Railsback et al. (2006)	Lake fish (roach), stream fish, and tropical pelagic predatory fish	Food, solar radiation, and temperature
Insects	Cummins et al. (2012),Arrignon and et al. (2007) Linard et al. (2009), Shaman (2007)	Fly (*Episyrphus balteatus*); and mosquitoes	Light, temperature, blood sources and food resources
Large carnivores	Sean et al. (2001), Comiskey and et al. (1997)	Panther, and tiger	Territory, and prey distribution
Large ungulates	Abbott et al. (1997), Dumont and Hill (2001) Morales et al. (2005),Turner et al. (1994)	Bison, elk, sheep, and white-tailed deer	Biomass, snow, topography, and water
Large omnivores	Hemelrijk (1999), Sellers et al. (2007)	Baboons, and macaques	Habitat types, water, sleeping sites, refuge, or distribution of conspecific neighbours

Table 1.1: Representative agent-based models of animal movement (adopted from Tang and Bennett (2010)).

Changes in the internal states are driven by behavioural rules and information acquired using sensors. This in return facilitates acquisition of a new information from the surrounding environment. The internal states are captured as the properties of each animal-agent and recorded and updated individually at each successive repetition of the algorithm.
The process of animal orientation in the landscape is associated with the updates of the short- and long-term memory (spatial and non-spatial) by the means of cognitive capacities of the animal (such as sensing and learning), (see Tang and Bennett (2010)).
In the case of the ABM of mosquito host-seeking process developed in this project, the environment is represented by a 2D landscape amended with the sites of interest, i.e., humans and households available for blood-feeding. Additionally, every agent has a set of attributed internal states, such as hunger, accumulated dosage of insecticide and the level of persistence associated with the host-seeking attempts. Motion capacities are captured by taking into account the mode of movement, switching from a pure random walk in the absence of sensory cues, to a directionally biased random walk, after entering the plume of carbon dioxide. To account for a short-distance behaviour, where additional sensory information induces higher attraction to the host, a third mode of movement is included. In all the cases, the speed of flight typical for most of the mosquito species is taken into account. Next, navigation capacities are defined as an ability to orient in the odour plume emitted from the hosts known as *klinotaxis*, where mosquito uses its memory of CO_2 concentration from the past for choosing a direction of movement.

1.3.2 Modelling external factors

Heterogeneous landscape navigated by animals typically features various characteristics associated with obstacles, resource allocations and other spatially varying attributes, e.g., temperature, precipitation and light intensity. These factors can change their characteristics across different spatial and temporal scales. Animals experience adaptation to their environment and act in response to the local surroundings. For example, the environmental factors that influence fish movement include solar radiation, food and temperature (see Hölker and Breckling (2005)). The environmental factors that drive mosquito movement, on the other hand, can be characterized by wind currents, availability of *oviposition* sites and blood sources, temperature and solar radiation (see Cummins et al. (2012), Arrignon and et al. (2007), Linard et al. (2009)).
The influence of environmental characteristics can be generally classified into two main categories: attractions (e.g., food and reproduction possibilities) and risks (e.g., predation and threats for survival caused by weather conditions). These features can be modelled as attraction and repulsion forces that govern animal navigation. Additionally, animal movement and interactions with environment can modify characteristics of these driving forces that may reciprocally modify animal movement patterns via feedback mechanism, (see Tang and Bennett (2010)).
In the ABM of mosquito host-seeking behaviour presented in this study the attractive potential driving mosquito movement is modelled as CO_2 emitted by human host. The potential is given as a solution of the diffusion equation with a point source specified as a

Gaussian kernel centred at the spacial position of the host $\mathbf{x}^h$:

$$C(\mathbf{x}, \mathbf{x^h}) = \exp\left[-\frac{d^2(\mathbf{x}, \mathbf{x}^h)}{2\sigma_a^2}\right], \tag{1.10}$$

where $\mathbf{x}$ is mosquito position, and C denotes the concentration that drives mosquito attraction in response to the host at a distance $d(\mathbf{x}, \mathbf{x}^h)$. The standard deviation of the Gaussian σ_a governs the maximal distance at which the mosquito is capable of recognizing the odour emitted from the host. At a short distance to the host (less then 3 meters), mosquitoes are capable of perceiving information by the heat sensors located around their mouth parts, which is modelled as a concentration scaling factor facilitating more directional movement towards the human. Here, the repulsive force is understood as the *contact irritancy* induced by the LLINs impregnated with the chemicals. This impact is introduced as a probability of rejection of a new position x conditioned on the presence of the chemical given by a logistic function which is parametrized as

$$\alpha_r(\mathbf{x}|d_{50}, r, s) = r\left[1 - 1/\Big(1 + \exp\big(-\big(d(\mathbf{x}, \mathbf{x}^h) - d_{50}\big)/s\big)\Big)\right], \tag{1.11}$$

where $d(\mathbf{x}, \mathbf{x}^h)$ stands for the distance from the mosquito to the net-protected human. The parameters d_{50} and s govern the range of spacial coverage and the spread of repellent, r denotes the intensity of repulsion.

1.3.3 Modelling motion capacities

Different animals possess different motion capacities, such as foraging, walking and flying. The mode of motion depends on environmental factors (e.g., risk avoidance and hunting). Movement of an individual animal is commonly modelled as a random walk. Depending on the movement modes, various modifications of the random walk are employed for movement modelling. Depending on the case, the biased, directed or correlated random walks can serve as the statistically appropriate representations, (see Tang and Bennett (2010)).

Many studies involve oriented movement of animal-agents towards the target. This can be modelled, for example, by using correlated random walk that describes directional movement:

$$\begin{pmatrix} x_{latitude,t+1} \\ x_{longitude,t+1} \\ \Phi_{t+1} \end{pmatrix} = \begin{pmatrix} x_{latitude,t} + d_{t+1} sin(\Phi_{t+1}) \\ x_{longitude,t} + d_{t+1} cos(\Phi_{t+1}) \\ f(\Phi_t) \end{pmatrix}, \tag{1.12}$$

where $f(\Phi_t) \sim$ VonMises(Φ_t, κ) and $d_t \sim$ Log normal (μ, σ^2). Here, Φ_{t+1} is the direction to the next location with mean direction Φ_t and dispersion parameter κ, and d_{t+1} is the distance to the next location with log-mean μ and log-variance σ^2, (see Patterson et al. (2008)).

The von Mises distribution is a stationary distribution of drifting and diffusive dynamics that occurs on the circle in harmonic potential. In a specific case, when no directional bias is assumed, i.e., $\kappa = 0$, the von Mises distribution reduces to the circular uniform

distribution, (see Risken and Haken (1989)).
However, in the ABMs presented in this study, oriented motion towards the target is modelled using *accept/reject* probabilities conditioned on the difference of the attractive potential that is calculated at the most recent position with respect to the previous position. In this case, the *candidate position* is randomly proposed using uniformly distributed random direction with respect to the previous spatial location.

1.3.4 Modelling interactive agents

Modelling complex systems consisting of a large number of interacting parts has been conducted within the frameworks of diverse scientific disciplines. Being a part of the aggregate structure, microscopic entities exhibit interrelated dynamics arising from the interactions with the co-species objects. This often leads to ordering phenomena and decrease of the entropy of the whole system, widely known as emergence. In physics, for example, the ordering phenomena and phase transitions have had prevailing importance in the last 50 years, bringing the inspiration for explaining and modelling emergent phenomena in the other spheres. Other frequently encountered examples of the processes simulated in ecology, economic science, physics, mobile robotics and supply chain management also feature the mechanisms of collective behaviour, (see Giardina (2008)). Depending on the field of application, e.g., either swarming animals, market agents, molecular clusters of reactive compounds or individual units are treated as the elementary units of the macroscopic system.
When considering the microscopic level of the system, the information determining the object dynamics can be acquired from direct interactions with the other objects or via exchange proceeding through the medium. Some of the applications incorporate multiple types of objects that feature different properties, but influence the objects of the other types acting in the same environment. As an example, one can consider the automated trading with human-participants and machine-traders, having the similar target of maximizing the profit, but different means of price prediction and hedging.
Modelling of interactive behaviour is frequently bound to the agent-based paradigm due to intuitive representation. However, this approach requires extensive computational capacities, while lacking analytic tools available for continuous modelling. In some cases, a hybrid modelling is applied, combining the advantages from both approaches. In this case, the medium is partitioned into isolated domains, where microscopic entities are allowed to change their position, migrating in-between the sub-partitions. Afterwards, classical modelling (e.g., compartmental ODE models or discrete-event simulations) is applied separately to each of the spatial domains, while tracking the histories of individual objects that impact local composition of macroscopic quantities, (see, for example, Figueredo et al. (2014)).
Here, an introductory example of the ABM approach applied for modelling the swarming behaviour is given, by treating the dynamics of two collective animal species with different degree of perception of the co-specie individuals. All the individuals are following the flowchart rules specified by the algorithm, (see Shcherbacheva and Kauranne (2013)).

Since the main focus of this subsection is on studying the overall impact of perception on aggregate movement of the swarm, the same spatial domain is considered for all the animal groups. This domain is located in 2D space and centred in a potential well that represents the local area constantly circumvented by animals. Hence, the aggregate dynamics is restricted to a finite space, but no explicit boundaries are imposed on the movement. This area contains the attraction site represented as a Gaussian kernel situated in the centre of the patch, with standard deviation $\sigma_a = 1000$m selected such that the attraction acts globally inside of the domain. Additionally, the habitat is amended with four local repulsion sites positioned at the corners and covering the patches of the width $L = 4$m. This local diversion acting on the swarm can be attributed to, e.g., repulsive smells or obstacles (e.g., vegetation, buildings). The diversion is introduced as the probability of rejection for position $\mathbf{x}_i^n$ given as a Heaviside step function, i.e., the random positions that are within the distance closer than L from the repulsion site are rejected. In all the simulations, the random walk step is considered as a proposal when the individual is changing its position. Given that the agent is occupying the position $\mathbf{x}^{n-1}$ at iteration $n-1$, the next *candidate step* $\mathbf{x}^n$ is randomly proposed $\mathbf{x}^n$ by

$$\mathbf{x}^n = \mathbf{x}^{n-1} + dW, \quad dW \sim N(\mu, \Sigma) \tag{1.13}$$

where a 2D Gaussian $N(\mu, \mathbf{\Sigma})$ is specified to govern the speed of the random walk. It should be noted that mosquito host-seeking in response to the odour emitted from human host is also modelled by the mechanism of accept-reject stepping, see Section 2. In the case of mosquitoes, collective effects are not included into the model.

Here, the movement of animal group is driven both by the exogenous factors - such as the potential well that imposes the attractive influence, the obstacles that each impose a local repulsive potentials - and by the internal potential originating from the interactions of the group members. For simplicity, the exogenous impacts are assumed to be constant in time. However, in reality the environment typically exhibits instant and periodic changes, e.g., intermittent air or water currents. As a summary, the aggregate dynamics of the animals is maintained by the aggregation force that preserves the swarming dynamics, and the short-range repulsive interaction that eliminates the collisions.

The two species considered in this study are referred to by familiar names to associate each of them with a similar real species. The difference of the species is attributed to their perception of the co-specie animals. In the first case, the birds are assumed to visually recognize their fellow individuals, but up to a certain finite distance in direction of their movement. Simultaneously, fish recognizes the movement of the school with its special sensing region - the lateral line, which enables to sense the fellow individuals beyond the scope of vision.

The tendencies to aggregate and to avoid overcrowding are characteristic for both of the animal species considered in this study. Here, these types of behaviour are reproduced by the means of the *Kalman dynamics*, a term introduced following the statistical parameter estimation approach known as Kalman filter, which enables to obtain an optimal estimate of the state variables attributed to dynamic system based on the model and observations, given together with their uncertainties, (see Kalman (1960)). Generally, the state estimate

of the system is taken as the weighted average of a prior state and the state observation, where the weights are dependent on the level of noise associated with these two terms. Assume that at a step $n-1$ the animals occupy spatial positions denoted as

$$\mathbf{X}^{n-1} = \left(\mathbf{x}_1^{n-1}, \mathbf{x}_2^{n-1}, \ldots, \mathbf{x}_N^{n-1}\right), \tag{1.14}$$

where $\mathbf{x}_i^{n-1}$ stands for position of the ith individual at the $(n-1)$th step, and N is the number of individuals in the group.
Initially, all the agents are occupying randomly selected spatial locations inside of the domain of interest. At each step of the simulations, the candidate positions $\mathbf{x}_i^n, i = 1, 2, \ldots, N$ are proposed, independently for each of the individuals, as given by Equation 1.13. After that, the candidate positions are preliminarily accepted (or rejected) following the accept/reject procedure with the aim of accounting for the orientation towards an increase of the attractive potential and the risk avoidance. Finally, the preliminarily accepted candidate positions are adjusted by the weighted term referred to as an observational increment with the aim of imposing the cohesive movement towards the other individuals in the swarm:

$$\bar{\mathbf{x}}^n = \mathbf{x}_i^n + G_a|\mathbf{y}_i^a - \mathbf{x}_i^n|. \tag{1.15}$$

Here, $\mathbf{y}_i^a$ stands for the state observation of the ith individual related to cohesion, and $0 < G_a < 1$ is the strength of cohesion. Attaining a certain strength of cohesion can be achieved by matching a suitable value of the coefficient G_a. Note that increasing the G_a results in an enhancement of aggregation. The difference between the animal species is introduced by the method of calculating the observational state related to cohesion, which is explained next.
The animals belonging to the first type (*flocking birds*) are assumed to synchronize their movement using vision of their neighbours located ahead. Here, it is assumed that only five nearest neighbours in front of the individual are visible for the birds. Observed positions of the fellow-individuals are averaged for computing an artificial state observation related to cohesion:

$$\mathbf{y}_i^a = \frac{1}{N_O} \sum_{j=j_1}^{j_{N_0}} \mathbf{x}_j^n, \tag{1.16}$$

where $j_1, \ldots, j_{N_O}$ are the indexes of $N_O = 5$ closest individuals located to the side and in front of the ith agent.
The *schooling* dynamics is introduced in a similar way to the flocking, with the exception of observations associated with the aggregation. Sensing fellow individuals at a distance which is beyond the vision is introduced in the state observation related to cohesion, which is computed as follows:

$$\mathbf{y}_i^a = \sum_{j=1 j\neq i}^{N} \exp\left[-\lambda d(\mathbf{x}_i^n, \mathbf{x}_j^n)\right] \mathbf{x}_j^n, \tag{1.17}$$

where $d(\mathbf{x}_i^n, \mathbf{x}_j^n)$ is the distance between the ith and the jth individuals at the nth step, λ is the constant which governs the range of sensing. Note that the weights associated with each of the individuals exponentially decrease with the distance.
Similarly to the case of cohesion, a short-range repulsive force between the swarm members is introduced as:

$$\bar{\mathbf{x}}_i^n = \mathbf{x}_i^n - G_r|\mathbf{y}_i^r - \mathbf{x}_i^n|, \tag{1.18}$$

where $0 < G_r < 1$ stands for the strength of repulsion. The state observation of the ith individual related to repulsion $\mathbf{y}_i^r$ is given as the average calculated over the set of all the neighbouring individuals located closer than at a minimum distance d_{min} to the ith individual:

$$\mathbf{y}_i^r = \frac{1}{|N_r^i|} \sum_{j \in N_r} \mathbf{x}_j^n, \tag{1.19}$$

where

$$N_r^i = \{j | d(\mathbf{x}_i^n, \mathbf{x}_j^n) < d_{min}\}.$$

The simulation results obtained for the two species and the case of mosquitoes (non-interactive agents) are illustrated in Figure 1.4. Herewith, each species is plotted in a separate row. The first two columns of the plots, corresponding to the flocking and schooling, stand for the intermediate states of the swarming, in each respective case. The upper-most left figure represents the common random initial state of all the swarms. Mosquito case was considered for the reference, since in this situation the agents only move in response to the global attraction force, in the absence of the collective behaviour. The basic movement for all the swarms was simulated as an accept-reject stepping, which is explained in Section 2 for the case of mosquitoes, where a more detailed modelling approach was developed to attain the model outputs reproducing the experimental data from Kitau et al. (2012).
According to the plots, it can be inferred that the shape of the swarm is different for birds and fish. These two species both orient towards their fellow individuals, in a way that influences the resulting shape of the swarm that they reproduce. As a result, birds, are circulating in a connected chain, while fish display clustering behaviour instead. As a result, they demonstrate the effect imposed by the spatial range of perception associated to each of the synthetic species on the macroscopic dynamics of the group. The summary of associated parameters employed in the simulations is given in the Table 1.2. This subsection provides only a brief outline of the aggregate motion simulations. More detailed explanations are available in the paper Shcherbacheva and Kauranne (2013).

Table 1.2: Model coefficients included into experimental runs together with their values

Parameter symbol	Parameter description	Parameter value
L	width of the repulsive domain	4[m]
G_a	strength of the cohesion	0.7
G_r	short-range repulsion coefficient	0.9
λ	sensitivity decay coefficient (for birds)	1
σ	scaling coefficient for global attraction	$1e-3$

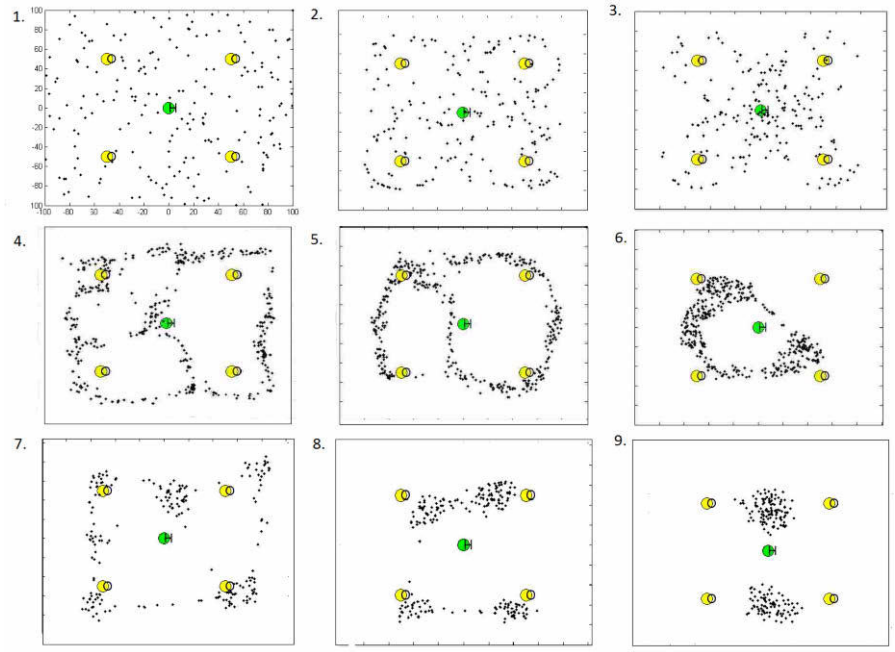

Figure 1.3: 1. Initial layout. 2. Mosquito swarm distribution at an intermediate stage. 3. The final distribution of the mosquito swarm. 4.-5. Intermediate distributions of birds. 6. The final distribution of birds. 7.-8. Intermediate distributions of fish. 9. The final distribution of fish.

1.4 Motivation, objectives and research questions

Movement ecology studies the phenomena underlying collective behaviour of the animals and movement in response to external stimulus imposed by the environment. Generally, collective behaviour and *emergence* (self-organization) are featured by many systems considered in, e.g., physics and economics, social science, control theory and mobile robotics, (see Giardina (2008)). However, in natural sciences collective phenomena are studied in more details due to broader modelling paradigm. The individual units treated in animal aggregation are more complex and possess cognitive and adaptation abilities that vary from species to species. However, only a few key characteristics strongly impact the formation of animal behaviour.
From more broad prospective, the characteristics of the individual can be crucial for capturing the mechanisms of, e.g., swarming and flocking, prey-predator relations and disease spread by insects. Unfortunately, there is no standardized approach to distinguish essential components from minor ones; this is commonly determined by specific formulation of the research problem to be addressed. This question is generally non-trivial, and is known as a problem of 'relevant detail', (see Giardina (2008)). In this project a host-seeking behaviour of malaria vector mosquito is modelled in the presence of Long-Lasting Insecticidal nets (LLINs). The most parsimonious parametrization of the model yet including all the meaningful factors is developed. The objective of this study is to address several topics by following the agent-based methodology:

1. What is the mechanism of host-seeking behaviour of malaria vector mosquitoes and what factors can explain the difference in the efficiency of the LLIN *vector control* in application to different species of mosquitoes?

2. How does the *in situ* mosquito behaviour influence the global characteristics of malaria transmission?

3. What implications for malaria transmission result from mosquito behaviour modified by the malaria parasite?

4. How do settlement patterns of the humans affect host-seeking behaviour of mosquitoes and what is the overall impact of household size on malaria transmission?

Model calibrations presented in this work are based on the data sets from Kitau et al. (2012). Although this kind of data is not sufficient to determine all of the parameters, the clear difference is observed between the efficiencies of the LLIN control in application to *An. gambiae* as compared to *An. arabiensis* mosquitoes from the estimated posterior distributions of parameters.
As the outcome of this work, partial answers to the above-postulated questions are given. For the detailed explanations and interpretations of the results, refer to Section 2 (see pp. 57-58, p. 66), Section 3 (see p. 75, pp. 77-78) and Conclusion.

1.5 Author's contribution and acknowledgements

The thesis is written in the form of a Monograph, based on the publications Shcherbacheva and Kauranne (2013), Shcherbacheva and Haario (2017), Shcherbacheva et al. (2018) given in the References. The author was the first writer in all these papers, and was carrying out all the coding implementations in Matlab and CUDA tool-chain and simulations for producing the results in all the published papers.
Professor Heikki Haario proposed the modelling approach, which is developed and extended in the present work, and contributed to the writing process of the papers Shcherbacheva and Haario (2017), Shcherbacheva et al. (2018). Dr. Gerry Killeen collaborated with the author and gave his guidelines for modelling the host-seeking behaviour of malaria vector mosquitoes as an expert in the field of entomology. Dr. Tuomo Kauranne assisted with writing the publication Shcherbacheva and Kauranne (2013).

2 ABMs of malaria transmission

2.1 Background

Malaria is a lethal disease threatening almost half of the human populace, caused by *Plasmodia* parasites and transmitted by *Anopheles* mosquitoes. Global efforts have been taken, resulting in malaria eradicated from 79 countries in the world within the period from 1979 to 2010, (see Feachem et al. (2010)). Commonly, a significant reduction in malaria burden was achieved through the *intervention strategies*, such as insecticide-treated bed nets (ITNs), indoor residual spraying (IRS), long-lasting insecticidal nets (LLINs) and artemisinin-based combination therapy (ACT), (see (WHO)). For evaluating the performance of strategies and planning supplementary measures, experimental data are typically collected and analysed, which is a time and resource-consuming procedure. In the situations, where field data are not available or scarce, mathematical modelling helps to fill the gaps, gaining knowledge by the means of the inference and prediction, (see McKenzie and Samba (2004)).

Mathematical modelling of infectious diseases has been dominated by compartmental models of Ross-MacDonald type (Ross (1903)), with the main focus on populations and transmission dynamics. Commonly, the system of equations specifies the transitions between the states of infection for vectors/humans. Following the progress in malaria research, more elaborate compartments were introduced. This enabled studying of many important factors, such as parasite drug-resistance (Gurarie and McKenzie (2006)), inter-human variation in immunity (Gatton and Cheng (2004), Gurarie and McKenzie (2007)) and vaccination efficiency (Anderson et al. (1989), Dietz et al. (2006)), age-specific biting rates and differential attractiveness for mosquitoes (Chamchod and Britton (2011)). Notwithstanding the fact that compartmental models are capable of capturing spatial heterogeneity (Acevedo et al. (2015)) and variations within human population (Maude et al. (2009)), in the areas of high spatial variation they often feature convergence issues, (see Smith et al. (2018)).

As an alternative approach, ABMs of malaria are gaining popularity with the increase in computer power. By its design, the ABM approach captures the influence of individual-level behaviour on transmission dynamics, which is essential for representing increased stochasticity in low-transmission environment. Additionally, the ABMs offer the benefits of high-resolution spatial simulations. Accounting for patient individuality and spatial heterogeneity appears highly crucial in vector control; especially, when status of disease is close to elimination. Figure 2.2 (adopted from Smith et al. (2018)) outlines the timeline of published papers reporting on the ABMs of malaria transmission, from the earliest to the most recent ones, including the author's contributions, Shcherbacheva and Haario (2017) and Shcherbacheva et al. (2018). In this subsection the author mostly aims at explaining the model in the context of existing classification.

Within the ABM framework, some of the participants of transmission process (conventionally, *vectors, humans* or/and *parasites*) are modelled individually, with a set of properties attributed to each of the agents, containing associated state variables, individual actions and parameters. Commonly, the levels of detail depend on research questions of

interest. However, factors underlying disease propagation are so complex, that no one model is capable of taking all of them into consideration.
In the context of malaria spread, different ABMs concentrate on different aspects of transmission. The questions of research included studying the impact of intervention strategies (Zhu et al. (2015a)) and their cost-effectiveness analysis (CEA), human infectivity, (Ross et al. (2006)) and immunity (Maire et al. (2006), Smith et al. (2006), Gurarie and McKenzie (2007), Griffin et al. (2010), Yamana et al. (2013) and Nguyen et al. (2015)), mosquito life cycle (Chitnis et al. (2012), Zhu et al. (2015b)), physical environments (Bomblies et al. (2008), Gu and Novak (2009), Zhu et al. (2015a), Zhu et al. (2015b)), populations dynamics (Depinay et al. (2004)) and potential impact of climate change (Bomblies and Eltahir (2009)).
Here, the ABM of mosquito host-seeking behaviour was developed with the main focus on studying the efficiency of spatial repellents and long-lasting insecticidal nets (LLINs) in application to malaria vector control. Herewith, the process of acquiring the infection (from mosquito to human and reverse) was not explicitly included into simulations. Instead, the biting and mortality rates are the key points of simulation. The former two factors are dependent on the spatial locations of the hosts and available interventions. For that purpose, the long- and short-range attractions of mosquitoes towards the humans are explicitly modelled, together with the repulsion and poisoning effects caused by insecticides. In a two-dimensional landscape, mosquitoes search for the host by moving in direction of the carbon dioxide concentration increase. Consequently, the insecticidal nets reduce the biting rates, while simultaneously decreasing the population of mosquitoes. Initially, in the paper Shcherbacheva et al. (2018), the *in situ* mosquito behaviour and the poisoning/repulsive effects of the LLINs were calibrated to the contact and mortality rates as given by the data from Kitau et al. (2012). In this work, the hut-level model is subsequently extended to the household-level and the community-scale simulations (see Figure 1.2), where preliminary calibrated parameters attributed to the properties of four different insecticidal treatments are employed in the simulations.
By algorithmic design, the ABMs of malaria transmission can be classified into three categories: ABMs originating from compartmental models with probabilities used instead of the flow rates for determining individual transitions of the agents from one state to another occurring at a given step (Dietz et al. (2006), Gurarie and McKenzie (2007) and Griffin et al. (2010)); models based on host parasite densities, where the state changes of the agents are specified as a set of equations with coefficients sampled from empirically defined distributions to generate variations within the agents, (see Smith et al. (2006)). Finally, the third method is based on the flowchart diagram which specifies the behavioural rules and the actions taken by the individual (Gu and Novak (2009), Cummins et al. (2012)) also featuring events that occur with given probabilities. In the present project, a model of mosquito host-seeking behaviour was developed following the third approach, (Shcherbacheva et al. (2018)). Figure 2.1 represents the flow chart of vector actions, as it was implemented in the algorithm.
Depending on the question at hand and relevant factors, a model may include one or several agent types, with the most frequent role attributed to *vectors, humans* or *parasites* Smith et al. (2018). In the present study a number of vector-agents, each attributed

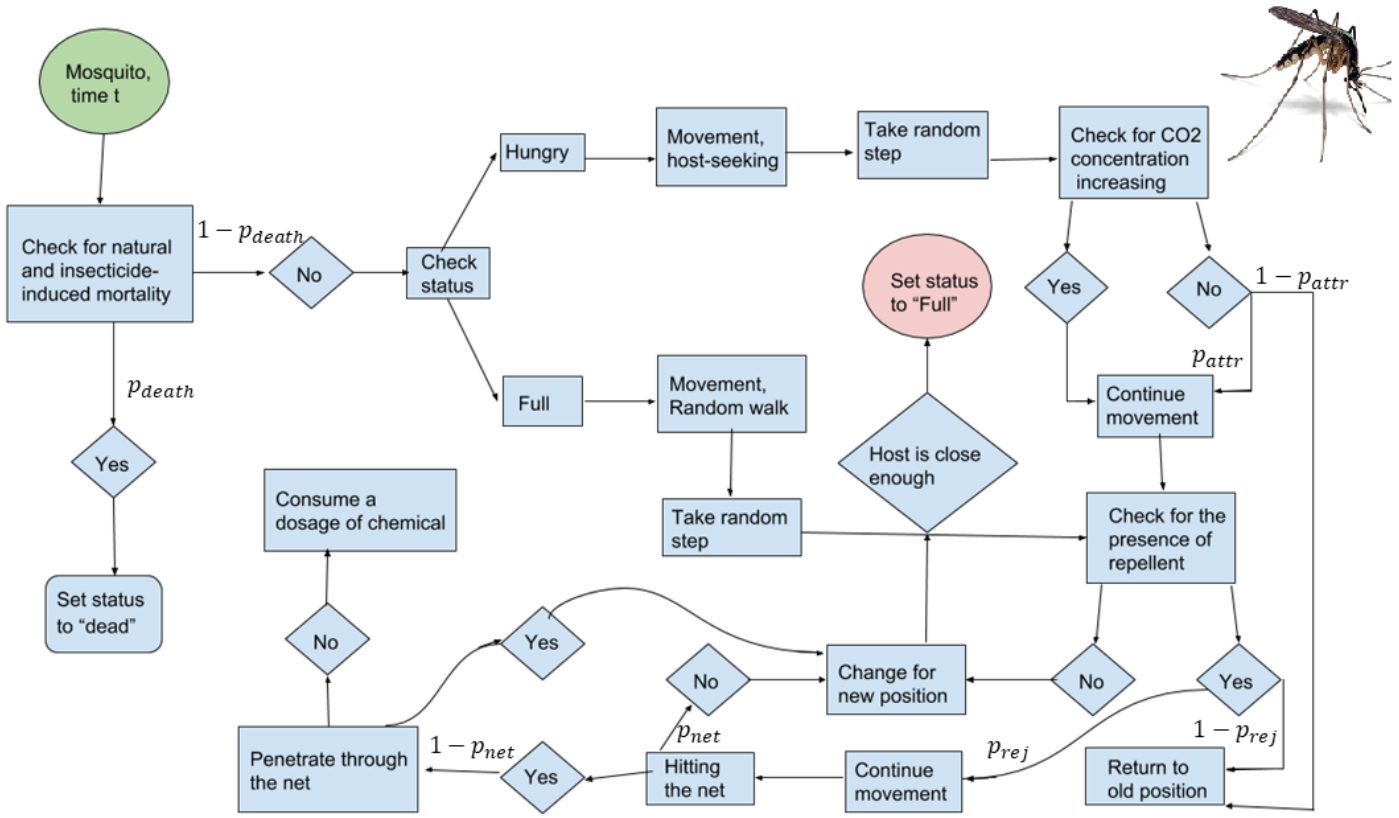

Figure 2.1: A decision tree representing the main features of the algorithm of the ABM of mosquito host-seeking behaviour in the presence of the LLINs introduced in Shcherbacheva et al. (2018). Here, some of the choices are probabilistic, conditioned on the state of the agent. p_{death} stands for the probability of death, p_{net} is the probability of being blocked by the physical barrier created by the net, p_{attr} is the probability of accepting the proposed step, p_{rej} is the probability of rejecting the proposed step due to the impact of repellent.

with the list of properties (e.g., infection, spacial location, blood-hunger state, accumulated dosages of chemical), are tracked and updated individually during the simulation. Humans were also modelled as individual agents, attributed with the state of infection, usage of the LLINs and spatial location. Different from mosquitoes, the humans don't undertake any actions and their attributes are constant in time. However, various detailed impacts of the disease dynamics can be included. In particular, the approach incorporates an excessive exposure of the LLIN non-users when sleeping next to protected individuals and alterations in vector induced by the parasite, where mosquitoes tend to take multiple blood meals on different hosts.

Depending on landscape representation, ABMs can feature a continuous environment, (Cummins et al. (2012)), grid partition with uniform size of the cells and patches of varying size depending on typical speed of mosquito flight or relative location of resources, (Gu and Novak (2009)). In the present model, the space is continuous, and the movement of mosquitoes is driven depending on Euclidean distances to the humans and households. In the absence of the sensory cues, the movement of mosquito constitutes pure random walk, which is common for the ABMs that incorporate animal navigation, (Tang and Bennett (2010)). When located sufficiently close for sensing the host, mosquito exhibits directionally biased random movement also typical for this modelling approach, (see Tang and Bennett (2010), Cummins et al. (2012)).

Models with mosquitoes as agents are typically dominated by mosquitoes belonging to *Anopheles* species, including *An. vagus* (Alam et al. (2017)), *An. stephensi* (Churcher et al. (2010)), *An. arabiensis* (Eckhoff et al. (2016)) and *An. darlingi* (Pizzitutti et al. (2015), Pizzitutti et al. (2018)). Some of the models were non-specific to *Anopheles* species, while some of the models include several species of *Anopheles*. The model proposed in the present work was developed for *An. gambiae* and *An. arabiensis*, motivated by the difference in their host-seeking behaviour when confronted with the LLIN. The difference between *An. gambiae* and *An. arabiensis* in their responses to insecticide results in higher efficiency of LLIN control in application to *An. gambiae* as compared to *An. arabiensis*, (see Kitau et al. (2012), Killeen and Chitnis (2014)). Potentially, our approach is capable of modelling other mosquito species, when sufficient experimental data are available for identification of mosquito responses. Additionally, since only female mosquitoes transmit the diseases upon blood-feeding, and mating is beyond the scope of this project, the *male* mosquitoes are not included into the ABM simulations.

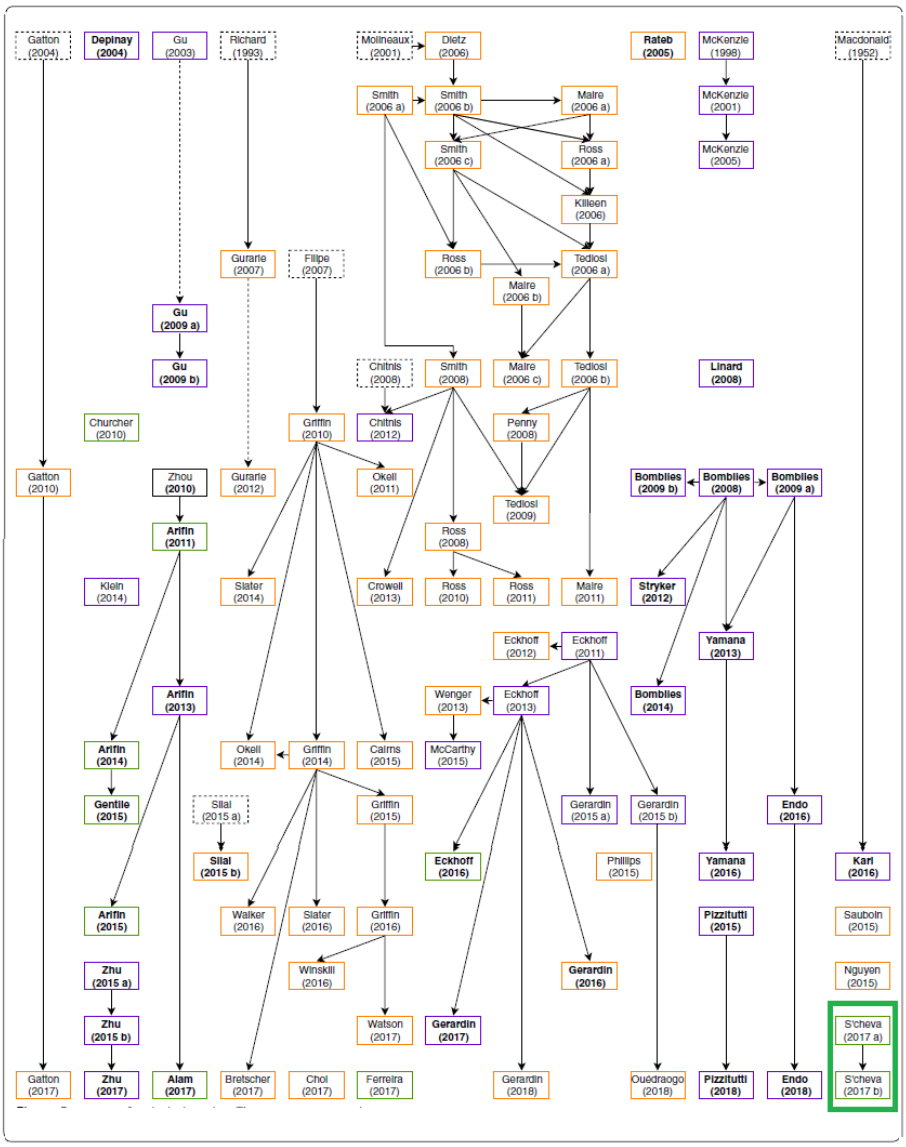

Figure 2.2: Overview of ABM approach of malaria transmission (adopted from Smith et al. (2018). The most recent studies are towards the bottom of the diagram. Solid arrows indicate papers directly linked to one another. Dotted arrows indicate models by the same lead author that are not related in methodology. Papers named in bold are spatially explicit. Boxes coloured orange, green and purple include human agents, mosquito agents or both, respectively. The papers by our authorship are highlighted in green rectangle (see the right bottom corner of the table) with the permission of Smith et al. (2018).

There exist a number of extensive ABM frameworks, such as OpenMalaria (Smith et al. (2006)), EMOD (Eckhoff (2011)) and HYDREMATS (Bomblies et al. (2008)), with many research questions investigated by the means of introducing additional modules into available environments. However, for the purposes of the present study the author developed an in-house implementation inside the MATLAB environment and by the means of the CUDA toolchain. This effort was taken to enable efficient calibration of the model using verified statistical toolbox which has been previously developed in Haario et al. (2001) and Haario et al. (2006).
The approach proposed in this work includes three specific features: accounting for species-specific behaviour (*anthropophilic* or *opportunistic* preferences of mosquitoes), possibility to to account for the other factors that impact the *in situ* behaviour of mosquitoes (socio-economic conditions and parasite ecology) and parameter identification conducted to estimate the effects of different chemicals (*contact irritancy*, *excito-repellency* and poisoning). It should be noted that parameter values employed in the ABMs of malaria transmission typically originate from the literature or simulations conducted to find the baseline values, (see Smith et al. (2018)). In this work, extensive parameter estimation is carried out by the means of the MCMC sampling, see Section 2.5 for more details.
The remaining part of the chapter introduces the ABM of mosquito host-seeking behaviour developed in this project. Basic components and parametrizations of various factors included into modelling, such as mosquito attraction to humans and the effects of impregnated nets are specified and explained. Summary of the details behind the simulations is given in Subsection 2.4. Next, Subsection 2.5 gives an overview of the techniques enabling parameter estimation of the ABMs, with a special emphasis placed on the Markov Chain Monte Carlo (MCMC) method employed for calibration of the ABM against real data from Kitau et al. (2012).
An extension from the hut-to-community-level scenario is elaborated in Chapter 3, following the scheme presented in the Figure 1.2. Here, the effect of partial coverage of population with the nets is quantified. Additionally, it is demonstrated that the model is capable of accounting for the impact of parasite ecology and socio-economic factors.

2.2 Basic model of mosquito host-seeking behaviour

Here, the ABM of mosquito host-seeking behaviour in the hut-level experiment is introduced and developed. In model simulations, mosquito population is considered as a number of independent agents navigating the 2D landscape in pursuit of blood-feeding. The movement of mosquitoes is driven by several basic external factors: attraction to odour (e.g., carbon dioxide emitted from hosts and sensed by mosquitoes (see Bowen (1991), Dekker et al. (2005), Dekker and Carde (2011), Lehane (2005), Syed and Leal (2009), Vickers (2000))), avoidance of repellents, poisoning caused by insecticides impregnated on the LLINs and physical barrier imposed by the bed nets.
The model of mosquito attraction is built on the conjecture that a mosquito orients towards the direction of the odour increase using the process widely known as klinotaxis, as it was hypothesized in Vickers (2000). The underlying mechanism of orientation in odour plume implies that mosquito probes the host odour at one position, then moves to

the next position and resamples the odour, comparing its memory of the previously sensed concentrations to decide the next location, (see Cardé (1996), Cummins et al. (2012)).
Here, the aim is to build a model that incorporates the key factors only: orientation towards host, effects of insecticides on host-seeking behaviour and mortality. A number of selections has to be made for enclosing all the features. The preference was given to the most parsimonious model formulation, with minimal number of unknown parameters.
The flight of mosquitoes is treated as a random walk featuring a directional bias with discrete time stepping. Attraction towards the source of CO_2 is specified as an *accept/reject* movement: after a random candidate position is proposed by the Brownian motion, the probability of accepting the new position for a given agent is specified to favour candidate steps taken in the direction of the CO_2 concentration increase, i.e., towards the source of attraction, (see Metropolis et al. (1953)). Moreover, the probability of acceptance is also affected by the presence of untreated or treated nets and the barrier imposed by the walls in human dwelling. These effects are included by a rejection function. Practically, untreated net is modelled as an obstacle with almost zero probability of mosquito entering the hedged space.
Additionally, the model incorporates both natural and insecticide-induced mortality caused by treated nets. The latter is dependent on amount of chemical accumulated in mosquito, i.e., practically, conditioned on the number of contacts with the surface impregnated with the insecticide. Following the ABM approach, each mosquito is tracked and updated individually within the simulation. The current condition of mosquito is represented by a vector of state variables, including position, accumulated chemical and blood-hunger status.
Assume that at time instant $n-1$ mosquito-agent occupies spatial location, then the mosquito can randomly chose a candidate position $\mathbf{x}^n$, where the new and the previous positions are related by the formula

$$\mathbf{x}^n = \mathbf{x}^{n-1} + \delta\mathbf{W}, \tag{2.1}$$

Here, an increment $\delta\mathbf{W}$ is proposed as a random position on a zone in circle centred at the origin of the coordinate system with direction randomly sampled from $U(0, 2\pi)$, and the length of the step sampled from the normal distribution $||\delta\mathbf{W}|| \sim N(\mathbf{R}, \sigma^2 I)$. In simulations, the values of parameters $R = 0.4$m and $\sigma = 0.1$m are taken such that the movement of the agents features characteristics similar to the real mosquito flight, where the speed of flight typically varies in the limits 0.4-1.1 m/s for majority of the mosquito species, as it was concluded in Snow (1980).
One iteration of the algorithm was set to 2 seconds with the intent of reducing the CPU time. Herewith, the spatial units used in simulations are expressed in meters. Although more sophisticated models for the insect flight have been proposed, (see Kareiva and Shigesada (1983), Dale and Collett (2001), Shimizu et al. (2002), Zbikowski et al. (2006), Roshanbin et al. (2009), Wu (2011), Senda et al. (2012)), the above-explained simple approach was found sufficiently adequate for the objectives of this study.
In the penury of any sensory cues emitted from the host, the mosquito flight constitutes pure random motion, as explained above. Next, a new modelling feature is introduced

to imitate the directional motion towards the source of the attractive odour. Identification and localization of a human host by mosquitoes occurs via several processes. As a long-range stimuli, they navigate in response to carbon dioxide (CO_2) plumes emanated from humans. Additionally, at a short distance to the host, mosquitoes are able to orient by heat sensors, vision and by smelling evaporations emanated from human body. Recent research has revealed that a mixture of different odours and chemical ingredients contained in a human sweat contribute to the human attractiveness for mosquitoes. *Inter alia*, the attraction is induced by nonanol, short chain carboxylic acids, ammonia, lactic acid and many other substances associated with the sweat, (see Bowen (1991), Dekker et al. (2005), Lehane (2005), Syed and Leal (2009), Dekker and Carde (2011), Smallegange et al. (2011), Verhulst et al. (2013)). Supplementary to this, mosquitoes distinguish movement, big visual features (such as buildings and vegetation) and colours. Commonly, mosquitoes are capable of sensing the human host only at a distance less then 80 meters, (see Cardé (1996)).

Initially the model is restricted to the host-seeking process inside the hut. In this study, the concentration of the odour attractant emitted from individual human is given as a solution of the diffusion equation with a point source, i.e., a Gaussian potential with the centre positioned in the spatial location of the host $\mathbf{x}^h$:

$$C(\mathbf{x}, \mathbf{x^h}) = \exp\left[-\frac{d^2(\mathbf{x}, \mathbf{x}^h)}{2\sigma_a^2}\right], \tag{2.2}$$

where $\mathbf{x}$ denotes the position of mosquito, C is a concentration that creates the stimuli sensed by mosquito at a distance $d(\mathbf{x}, \mathbf{x}^h)$ to the host. The sensitivity range attributed to mosquitoes is modelled by the means of the standard deviation σ_a, which gives an endmost distance at which mosquito is sensitive to the host. Naturally, when taking into account other meaningful factors that impact the dispersion of mosquitoes, the concentration can be specified in a different way, e.g., by using advection-reaction-diffusion equations, which include the air flows and the intermittent concentration plumes, etc., (see Cummins et al. (2012)). Here, it should be noticed that since only scaled concentrations are utilized in the accept-reject procedure, the true value of concentrations are not represented in the model. Furthermore, only the ratios of the concentration-dependent attraction function, which is specified below, are needed for modelling. The process of host-seeking is given by a random walk with accept-reject stepping, where the acceptance probabilities are estimated to fit the observed effects associated with mosquito responses to the host, the presence of the LLIN (such as repulsion and early exit) and poisoning by insecticides. This is achieved by introducing the model features adopted from the Metropolis algorithm, (see Metropolis et al. (1953)).

Assume that the attraction potential function $p(\mathbf{x})$ is specified for each spatial location $\mathbf{x}$, conditioned on the attractant concentration and other relevant factors. Then, assume that from point $\mathbf{x}^{n-1}$ the new position $\mathbf{x}^n$ is randomly proposed. Supposing that the corresponding attraction values associated with the points are p_{n-1}, p_n, the candidate point is

accepted with probability

$$\alpha_a(\mathbf{x^n}|\mathbf{x^{n-1}}) = \min\left(1, \frac{p_{n\cdot}}{p_{n-1}}\right) \tag{2.3}$$

The CO_2 concentration is viewed as a main attraction stimuli for mosquitoes. In order to account for other short-distance attraction factors in a parsimonious way, we define the attraction potential function as

$$p(\mathbf{x}) = \exp\left(C(\mathbf{x})/\sigma_{acc}\right) \tag{2.4}$$

with a scaling factor σ_{acc} is conditioned on the distance to the host. Additionally, we account for increasing greediness of mosquito, as a result of activation of the heat sensors at a short distance to the host by introducing a linearly distance-dependent scaling factor as

$$\sigma_{acc}(\mathbf{x}) = \begin{cases} \sigma^1_{\text{acc}} + \sigma^2_{\text{acc}} d(\mathbf{x}, \mathbf{x}^h), & d(\mathbf{x}, \mathbf{x}^h) \leq 80 \\ \sigma^{\text{max}}_{\text{acc}}, & d(\mathbf{x}, \mathbf{x}^h) > 80 \end{cases} \tag{2.5}$$

The above function increases from the minimum value σ^1_{acc} with a slope given by the parameter σ^2_{acc} until it is replaced by a constant suitable for producing a purely random movement outside of the plume. More details on specifying parameters $\sigma^{\text{min}}_{\text{acc}}$ and $\sigma^{\text{max}}_{\text{acc}}$ are explained in the next section.

Figure 2.3 displays the broken line shape which was selected for σ_{acc}, together with the corresponding probability of accepting the steps away from host. Note that the functional behaviour of the scaling factor results in such a movement that steps taken in direction of the host are always accepted. Moreover, the parameters of functional dependence for σ_{acc} can be bounded so that the acceptance probability specified by Equation 2.3 is actually 1 at the distance of 80m from a host. This means that all the moves are accepted, when the distance from the host comprises more then 80m, i.e., the movement reduces to the pure random walk out of limits of the concentration plume. More details of numerical implementation are given below, in the next section.

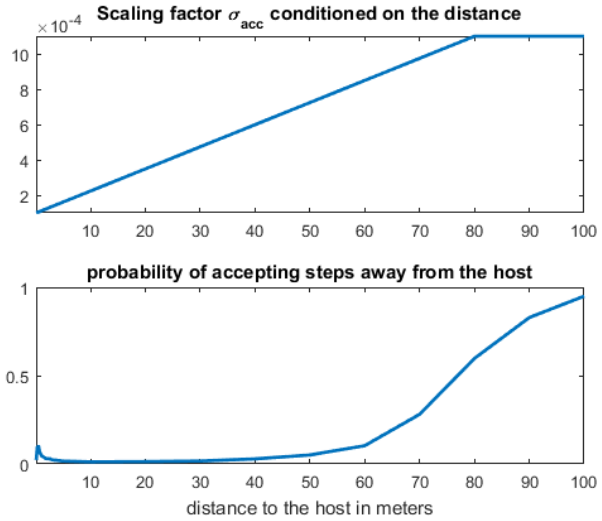

Figure 2.3: Scaling factor σ_{acc} conditioned on distance to the host (top), average probability of accepting steps taken away from the host as a function of distance to the host (bottom).

By design, the algorithm basically resembles a well-know Simulated Annealing optimization method, proposed in Kirkpatrick et al. (1983). Here, the difference comes only from the 'annealing temperature schedule' replaced with the 'greediness scale', which is related to the distance from mosquito to the host.
As displayed in Figure 2.3, the rate of acceptance for the steps away from the plume decays as the insect approaches the host. However, in the close proximity to the host, the latter rate locally increases, while still remaining small. This property can be attributed to a genuine insect behaviour, since mosquitoes of different species tend to exhibit more tortuous flights in proximity to the host, as it was reported in Spitzen et al. (2013). This tendency is associated with scanning of the environment before landing.

2.2.1 Modelling treated and untreated nets

The impact of control measures is introduced by the means of the logistic function:

$$y = \frac{1}{1 + \exp(-x/s)}, \tag{2.6}$$

which exhibits S-shape behaviour. The function is characterized by exponential increase of the growth , which slows down when $|x| \to \infty$.
In order to model a *contact irritancy* induced by the net, the function was modified so that the rejection probability at the candidate position $\mathbf{x}$ attenuates as the distance to the host

grows, parametrized as

$$\alpha_r(\mathbf{x}|d_{50}, r, s) = r\left[1 - 1/\Big(1 + \exp\big(-\big(d(\mathbf{x}, \mathbf{x}^h) - d_{50}\big)/s\big)\Big)\right], \tag{2.7}$$

where $d(\mathbf{x}, \mathbf{x}^h)$ denotes the distance from the mosquito to the protected human. The parameters d_{50} and s determine the range of coverage and the spread of repellent, r stands for intensity of repulsion.

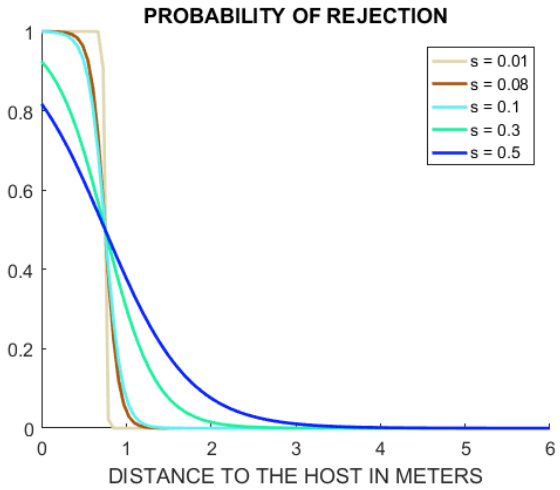

Figure 2.4: Probability of rejection associated with repellent given by Equation 2.7 for different values of s, with $d_{50} = 0.75$ and $r = 1$.

In the present work, bed nets of fixed size of 1.5m are considered, where the size is specified in accordance with the WHO reports. As an option, untreated nets can be given as the probability of rejection reduced to the Heaviside function, which is a specific case of Equation 2.7 with $s << 1$. Here, the torn nets are imitated that are typically available in rural conditions, (see Kitau et al. (2012), Okumu et al. (2013)), which is simulated with a penetration probability $1 - p_{net} << 1$, that gives the non-zero chance to get through the net barrier. Following this choice, the candidate position which is inside the net is accepted with probability $1 - p_{net}$. Here, the model parameters are identified related to untreated net using the experimental data from Kitau et al. (2012). See the Subsection 2.3 for detailed explanation of the data sets.
The effect of the LLIN is simulated in two subsequent steps. Initially, the impact of spatial repellent is imitated by conducting the accept/reject procedure, with the probability of rejection specified by logistic equation, see Equation 2.7. Then, the physical obstacle created by the net is simulated, similar to the situation with the untreated net. Moreover, it is assumed that the poisoning action is induced by the LLINs, which is regarded as *insecticide-induced mortality*. Specifically, the probability of death increases when mosquito takes additional dosages of the chemical, see the next subsection for more details.

2.2.2 Mortality rates

In the present project, natural and insecticide-induced mortality are taken into account in the model. Natural mortality in a declining population can be modeled by the means of an ordinary differential equation

$$\frac{dP}{dt} = -\mu P, \tag{2.8}$$

where μ stands for the rate of decline, P denotes the population number. A discretization in time leading to agent-based rules instead of the rates is naturally given as:

$$\frac{P(t+\Delta t) - P(t)}{\Delta t} \approx -\mu P(t), \tag{2.9}$$

where $\Delta t = t_n - t_{n-1}$ is a unit time interval. In so doing, the equation can be represented as follows:

$$\frac{P(t+\Delta t)}{P(t)} \approx 1 - \mu \Delta t. \tag{2.10}$$

The latter formula expresses the relative decline of the population within a time period Δt. Hence, the probability of death per unit time Δt is specified as the decline rate multiplied by length of the time interval:

$$\alpha^{\Delta t} = \min\left\{1, \mu \Delta t\right\}. \tag{2.11}$$

Consequently, the probability of natural death in the ABM simulations is specified by the former formula, with $\Delta t = 2$ seconds, and with a value for μ taken from the literature, which conforms with the 34-hour natural mortality rates reported for *An. gambiae* and *An. arabiensis* as 10%, (see Clements and Paterson (1981)).
Herewith, the probability of death is updated and taken into account separately for each mosquito during the simulation. Following the results reported in Kitau et al. (2012), the probability of death resulting from a lethal dosage of chemical is similar for *An. gambiae* and *An. arabiensis*. In accordance with this, the same poisoning rates are assumed for these two species. Next, the poisoning from the chemicals is modelled, assuming that mosquito consumes a unit dosage upon physical contact with the net surface, impregnated with the insecticide. Insecticide-induced mortality rate $\alpha_p^{\Delta t}$ is conditioned on the effective amount of chemical, taken by mosquito within the simulation up to a time instant t. Here we introduce a dependence

$$\alpha_p^{\Delta t}(t) = \mu_p C_{tot}(t) \Delta t, \tag{2.12}$$

where the effective amount of chemical taken by mosquito is computed as the total accumulated dosage $C_{tot}(t)$ scaled by a chemical toxicity coefficient μ_p, which depends on a given insecticide disposed for LLIN treatment. The value of $C_{tot}(t)$ is given by the sum of steps in the repellent plume:

$$C_{tot} = \sum_{i=1}^{T} C_{rep}(\mathbf{x}^i) = \sum_{i=1}^{T} \alpha_r(\mathbf{x}^i | d_{50}, r = 1, s), \tag{2.13}$$

where, the value $\alpha_r(\mathbf{x}^i|d_{50}, r = 1, s)$ is associated with the dosage of the chemical spread in the air given by Equation 2.7 above. Taking into account the properties of modern insecticidal treatments, the spatial range of repellent is small ($s = 0.01$). Thus, it is assumed that the dosage is consumed upon the contact with the net, which is similar to the above formula. As a result, the total accumulated dosage C_{tot} is computed as the number of contacts with the net multiplied by a unit dosage consumed during the contact. In Equation 2.7 the arguments are set as follows: $d(\mathbf{x}, \mathbf{x}^h) - d_{50} = \epsilon$, with $\epsilon << 1$, and $r = 1$. This dosage is assumed to be the same for all the chemical treatments and all the mosquito species considered in the study.
The total probability of death per unit time interval Δt is given as a sum of the natural and chemically-induced probabilities of death:

$$\alpha_{death} = \min\{1, \alpha^{\Delta t} + \alpha_p^{\Delta t}\}. \tag{2.14}$$

At the beginning, when mosquito has not yet taken the poison, the death rate is reduced to the natural mortality. Gradually, as the dosage of the chemical is increasing in mosquito, α_{death} tends to one, where finally the chemical-induced death occurs from the lethal dosage of insecticide.
Remark 1. A delayed mortality is taken into account, as a result of prolonged impact of insecticides in mosquitoes. Note that this was also featured by the data reported in Kitau et al. (2012), since alive mosquitoes were gathered and kept under the glass for 24 h before recording delayed mortality happening after 10 hours in the hut. Here the process is imitated by keeping the death rate α_{death} from Equation 2.14 fixed after 10 hours spent in the hut. As a result, the probability of death after 24-hour time period is given by Equation 2.11, with $\Delta t = 24 \cdot 1800$:

$$\alpha_{24\text{h}}^{\Delta t} = \min\left\{1, \min\left\{1, \alpha^{\Delta t} + \alpha_p^{\Delta t}\right\}\right\} \tag{2.15}$$

Remark 2. The host-seeking process governed by the presence of attraction to the human is assumed to continue only during a certain time period, restricted by a maximal duration t_{max}. In the absence of the insecticides (which is further referred to as the control case) this limit is set to 5 hours, (see Reddy et al. (2011)). After t_{max} hours, the mosquito starts to exhibit a random walk independently of the presence of CO_2 concentration. However, the impact of the repellent and the space hedged by the physical net barrier still restrict the movements of mosquito. Also, the poisoning by chemicals has a continuous impact. It should be noted that the attractant cue does not affect the movement after mosquito abandons the host-seeking process, which happens either after the blood-meal sufficient for egg development has been taken upon the feeding, or after t_{max} spent in futile blood-feeding attempts. In the hut-level simulations it is assumed that the sufficient portion of blood is received upon one successful contact with the human. In addition, as it was revealed by the simulations, the resting time after the feeding does not change the overall statistical result of the computational experiment when introduced into the algorithm. Therefore, this effect was omitted for the sake of parsimony.

2.3 Extended model

The data acquired from trials in Kitau et al. (2012) are utilized for modelling and calibration. Specifically, the datasets include the contact, exit and mortality rates observed for mosquitoes in the presence of different insecticidal treatments, see the summary in Figure 2.5. According to the data, two anthropophilic mosquitoes (*An. gambiae* and *An. funestus*) exhibit higher insecticide-induced mortality as compared to opportunistic *An. arabiensis*. Many conjectures can be proposed for explaining the underlying differences in host-seeking traits of the species. A straightforward explanation, presented in Vaughan et al. (1991), implies that *An. arabiensis* is a faster feeder as compared to *An. gambiae*, which results in less prolonged time spent in contact with the net surface; *An. arabiensis* exposure to insecticide is therefore shorter, which results in a lower amount of poison consumed. A further conjecture supposes that *An gambiae* and *An. arabiensis* feature dissimilar persistances of blood-feeding attempts, which is due to the fact that the odorant receptors of anthropophilic *An. gambiae* are more accurately adjusted to ingredients contained in the human sweat, (see Broek and Otter (1999), Lorenz et al. (2013)).
In the paper Shcherbacheva et al. (2018), the reduced persistence of host-seeking attempts specific for *An. arabiensis* was implemented using two different model parameterizations. First parameterization assumed a shorter time spent in host-seeking process t^A_{max} for *An. arabiensis* when confronted with LLIN, as compared to the untreated net case. This parameter was estimated separately, assuming all the other impacts to be similar for the two species. Another alternative version suggested a reduced directional bias towards the host (for *An. arabiensis*) in the presence of the LLIN. In this case, the parameter determining the scaling factor for attraction $\sigma^{1,A}_{acc}$ was estimated for *An. arabiensis*, together with the reduced host-seeking time t^{LLIN}_{max}, which was assumed similar for both mosquito species. These two parametrizations were found sufficient only for fitting the case of the IconMaxx insecticidal treatment. Other data sets from Kitau et al. (2012) feature higher exit and lower contact rates alongside more than twice higher mortality rate for *An. gambiae* (*An. funestus*) as compared to *An. arabiensis*. This is different in the case of IconMaxx. Specifically, the corresponding death rate of *An. gambiae* is not up to twice higher than that of *An. arabiensis*, and the insecticide-induced exit rate produced with the IconMaxx was not very high in comparison with the other chemicals considered in this study, (see Shcherbacheva et al. (2018)).
In order to make the model capable of reproducing the properties attributed to the other insecticidal treatments, three additional effects caused by the chemicals are introduced: metabolic detoxification, (Yahouódo et al. (2017), Nardini et al. (2012)), delayed impact, (Kitau et al. (2012)) and excito-repellency (or insecticide-induced exiting), (Okumu (2012), Kitau et al. (2012)). Given this version, four chemicals are included into the study: Alphacypermethrin, Carbosulphan, Deltamethrin and IconMaxx, with the model calibrations performed accordingly.

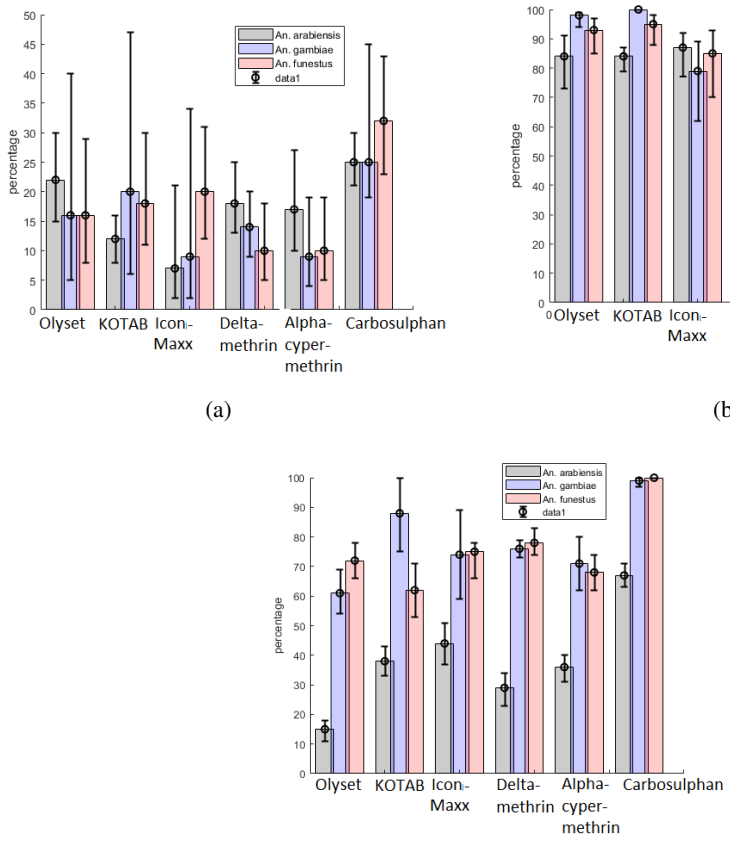

(a) (b)

(c)

Figure 2.5: Summary of the data sets from Kitau et al. (2012) for several insecticidal treatments. Percentages of the (a) blood-feed and (b) exited mosquitoes. (c) Percentage of insecticide-induced mortality cases in mosquito populations. The black bars indicate 95% confidence intervals.

As a first extension of the basic model, the scaling factor is further specified such that it depends not only on the distance to the host, but also on the influence of repellent. Again, this extension was made to properly fit the exit rates, as the scaling factor accounts for the generally higher exit rate when confronted with the treated nets as compared to the control case with the untreated nets. For that purpose, an *excito-repellency* parameter μ_e is introduced (see Okumu (2012)), that depends on the chemical treatment used for impregnating a given LLIN and on mosquito specie, parametrized as

$$\sigma_{acc}(\mathbf{x}, C_{tot}) = \sigma_{acc}(\mathbf{x}) + \mu_e \cdot C_{tot}, \tag{2.16}$$

where C_{tot} denotes the total dosage of the chemical consumed by a mosquito computed by Equation 2.13.
Secondly, the detoxification is also taken into account, occurring with a rate α. Given the

previous dosage of the chemical $C_{tot}(n)$ at the step n, the dosage at the next step $n+1$ is calculated as

$$C_{tot}(n+1) = C_{tot}(n) - \alpha \Delta t C_{tot}(n) + \alpha_r(\mathbf{x}^{n+1}|d_{50}, r = 1, s), \tag{2.17}$$

where the detoxification rate α is conditioned on the chemical and mosquito species, and the last term comes from Equation 2.7. This equation is similar to Equation 2.13, with the total dosage accumulating during the movement, but detoxifying with time.

The last feature introduced into the extended version is a change in how the delayed mortality is taken into account, which was motivated by the following reasoning. Since insecticidal effect is primarily attributed to the contact of mosquito shell with the surface, some time is needed for chemical to get through the shell and reach the neural system of insect, which in turn depends on physiological characteristics of mosquito, such as sensitivity of target proteins and the thickness of cuticle, (see Yahouódo et al. (2017)). Due to the high exit rates reported in Kitau et al. (2012), it was conjectured that the major insecticidal-induced mortality must have occurred after exiting from the hut. To that end, the model accounts for the poisoning to impact the mortality only after 10 hours in the hut.

As a summary, two case studies are presented here. Firstly, the initial parametrization given in Shcherbacheva et al. (2018) is considered, where only one chemical case is taken into consideration. In that case, two different versions of parametrization were developed, as discussed above. In the next subsection the results are given and explained for both parametrizations. Next, the results obtained with the extended version are presented.

The model developed in this study consists of four basic components, where each of the components features a number of associated attributes, see the summary in the Table 2.1. Additionally, we list the properties that are assigned individually for each of the mosquito-agents and updated within the simulation, see Table 2.2 below.

Table 2.1: Model components

Model component	Attributes	Definition
Host-seeking		
	· CO_2 Concentration	Equation 2.2
	· Time spend indoors	
	· Klinotaxis.	
	· Distance-dependent attraction	Equation 2.5
Motion		
	· Accept/reject stepping	Equation 2.3
	· Excito-repellency	Equation 2.16
Poisoning		
	· Accumulating the chemical dosage	Equation 2.13
	· Detoxification.	Equation 2.17
Death		
	· Natural mortality	Equation 2.11
	· Insecticide-induced mortality	Equation 2.12
	· Delayed mortality	Equation 2.15

Table 2.2: Property list of each agent and relevant model component.

Property index	Property	Model component
1	Spatial position	Motion
2	Inside/Outside the hut	Motion
3	Inside/Outside the net	Motion
4	Trapped	Motion
5	CO_2 concentration	Motion
6	Fed	Host-seeking
7	Time indoors	Host-seeking
8	Klinotaxis.	Host-seeking
9	Dead	Death (Poisoning)
10	Accumulated dosage of chemical	Poisoning

2.4 Numerical simulations

Next, the numerical details of the simulations are given and explained. In the simulation model, the mosquitoes are treated as a number of agents in a two-dimensional rectangular domain $[x_{min}, x_{max}] \times [y_{min}, y_{max}]$, initially located at uniformly selected random spatial sites. For the steps outside of the domain, see the step 11 of the Algorithm 2.1. For any discrete time step n and for every agent, the outline of the location change from the present position $\mathbf{x}^{n-1}$ is specified in the Algorithm 2.1 given below:

Algorithm 2.1 Model algorithm

1. Propose candidate position $\mathbf{x}^n$ by amending the previous position with a stochastic increment, i.e., compute $\mathbf{x}^n$ by Equation 2.1;
2. Account for natural mortality. Generate random number $u \sim U[0,1]$. Remove the agent if $u < \alpha^{\Delta t}$;
3. Account for insecticide-induced mortality. Generate random number $u \sim U[0,1]$. Remove the agent if $u < \alpha_p^{\Delta t}$;
4. Evaluate the concentration of carbon dioxide $C(\mathbf{x}^n)$ at new position $\mathbf{x}^n$ as it was specified in Equation 2.2;
5. Calculate the scaling factor $\sigma_{acc}(\mathbf{x}^n)$ as given by Equation 2.5;
6. Recalculate the scaling factor, taking into account the excito-repellency, conditioned on the accumulated amount of the chemical by Equation 2.16;
7. Compute probability of acceptance by attraction, $\alpha_a(\mathbf{x}^n|\mathbf{x}^{n-1})$ for position $\mathbf{x}^n$ by Equation 2.3;
8. Compute the probability of rejection α_{rej} associated with repellent $\alpha_r(\mathbf{x}^n|d_p, s)$ by Equation 2.7;
9. Generate random number $u \sim U[0,1]$, if $u < min\{1, \alpha_a(1-\alpha_r)\}$, mark position $\mathbf{x}^n$ as preliminarily accepted, otherwise, mark position as rejected and remain at the old position $\mathbf{x}^n = \mathbf{x}^{n-1}$;
10. Account for the barrier imposed by the net. If candidate step $\mathbf{x}^n$ is inside and old position $\mathbf{x}^{n-1}$ is outside of the net, and position $\mathbf{x}^n$ was preliminarily accepted, generate random number u. If $u < 1 - p_{net}$, accept the new position $\mathbf{x}^n$. Otherwise, select the closest point on the net $\mathbf{x}^{net}$ to $\mathbf{x}^{n-1}$ and assign new position $\mathbf{x}^n = \mathbf{x}^{net}$;
11. Account for the walls. If candidate step $\mathbf{x}^n$ is outside and old position $\mathbf{x}^{n-1}$ is inside of the hut and position $\mathbf{x}^n$ was preliminarily accepted, generate random number u. If $u < p_{hut}$, accept the new position $\mathbf{x}^n$. Otherwise, chose closest point on the wall $\mathbf{x}^{wall}$ to $\mathbf{x}^{n-1}$ and assign new position $\mathbf{x}^n = \mathbf{x}^{wall}$;
12. Update the total accumulated dosage of the chemical C_{tot} increasing upon the contact with the net by Equation 2.17;
13. Account for detoxification of the total accumulated dosage of chemical C_{tot} with the rate α;
14. Update the property list of mosquito;
15. Move to step 1, $n \to n+1$

In the above algorithm some of the steps are implemented by the different means in simulations of the basic and the extended model versions. Here, the differences in the formulas included into the algorithm are summarized. Firstly, when computing the death rate, in

the basic model we account for both natural and insecticide-induced mortality at each successive iteration, during the host-seeking period inside of the hut, which is given by the Equation 2.14. In the extended version only the natural death is taken into account during the host-seeking, which results in the probability of death given as $\alpha^{\Delta t}$, which is similar for every iteration of the algorithm. Here $\alpha^{\Delta t}$ is calculated from percentage of the dead mosquitoes per 34 hours, which is given as 10% for most of the mosquito species, as discussed above.

At step 6, when calculating the scaling factor, the short-range attraction is always accounted for, by the Equation 2.5 in all the model versions. Additionally, in the simulations of the extended model, the scaling factor increases with the accumulated dosage of the chemical C_{tot} to imitate the early exit in the presence of LLIN, which is calculated by Equation 2.16. In addition, step 13, where the detoxification is taken into account, is calculated only in the case of the extended model version.

Finally, a delayed action of the insecticide is modelled, which is assumed to impact the mortality only after 10 hours spent in the hut, due to high exit inherent in all the data sets in Kitau et al. (2012). Specifically, after host-seeking process mosquitoes are collected and kept under the glass treated with glucose solution, for the purpose of scoring the delayed mortality, (see Kitau et al. (2012)). Actually, all the model versions can be simulated using the above-stated algorithm. In case of the basic version, the rates of detoxification and excito-repellency are to be set to zero. Note that there is no difference in the formulas involved in Algorithm 2 for the two parametrizations developed in Shcherbacheva et al. (2018). The only difference comes from parameter combinations selected for estimation. More details are explained in Section 2.4.

Multiple parameters introduced into the model are associated with the relevant physical effects. Therefore, fixed values are used for these parameters in all the simulations, see the summary given in Table 2.3 below.

Table 2.3: Fixed parameters.

Parameter symbols	Parameter description	Parameter values	source
μ_s	average flight speed	0.4 m/s	Snow (1980), Spitzen et al. (2013)
σ	standard deviation of the flight speed	0.1 m	Snow (1980) Spitzen et al. (2013)
$3\sigma_a$	distance at which mosquito is able to sense a host	80 m	Gillies and Wilkes (1968)
	size of experimental hut	3 m	WHO (2006)
d_p	width of the net	1.5 m	WHO (2006)
ϵ	minimal distance between mosquito and host treated as an exposure	0.65 m	
t_{max}	maximal host-seeking time in absence of chemicals	5h	Gillies (1957) Kawada et al. (2014)
s	slope of repellent, characterizes spatial spread of repellent	0.015	Killeen et al. (2011)
σ_m	effective range of the poison	<10 cm	Killeen et al. (2011)

Regarding the attraction scaling coefficient, it was found that the values of parameters $\sigma^1_{acc}, \sigma^2_{acc}$ introduced in the function σ_{acc} can be assigned and taken as fixed within the simulations by the following reasoning. At a distance of approximately 80 m, i.e., beyond the CO_2 plume, mosquito exhibits purely random motion, since $C \simeq 0$. However, in the hut-level experiment this distance is never attained. Anyway, the upper limit for σ_{acc} was set to a large enough value to generate Brownian motion outside of the concentration plume. Utilizing Equation 2.5 and accounting for $\sigma^1_{acc} << 1$, we find by the requirement

$$\sigma_{acc}(\mathbf{x}|d(\mathbf{x}, \mathbf{x}^h) = 80) = 0.001 \tag{2.18}$$

that the slope for the attraction scaling coefficient can be specified as $\sigma^2_{acc} = 0.001/80$, where the value 0.001 is originating from the characteristic difference of the concentration values $\Delta C = C(\mathbf{x}^n, \mathbf{x}^h) - C(\mathbf{x}^{n-1}, \mathbf{x}^h)$ at a distance of $80m$ from the host, which was verified by the simulations. When the upper limit is fixed, only the lowest value of the attraction parameter remains for parameter identification, as it can be seen from Equation 2.5. However, it appeared that the data in Kitau et al. (2012) are only capable of giving an identification of the upper bound for σ^1_{acc}. From the range of possible values, the choice $\sigma^1_{acc} = 0.0001$ was taken.
Given the value for σ_{acc} as discussed above, the probability of accepting the steps away from the host decreases from one to almost zero, when the distance $d(\mathbf{x}^n, \mathbf{x}^h)$ reduces from 80 m to zero. Thus, the stepping is characterized by progressive transition from

purely random movement in the absence of the odour plume to directionally biased motion in proximity of the host. Better identification of the attraction parameters is possible by the means of more exhaustive data characterizing the flight of mosquitoes. However, the above-specified selections of parameters are sufficient for calibrating the model against the data from Kitau et al. (2012).

Eventually, certain specifications are to be made on how to handle the movement at the net and inside the net, on the walls of the hut, and at the exit from the hut. In case when the proposal steps falls on the space inside the net and is rejected (with probability p_{net}), the mosquito position is set to the closest site on the net $\mathbf{x}^n$ with respect to the old position $\mathbf{x}^{n-1}$, such that $d(\mathbf{x}^n, \mathbf{x}^h) = d_p$, where d_p is the net width specified in the Table 2.3 above. In the situation when the candidate position is accepted with probability $1 - p_{net}$, the direction of the LLIN repulsion is inverted to imitate the spread of the chemical close to the surface and insecticide-free space in the closeness to the human. In a similar way, if the proposed step receives the position outside of the hut, the acceptance occurs with probability p_{hut}, which is interpreted as mosquito entering one of the window traps. The list of properties associated with the trapped mosquitoes is not further modified, except their mortality status. In the case of rejection of the proposal step, mosquito is imitated to land on the wall. In this case the new location $\mathbf{x}^n$ is taken as the closest site on the wall to the old position $\mathbf{x}^{n-1}$. The size of the experimental hut is specified in Table 2.3 above.

In the algorithm, only the steps that influence the movement during the host-seeking were described. Additionally, the properties related to exit, feeding, mortality and host-seeking status (i.e., directional movement or purely random walk) are tracked and recorded individually for each agent. After mosquito is marked as dead, its attributes remain constant, but for trapped mosquito the mortality chance is taken into account at each step.

The feeding status of mosquito is set to fed if its new position is closer than ϵ to the centre point of the host, see Table 2.3 below. If mosquito is scored as fed, or if its time of host-seeking inside of the hut exceeds t_{max}, the mosquito starts to exhibit a pure random walk (or kinesis), so the probability of acceptance for new candidate positions by Equation 2.3 is always one. This means that at every successive step the proposed position is accepted, except in the situation when mosquito is hedged by the net or wall or affected by the presence of repellent.

The steps of the Algorithm 2 are iterated for the time period of one night, which is 10hrs. After that, the delayed mortality is accounted for, as it was explained before. As a result, each run of the algorithm is conducted for a 34-hour hut experiment. The simulation results are dependent on random numbers, so the outcome of each experiment is stochastic. To ensure statistical accuracy needed for calibration of model parameters, we take the averaged model outputs, which is attained by multiple simulations, using a sufficiently large swarm of mosquitoes in each case. It should also be noted, that the data from Kitau et al. (2012) are given in percentages. For this reason, the absolute number of mosquitoes does influence the results.

Multiple repetitions of the experiment for a swarm of mosquitoes are substantially CPU demanding. Additionally, for extensive sampling of parameters, which is needed to study the identifiability conditioned on existing data, comprehensive computational methods are to be applied. To reduce the CPU time, the computations were conducted by the means

of combining the parallel implementation for the CUDA tool-chain with MATLAB programming. By design, the algorithm can be executed independently for every mosquito, which implies that the parallel computations are highly appropriate for the purposes of this study. It was found that the optimal combination of the size of the swarm and the number of repetitions which results in the minimal computational time alongside the sufficiently small variation of the outputs is attained for 6 repeated simulations carried out with a swarm of 600 mosquitoes. Naturally, an optimal combination depends on available computing capacity. Hence, the two-dimensional grid with respect to repetitions and the members of the swarm is specified for the GPU runs, where every thread is executing the above-described algorithm independently. It should also be noted that in the case of the LLINs the cost function is evaluated twice, which is separately for *An. gambiae* and *An. arabiensis*. The evaluation of the cost function conducted with CUDA implementation takes 2s, whereas the MATLAB counterpart is executed for 50s. This comparison was conducted for a CPU core-i7 2500K and GPU GetForce GTX TITAN.

2.5 Model calibration for ABM

2.5.1 Review of available methods

Agent-models are intensively adopted to examine questions of real-world mechanisms and phenomena. Due to this, calibration of model parameters to available data sets and patterns is frequently required. Additionally, a sensitivity analysis is essential for studying the behaviour of the model responses with respect to the input parameters, which facilitates the knowledge of relative importance of various mechanisms incorporated into the model structure. However, most of the recent agent-based simulation studies omit the questions of quantitative analysis, which is due to the emphasis placed mostly on representation and demonstration, rather then on getting actual calibration to the real system, (see Thiele et al. (2014)).
Usually, a range of plausible values are known for each of the parameters, which comes from some real-world constraints or available experimental data, e.g., obtained by checking variations in the repeated measurements. When adjusting the model to data sets, the initial guess for parameters are often retrieved manually, by trial and error. However, when the model is carefully elaborated, systematic model runs with varying parameter values are needed, for carrying out quantitative analysis of the relation between model response and the inputs, (see Thiele et al. (2014)).
Parametrization, i.e., finding an appropriate values of parameters, is often cumbersome due to lack of experimental data, their excessive uncertainty and large number of unknown parameters. In these situations, parameter identification or calibration techniques can be applied to retrieve suitable parameter values by employing optimization methods together with the inverse modelling techniques, also known as pattern-oriented parametrization/modelling (POM; Grimm et al. (2005)) or Monte Carlo Filtering, where patterns are utilized as criteria for distinguishing reasonable selections of parameter values (Grimm et al. (2005)). The main objective is identifying parameters that enable the model to generate patterns matching with the observations in a reasonable way. Next, we briefly recall

several widely-adopted notions and approaches related to model calibration, including the one that is put into practice within this project.

Fitting criteria. Fitting criteria can be aggregated into one measure, which determines the difference between model output and observed values. This is known as the best-fit strategy. Another approach is categorical calibration, when criteria are taken from different spatial and temporal scales of the model, i.e., *multi-criterion approach*, where each criterion is considered separately, and further all criteria are combined by Pareto optimization, (see Zitzler et al. (2000)). This technique is much less straightforward in implementation in comparison to cost-function approach, which is applied in the present project.

Design of Experiments (DoE). In DoE methodology, the independent variables are referred to as 'factors', and the dependent are termed as 'responses', (Box et al. (1978)). In the case of full factorial design all the possible factor combinations are explored. This type of study can be used for exploring small number of parameters, when the number of combinations can be kept small enough. Otherwise, *partial factorial design* can be applied instead, where only a subset of parameter combinations are chosen for examination, (see Box et al. (1978)).
Similar technique is offered by Latin hypercube sampling (LHS). This method is based on the *Latin square design*, which contains a single sample in each row and column of the hypercube partitioning, and was introduced by McKay et al. (1979). This sampling technique requires sub-division of the parameter space, i.e., a space constrained by the known ranges of parameters, into a number of sub-spaces of equal size, (see Marino et al. (2008)). The number of partitions N should be at least $k + 1$, where k is the number of the varied parameters, but usually much larger to ensure accuracy. After separating the sub-spaces, a random point is selected from each of the partitions. LHS is typically used to save computer processing time when running Monte Carlo simulations, (see Blower and Dowlatabadi (1994), Olsson et al. (2003)).

Other techniques. In many cases, when classical methods of model calibration are inapplicable, modellers adopt extended counterparts that are specifically tuned for handling stochastic models, (see Thiele et al. (2014)). In particular, many novel approaches originating from computer science provide advanced but often heuristic solutions for ABM calibration; machine learning (Lamperti et al. (2018)), evolutionary algorithms, kriging estimation (Conti and OHagan (2010), Rasmussen (2006)), indirect inference (e.g., Method of Simulated Moments, or MSM) (Franke (2009)) and Simulated Maximum Likelihood (Kukacka and Barunik (2017), Fievet and Sornette (2018)) methods can be exemplified, among the others.
Markov Chain Monte Carlo sampling. However, the statistical Bayesian approach was found applicable for the purposes of the present project. This approach is especially preferable, since instead of generating a single 'optimal' solution to parametrization, the Markov chain Monte Carlo (MCMC) sampling enables to approximate the parameter posterior distribution. This is important for quantifying the reliability of the resulting ABM for subsequent simulation tasks.

The main concept is to sample the candidate parameter selection from a preliminary specified proposal distribution, and then either accept or reject it, depending on the quality of the corresponding fit of the outputs to the data. The fundamental technique is given by the Metropolis algorithm, (see Metropolis et al. (1953)).
In this study the *Delayed rejection adaptive Metropolis algorithm* is employed, which was introduced in Haario et al. (2006). This method was chosen for its advanced ability to efficiently explore high-dimensional parameter space by adapting the proposal distribution from history of the sampler and through the two-stage sampling procedure. However, the number of parameters in the present model is not essentially large. In the next subsection we explain the design of the cost function and criteria used for comparing model outputs with experimental data from Kitau et al. (2012).

2.5.2 Data and the Likelihood function

The results of the hut experiments given in the data sets from Kitau et al. (2012) consist of the percentages of exited, blood-fed and dead mosquitoes. The replicated experiments were conducted separately for *An. gambiae* and *An. arabiensis*. In each case, the outcomes were averaged over six repetitions to reduce the uncertainty attributed to the differences in individual attractiveness of humans to female mosquitoes. The data and the 95% confidence intervals are shown in Table 2.9, see Figure 2.5 for graphical representation of the data sets.
In the present work, the simulated and the experimental data are compared on the bases of the sum of squares cost function, see Equation 2.19 below. Due to repeated measurements, the likelihood is assumed to be Gaussian in the absence of more detailed knowledge of the underlying distribution of the noise. Since no prior estimate of the parameter distributions was available, the uniform prior was chosen for sampling in all the cases considered in the present study. The approximation of the posterior distribution of parameters is obtained as a result of sampling the likelihood. In this regard, it can be questioned how accurately different model parameters can be identified by the means of the likelihood. No preliminary estimates are available to select an appropriate proposal distribution, but the adaptation procedure updated the proposal after each 100 iterations. It should be noted, that the sampled parameters of the posterior distribution represent the model evaluations that produce values within the noise level of the data given in the Table 2.9.
When calibrating the model, the fit with the data was evaluated via the cost function, which is a sum of squared residuals of the model outputs $\hat{Y}_i$ and the measurements, Y_i, also accounting for the measurement error variance. Thus, we have

$$\mathbb{S}_{sum} = \sum_{i=1}^{N_r} \frac{(Y_i - \hat{Y}_i)^2}{\sigma_i^2}. \tag{2.19}$$

Here N_r gives the number of measured responses over which the sum of squares is computed. This number is specified separately for the control and treated net cases in the next section. The measurement error variance σ_i is calculated separately for each of the

responses and each of the four chemicals considered in the present study, based on the confidence intervals reported in Table 2.9, assuming normally distributed data. This was done to achieve an agreement of the simulation results with the confidence intervals.
Note that these data are relative, giving the percentages of dead, fed and exited mosquitoes. Hence, simulated model outputs are independent on selections of repetitions and swarm size. However, since the model is stochastic, all the results need to be averaged over multiple repetitions. As noted above, the combination of 6 repetitions and the size of the swarm comprising 600 mosquitoes results in a reasonably small variance given the minimal CPU time. The total wall-clock time for evaluation of the cost-function, using parallel GPU calculations, was approximately 2 seconds as performed on a CPU core-i7 2500K, GPU GetForce GTX TITAN, as compared to 50 seconds when the run is conducted in MATLAB environment given same CPU core.

2.5.3 ABM parameter identification, control case

In the control case, the experimental hut trials are modelled with an untreated net. It is also assumed that *An. gambiae* and *An. arabiensis* feature similar host-seeking traits in the absence of the insecticide-impregnated net. However, in reality opportunistic *An. arabiensis* can blood-feed on the other animals, and hence display lower feeding rate as compared to anthropophilic *An. gambiae* that specializes solely on humans. But in the hut experiment there is no alternative source of blood. Hence, for simplicity, the similar contact rates are assumed. Therefore, same parameters are appropriate for both species in the absence of insecticide. Here, the maximum time that mosquito can spend at once in futile attempts to feed on the protected human host was fixed to $5h$, in the absence of any ingredients that alter the behaviour of mosquitoes. Note that the minimal value for the attraction parameter σ^1_{acc} is set to a fixed value by the argument explained in the previous chapter. Initially, the slope for the attraction scaling coefficient σ^2_{acc} was sampled together with the two above-mentioned parameters, but the available data do not allow unambiguous identification of this factor. Hence, it was fixed to a reasonable value, as discussed Section 2.4.
In this case two parameters are remaining for identification: probability of exiting the hut p_{hut} (as a hedged space) and probability of being blocked from feeding by the net p_{net}. These parameters are fitted against two responses ($N_r = 2$) available from the data sets in Kitau et al. (2012), specifically, the exophily and feeding percentages for the expression in Equation 2.19.

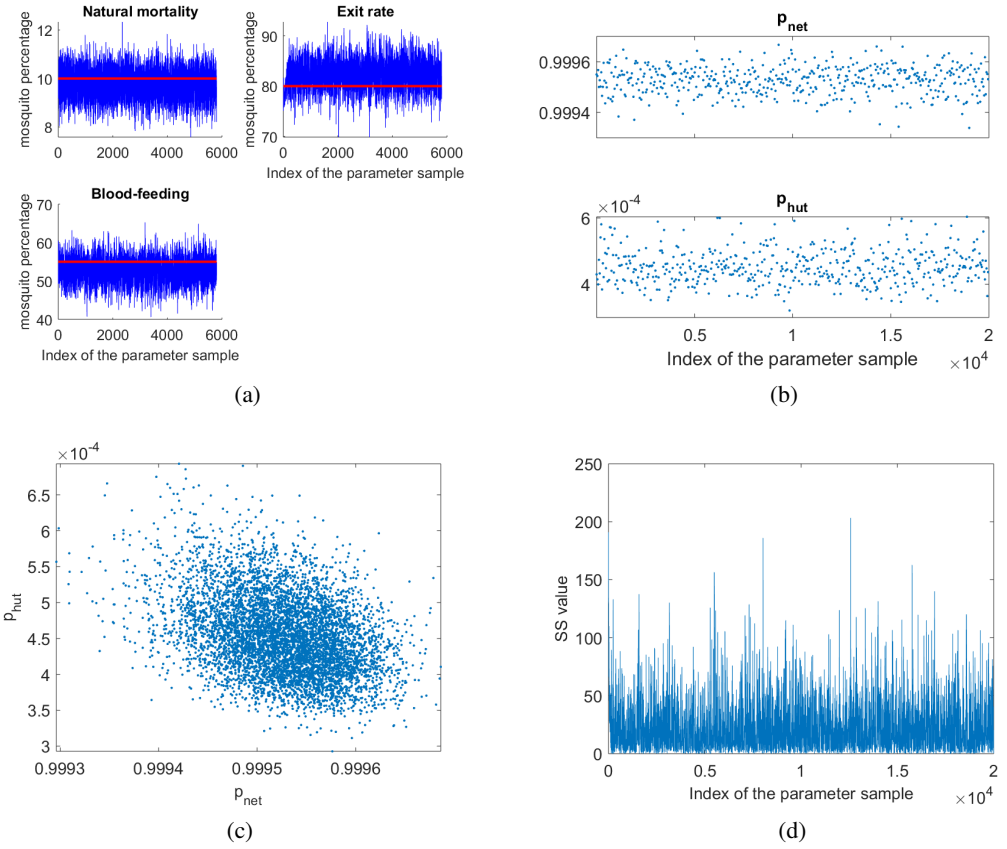

Figure 2.6: Parameter estimation results for the control case. (a) Model outputs obtained using the posterior distributions of parameters p_{net}, p_{hut} (blue trace lines) versus the mean values reported in Kitau et al. (2012) (red solid lines). (b) Parameter chains for probabilities of penetrating through the net p_{net} and exiting the hut p_{hut}. (c) Pairwise distribution of parameters p_{net} and p_{hut}. (d) Sum of squared residuals of the model outputs and the corresponding observations for each of the sampled parameter combinations calculated by Equation 2.19.

Table 2.4: Model parameters for control case and initial guess for the sampler.

Parameter symbols	Parameter description	Parameter value
p_{net}	probability of being blocked by physical barrier created by net	0.99967
p_{hut}	probability of exiting the hut	$5.9 \cdot 10^{-4}$

As a summary, the results of the parameter estimation by the MCMC method are displayed in Figure 2.6. The plots illustrate the sampled combinations of model parameters that generate the respective fits. Specifically, the sampled chains are presented separately for each of the parameters (summarized in Table 2.4), together with the joint 2D distribution and the sum of squared residuals (calculated by Equation 2.19). It can be seen from the estimation results, that the simulated fits of the model outputs, obtained using the posterior distributions of parameters, against the experimental data reported in Kitau et al. (2012) are indeed good. Moreover, the limits of the simulated model outputs match with the data sets for the control case given in Kitau et al. (2012). From the parameter chain plots it can be concluded that both of the parameters are well identified. According to the 2D plot, no significant correlation was revealed between the parameters.

2.5.4 ABM parameter identification, LLIN case

As discussed above, basic model version introduced in Shcherbacheva et al. (2018) is sufficient for fitting the case of the IconMaxx chemical. Firstly, the calibration of the model is presented for two slightly different parametrizations. Next, the data for the IconMaxx are fitted using the extended version of the model. Although the IconMaxx case is better fitted with the basic version, the other data sets from Kitau et al. (2012) inherit the patterns that impede the calibration of this model modification, as it was explained above. Hence, for the other chemicals the extended model is calibrated, with additional features included into the modelling approach. Given the extended version, the data sets for Alphacypermethrin, Carbosulphan and Deltamethrin insecticidal treatments are considered and calibrated. In these cases the model produces fair fits to the data.

Calibration of the basic model. As it was previously discussed in the Subsection (2.2.3), the difference in behavioural traits of the two mosquito species is noticeable only in the presence of the insecticide-impregnated nets. As it was mentioned above, several conjectures for modelling the difference were proposed in the literature. In all the simulations we assume that mosquito abandons host-seeking after spending the maximal t_{max} in the hut. After that, it starts exhibiting a pure random walk, without responding to the stimuli created by the presence of the CO_2 concentration. As a straightforward approach, we initially calibrated the model version, where only the maximal host seeking time t^A_{max} of *An. arabiensis* was identified together with the other parameters that stand for the impact of the LLINs, d_{50}, s, μ_p, simultaneously keeping t^G_{max} of *An. gambiae* fixed to the same value as it was set in the control case. However, this version did not result in a reasonable fit to the experimental data.

Next, two slightly more complex versions were proposed. Considering the first version

of the model, referred to as Version 1 below, the difference in host-seeking traits of the species is captured by calibrating the maximal host-seeking time t_{max}^{LLIN} in the presence of the insecticide separately for *An. gambiae* and *An. arabiensis*. In this case, the scaling coefficient σ_{acc} governing the attraction to the host remains the same as in the control case, similar for the two species. Additionally, the insecticide-induced mortality due to the LLINs is calibrated, also using the same rate coefficient for both of the mosquito species. In the second version of the model, further denoted as Version 2, the maximal host-seeking time when confronted with the LLIN is calibrated but assumed to be the same for both mosquitoes. Here, the difference in host-seeking behaviour is introduced by the means of the attraction scaling parameter $\sigma_{acc}^{1,A}$, which is identified *An. arabiensis* and was found to be larger as compared to the control case. This estimation was conducted to capture a reduced persistence of the host-seeking attempts of *An. arabiensis* in the presence of the insecticidal treatment, as conjectured in the literature, (see, e.g., Reddy et al. (2011)).
Note that parameters for penetrating through the net and exiting the hut are assumed to be the same as in the control case, and are fixed to the values given in the Table 2.2 above. Herewith, for the effect of repellent the function expressed by Equation 2.7 was employed. Here, the parameter d_{50} denotes the distance from the host where the concentration of the insecticide attains 50% of its total.
The outputs of the simulations are compared with the corresponding data reported in Kitau et al. (2012). Specifically, in this case there are six measured responses ($N_r = 6$ available for Equation 2.19): exit percentage, percentage of mosquitoes subject to the insecticide-induced mortality and percentage of fed mosquitoes, all separately for *An. gambiae* and *An. arabiensis*.
The summary of estimated parameters are given in Table 2.6 and Table 2.7, including the mean values of the sampled Monte Carlo chains. The model outputs against the corresponding data from the hut experiment for IconMaxx LN provided in Kitau et al. (2012) are plotted in Figures 2.7 and 2.9. Although the fits are not perfect, the simulated outputs match within the uncertainty bounds of the observed quantities. In addition, Table 2.5 below illustrates that both model versions are sufficient for fitting the data within the confidence bounds.
Next, the sampled parameter distributions that resulted in the above fits of the model to the experimental data are considered. Similar to the control case, both sampled values of the individual parameters and the pairwise distributions are visualized. As it was mentioned previously, the chemical treatment considered in this case (IconMaxx LN) has a short spatial range of action (approximately, 10cm), which is practically reflected in the value of the parameters s which stands for the spatial spread of the chemical. This value is kept fixed in all the subsequent simulations The separate MCMC chains for the rest of the parameters, i.e., $d_{50}, r, \mu_p, t_{max}^A, t_{max}^G$ for Version 1 are given in Figure 2.8. As it can be seen from this plot, although all the parameters are clearly bounded from above and below, large variations are still observed in the chains. Note that the adaptation procedure clearly improves the mixing, as indicated by the chain plots of parameter d_{50} in Figures 2.8 and 2.10. The information of the parameter correlations is available from the pairwise scatter plots displayed in the Figures 2.8 and 2.10. Specifically, the pairwise plot of the parameter values for t_{max}^A and t_{max}^G indicates a strong correlation between these two

factors; the host-seeking time of *An. gambiae* was estimated to be substantially longer, approximately twice larger as compared to that of *An. arabiensis*. Additionally, for both mosquito species the estimated host-seeking time is lower than that employed for the control case, which comprised 5 hours. It can be concluded, that although the data do not enable unambiguous estimation of parameters, they are sufficient for detecting some natural correlations between them.
The corresponding summaries for the for the Version 2 are presented in Figure 2.10. Similar to the Version 1, it can be seen, that while the values of parameters feature the upper and the lower limits, the correlations between the values still persist, together with relatively large variations for some of the parameters.
Overall, it can be concluded that the experimental data for IconMaxx employed for calibration in the present study are only sufficient to partly constrain the model parameters; substantially various values for the maximal host-seeking times and host-seeking persistence in the presence of the LLINs produce the outputs reasonably matching with the data set for IconMaxx taken from Kitau et al. (2012), i.e., fitting within the reported confidence limits. However, the global effect of the LLINs, different for *An. gambiae* and *An. arabiensis* can be naturally evaluated using the model, which is discussed in the next subsection.

Table 2.5: Model outputs for Versions 1 and 2 (denoted by **V1** and **V2**, respectively) versus reported in Kitau et al. (2012) field observations. LLIN is treated with long-lasting treatment kit (IconMaxx LN): insecticide-induced mortality, exophily and blood-feeding measured in percentages. Herewith, 95% confidence intervals are given in curly brackets.

	An. gambiae			***An. arabiensis***		
Source	**V1**	**V2**	**Kitau et al. (2012)**	**V1**	**V2**	**Kitau et al. (2012)**
Mortality	72	72	74 (59-89)	46	48	45 (37-51)
Exophily	77	77	79 (62-89)	88	82	87 (77-92)
Blood-feeding	10	10	9 (2-34)	7	5	7 (2-21)

Table 2.6: Model parameters and mean values of the MCMC sampled parameter chains (for Version 1), where the LLIN is treated with long-lasting treatment kit (IconMaxx LN).

Parameter symbols	Parameter description	Sampled mean
d_{50}	range of repellent coverage	0.755
μ_p	insecticide-induced death rate	$4.4 \cdot 10^{-8}$
r	intensity of repulsion	0.88
t^A_{max}	maximum host-seeking time for *An. arabiensis*	1.2 h
t^G_{max}	maximum host-seeking time for *An. gambiae*	4.0 h

Table 2.7: Model parameters and mean values of the MCMC sampled parameter chains (for Version 2), where the LLIN is treated with long-lasting treatment kits (IconMaxx LN).

Parameter symbols	Parameter description	Sampled mean
d_{50}	range of repellent coverage	0.755
μ_p	insecticide-induced death rate	$4.4 \cdot 10^{-8}$
r	intensity of repulsion	0.88
t^{LLIN}_{max}	maximum host-seeking time for both species	4.0 h
$\sigma^{1,A}_{acc}$	minimal value for the scaling factor (for *An. arabiensis*)	$7 \cdot 10^{-4}$

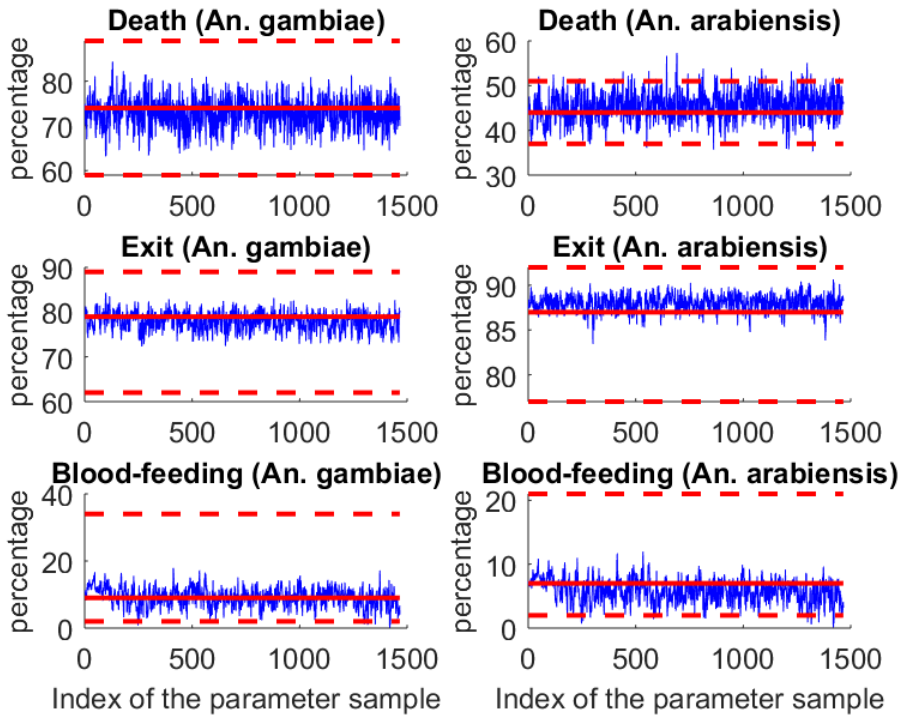

Figure 2.7: Results of the MCMC parameter estimation (Version 1), where LLIN is impregnated with the long-lasting treatment kit (IconMaxx LN). Model outputs obtained using the posterior distributions of parameters (blue trace lines) versus experimental data reported in Kitau et al. (2012) (mean values (red solid lines) and 95% confidence intervals (red dashed lines)).

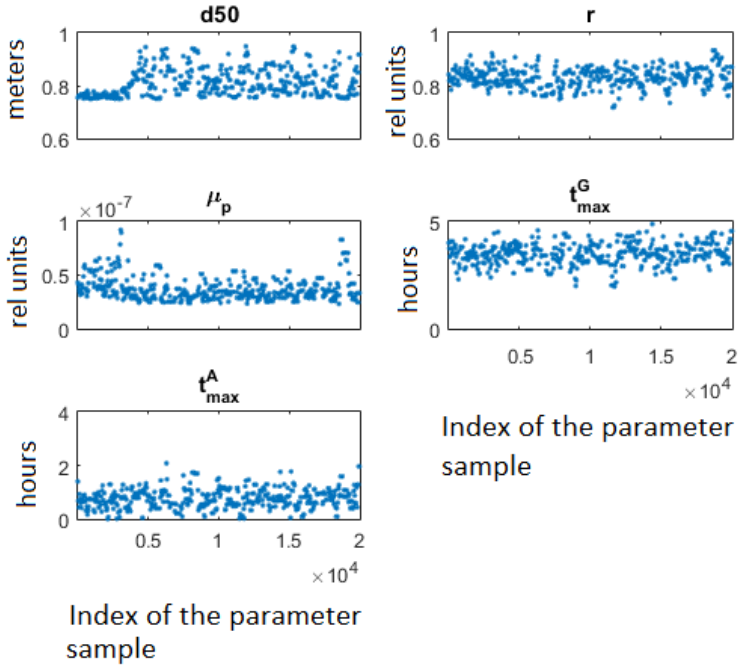

(a)

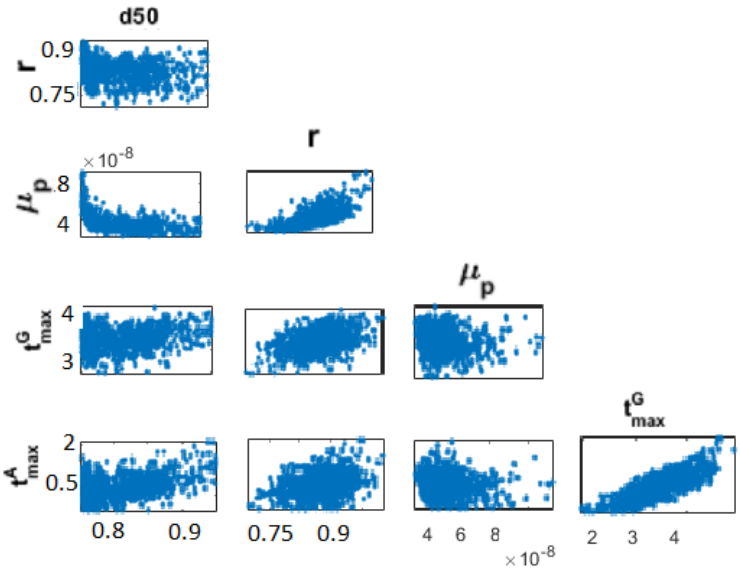

(b)

Figure 2.8: Results of the MCMC parameter estimation (Version 1), where LLIN is impregnated with the long-lasting treatment kit (IconMaxx LN). (a) Parameter chains and (c) pairwise distributions of model parameters summarized in Table 2.6.

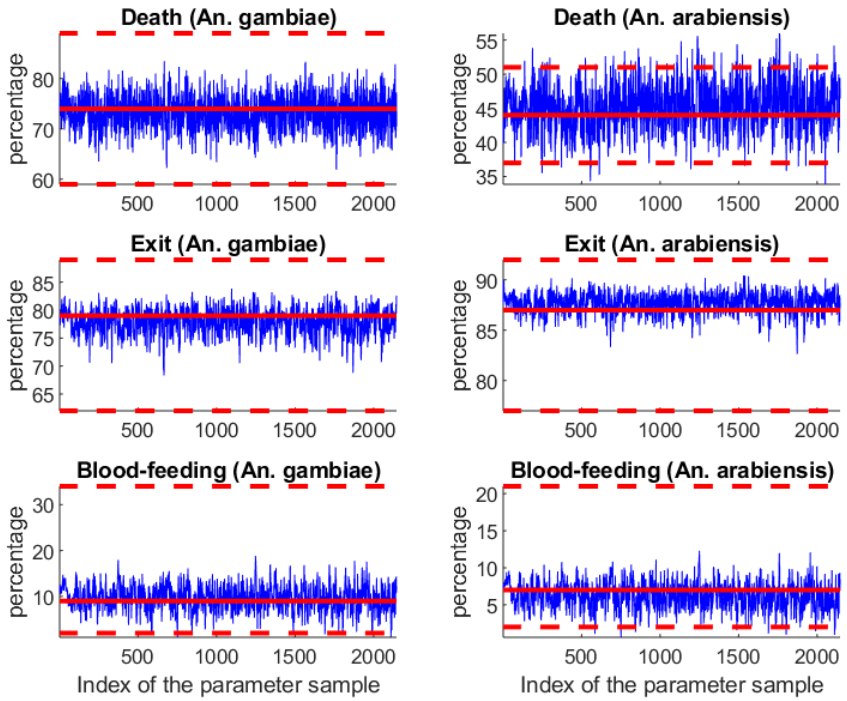

Figure 2.9: Results of the MCMC parameter estimation (Version 2), where LLIN is impregnated with the long-lasting treatment kit (IconMaxx LN). Model outputs obtained using the posterior distributions of parameters (blue trace lines) versus experimental data reported in Kitau et al. (2012) (mean values (red solid lines) and 95% confidence intervals (red dashed lines)).

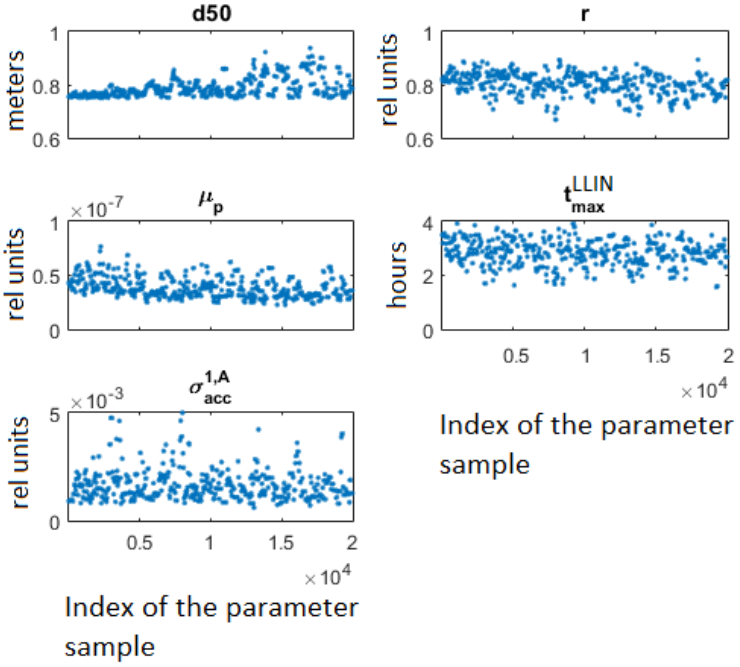

(a)

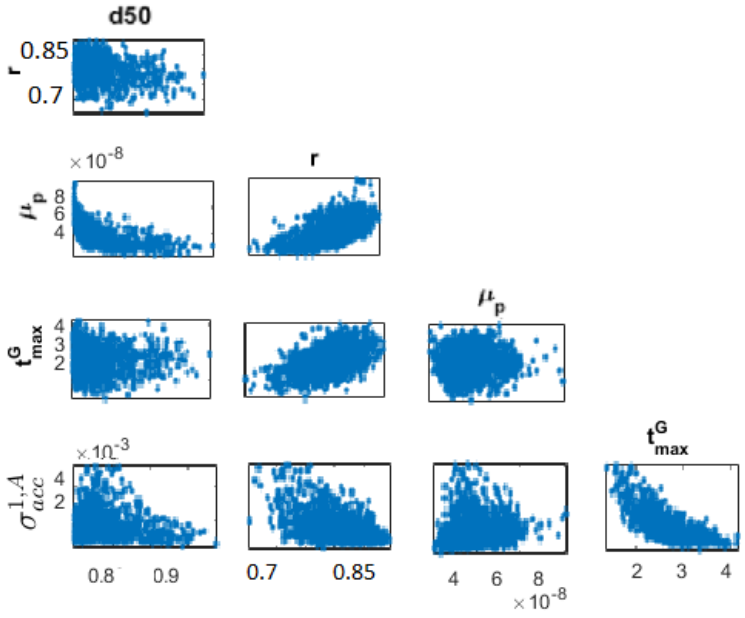

(b)

Figure 2.10: Results of the MCMC parameter estimation (Version 2), where LLIN is impregnated with the long-lasting treatment kit (IconMaxx LN). (a) Parameter chains and (c) pairwise distributions of model parameters summarized in Table 2.7.

Calibration of the extended model. Here we provide the results for calibration of the extended version of the model. As revealed by the field trials carried out with the LLINs impregnated with different chemicals in Kitau et al. (2012), the mortality attributed to *An. gambiae* is systematically and significantly higher as compared to that of *An. arabiensis*, alongside the exit rate which in majority of the data sets is lower for *An. arabiensis* than that for *An. gambiae*. Simultaneously, the experimental data indicated consistently higher feeding rates for *An. arabiensis* as compared to *An. gambiae*, with the exception for the IconMaxx LN situation.

Although several parametrizations have been attempted in Shcherbacheva et al. (2018) to reproduce the scenario attributed to the data sets for LLINs taken from Kitau et al. (2012), it appeared that the model fits the data in a reasonable way only for the IconMaxx insecticide data. Thus, the basic model is extended discussed above, such that good fits can be attained for the other data sets from Kitau et al. (2012).

As it was previously mentioned, the fact that *An. arabiensis* features higher (or similar) feeding rate than that of the *An. gambiae* and the substantially lower insecticide-induced mortality rate, contravenes with the principle adopted for the basic model version. This is due to to the fact that both the probability of death and that of successful feeding is proportional to the number of net contacts, so it is not plausible that mosquito could simultaneously feature excessive feeding rate and reduced mortality rate, unless some additional effects of the chemicals are taking place.

A number of probable explanations can be proposed for the mechanisms underlying the pattern inherent in the data sets. A simple reason could be that the rate of poisoning is different for these two species, such that *An. arabiensis* is suspected to feature higher *insecticide resistance*, and a bigger dosage of the chemical is need for killing this mosquito, as compared to *An. gambiae*. However, the bioassays in Kitau et al. (2012) state that a similar dosage resulted in the lethal outcomes for both *An. gambiae* and *An. arabiensis*. Here, mosquitoes are not assumed to consume the lethal dosage upon a single contact with the net, but they receive a sub-lethal dosage instead. For the difference in insecticidal poisoning, we postulate that the dosage of chemical which was consumed by mosquito gets detoxified with time at some rates, which are different for these two species, (see Brooks (1985)). Here we include two parameters that stand for the rates of detoxification in *An. gambiae* and *An. arabiensis*, respectively.

Thus, five parameters are fitted, $r, \alpha_G, \alpha_A, \mu_e^G, \mu_e^A$ explained in Table 2.8, in consideration of six measured responses: exophily, blood-feeding and insecticide-induced mortality; all of which are given separately for *An. gambiae* and *An. arabiensis*. The model is calibrated separately to Alphacypermethrin, Carbosulphan and Deltamethrin insecticidal treatments, using data sets from Kitau et al. (2012). Table 2.8 presents the parameters selected for the MCMC calibration. However, some of the parameters were not well-identified. In these cases the corresponding values were fixed, while calibrating the rest of the parameters. In Table 2.8, fixed and estimated parameters are indicated for all the chemical cases. Additionally, the chemically enhanced mortality rate coefficient μ_p displayed poor identification and was fixed ($\mu_p = 0.0005$) in all the parameter estimations conducted for the extended version. The parameter identification results are presented in Figures 2.11 to 2.13 for the Deltamethrin, Figures 2.14 to 2.16 for the Carbosulphan and

Figures 2.17 to 2.19 for the Alphacypermethrin cases, respectively. For the IconMaxx the basic parametrization is found to be sufficient, and the results displayed in Figures 2.7 to 2.10 are taken for comparison with the other chemical treatments considered here. Also, the average model outputs calculated with the posterior distributions of parameters together with the corresponding experimental data are presented in Table 2.9 for An. gambiae and An. arabiensis, and each of the chemicals, respectively.

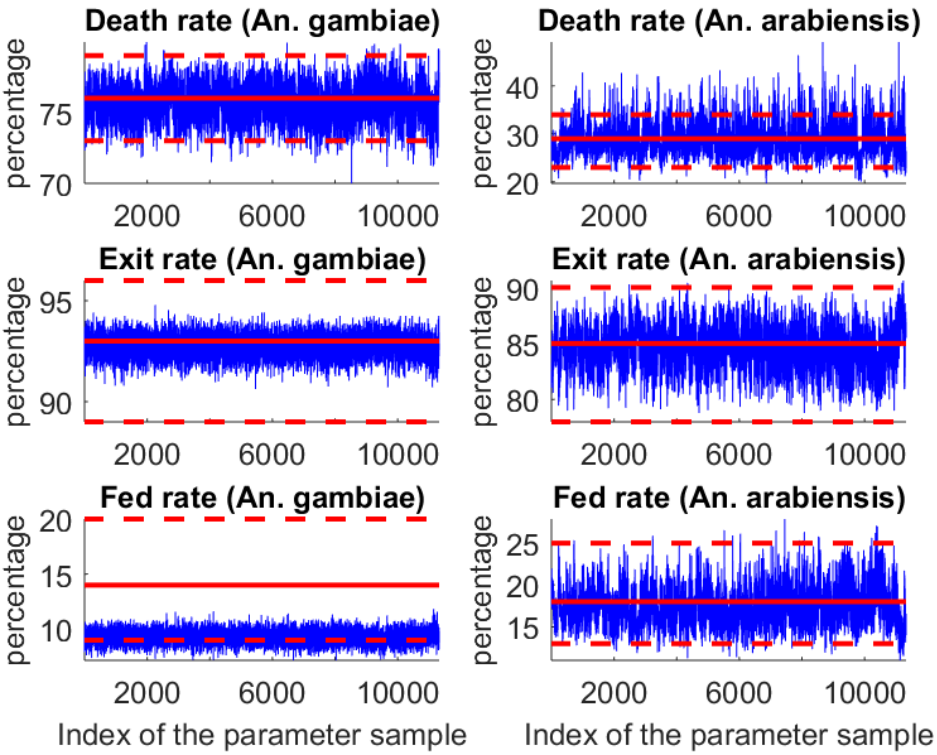

Figure 2.11: Results of the MCMC parameter estimation, where LLIN is impregnated with the long-lasting treatment kit (Deltamethrin). Model outputs obtained using the posterior distributions of parameters (blue trace lines) versus experimental data reported in Kitau et al. (2012) (mean values (red solid lines) and 95% confidence intervals (red dashed lines)).

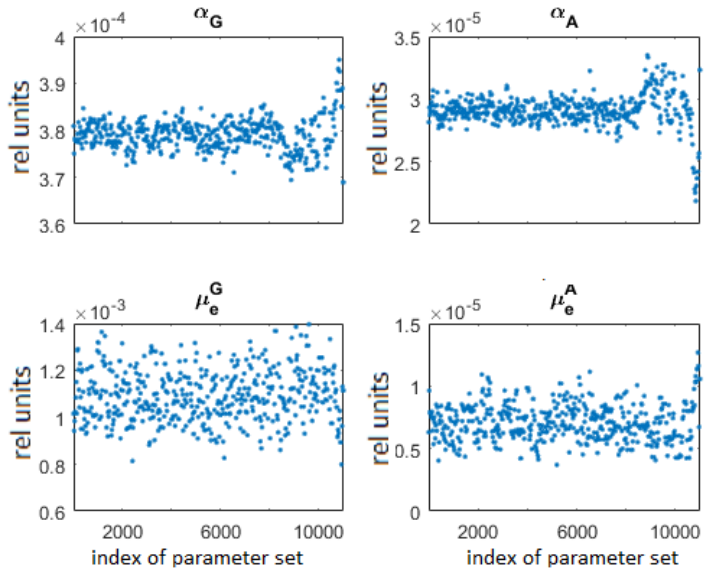

(a)

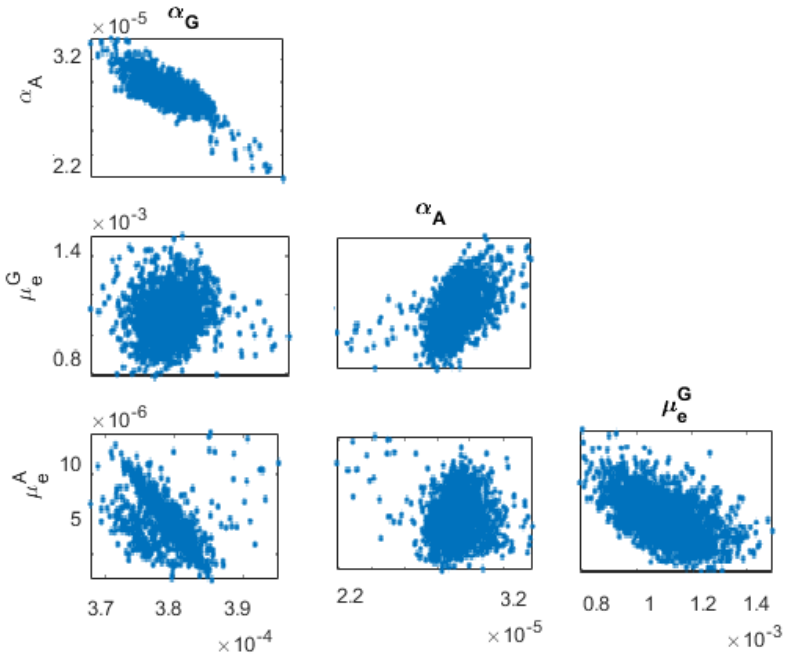

(b)

Figure 2.12: Results of the MCMC parameter estimation, where LLIN is impregnated with the long-lasting treatment kit (Deltamethrin). (a) Parameter chains and (b) pairwise distributions of model parameters summarized in Table 2.8.

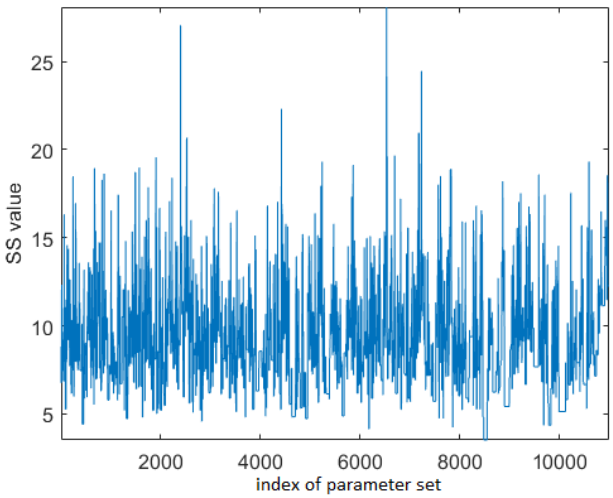

Figure 2.13: Results of the MCMC parameter estimation, where LLIN is impregnated with the long-lasting treatment kit (Deltamethrin). Sum of squared residuals for each of the sampled parameter combinations calculated by Equation 2.19.

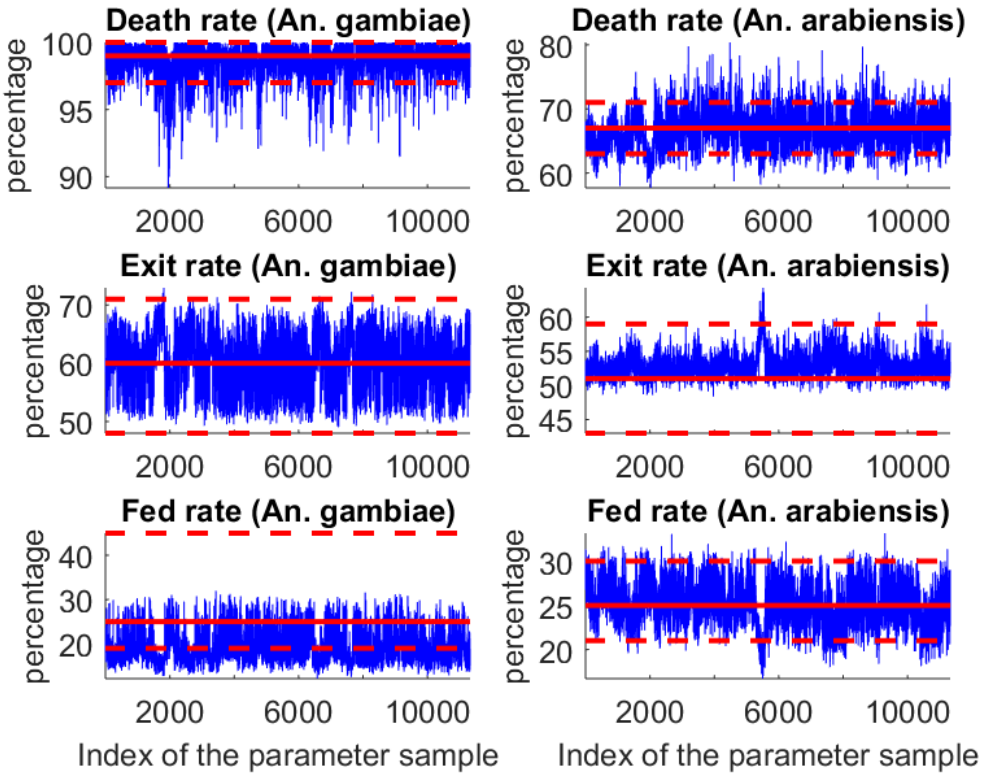

Figure 2.14: Results of the MCMC parameter estimation, where LLIN is impregnated with the long-lasting treatment kit (Carbosulphan). Model outputs obtained using the posterior distributions of parameters (blue trace lines) versus experimental data reported in Kitau et al. (2012) (mean values (red solid lines) and 95% confidence intervals (red dashed lines)).

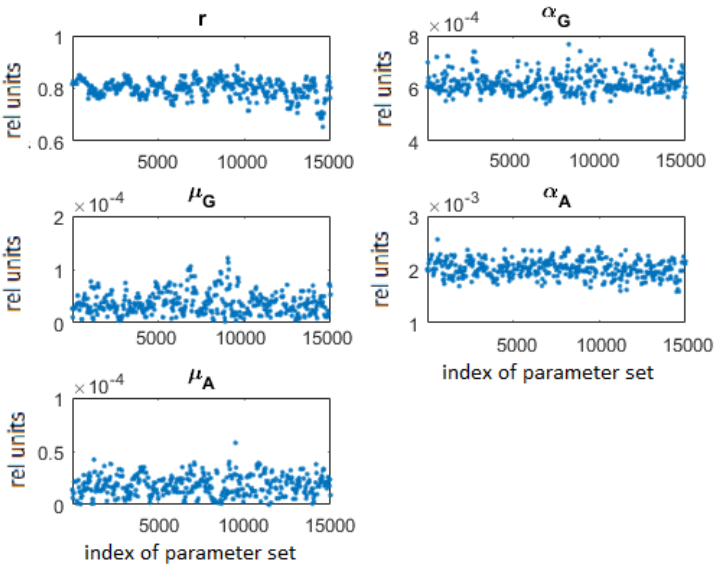

(a)

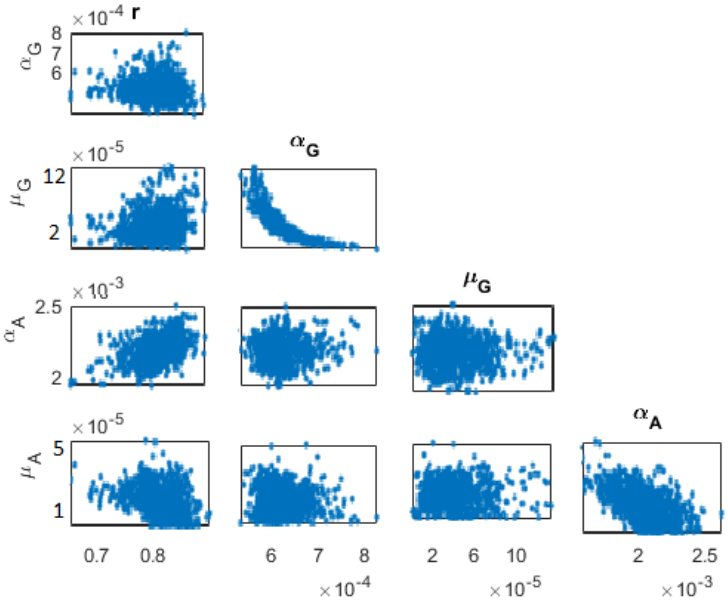

(b)

Figure 2.15: Results of the MCMC parameter estimation, where LLIN is impregnated with the long-lasting treatment kit (Carbosulphan). (a) Parameter chains and (b) pairwise distributions of model parameters summarized in Table 2.8.

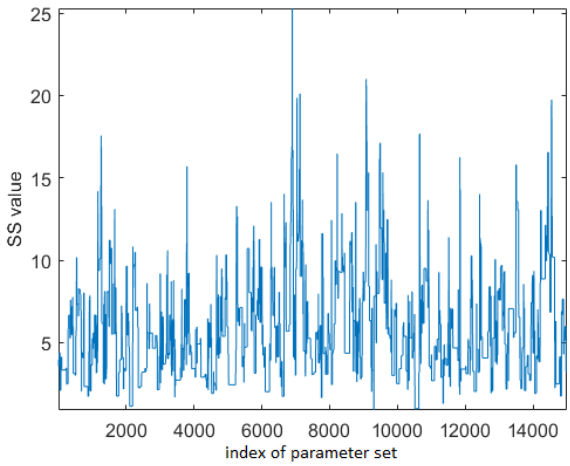

Figure 2.16: Results of the MCMC parameter estimation, where LLIN is impregnated with the long-lasting treatment kit (Carbosulphan). Sum of squared residuals for each of the sampled parameter combinations calculated by Equation 2.19.

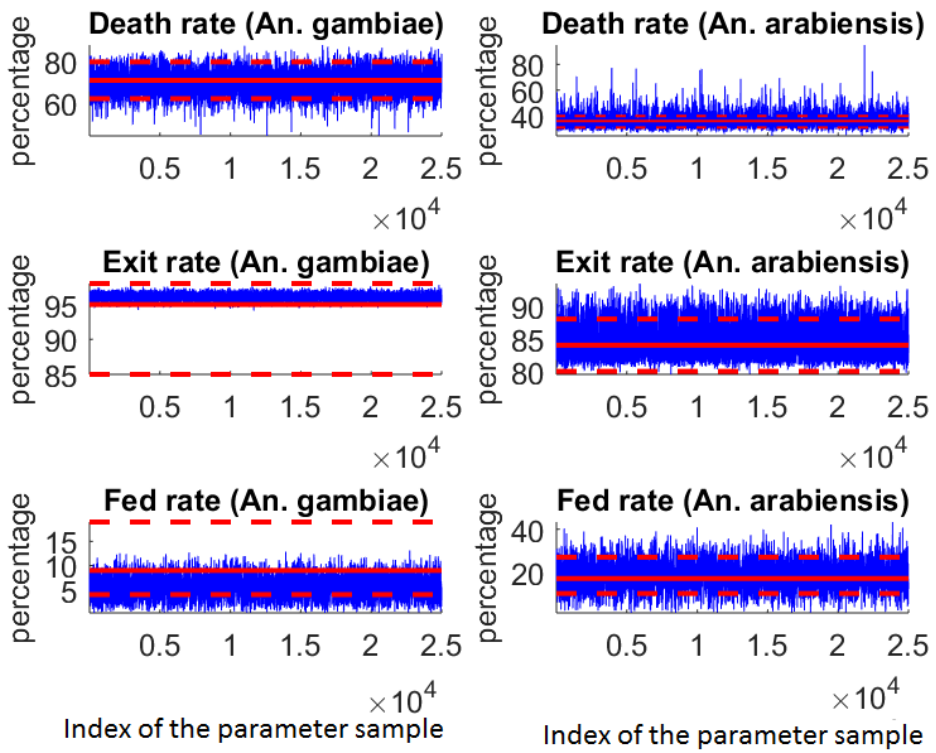

Figure 2.17: Results of the MCMC parameter estimation, where LLIN is impregnated with the long-lasting treatment kit (Alphacypermethrin). Model outputs obtained using the posterior distributions of parameters (blue trace lines) versus experimental data reported in Kitau et al. (2012) (mean values (red solid lines) and 95% confidence intervals (red dashed lines)).

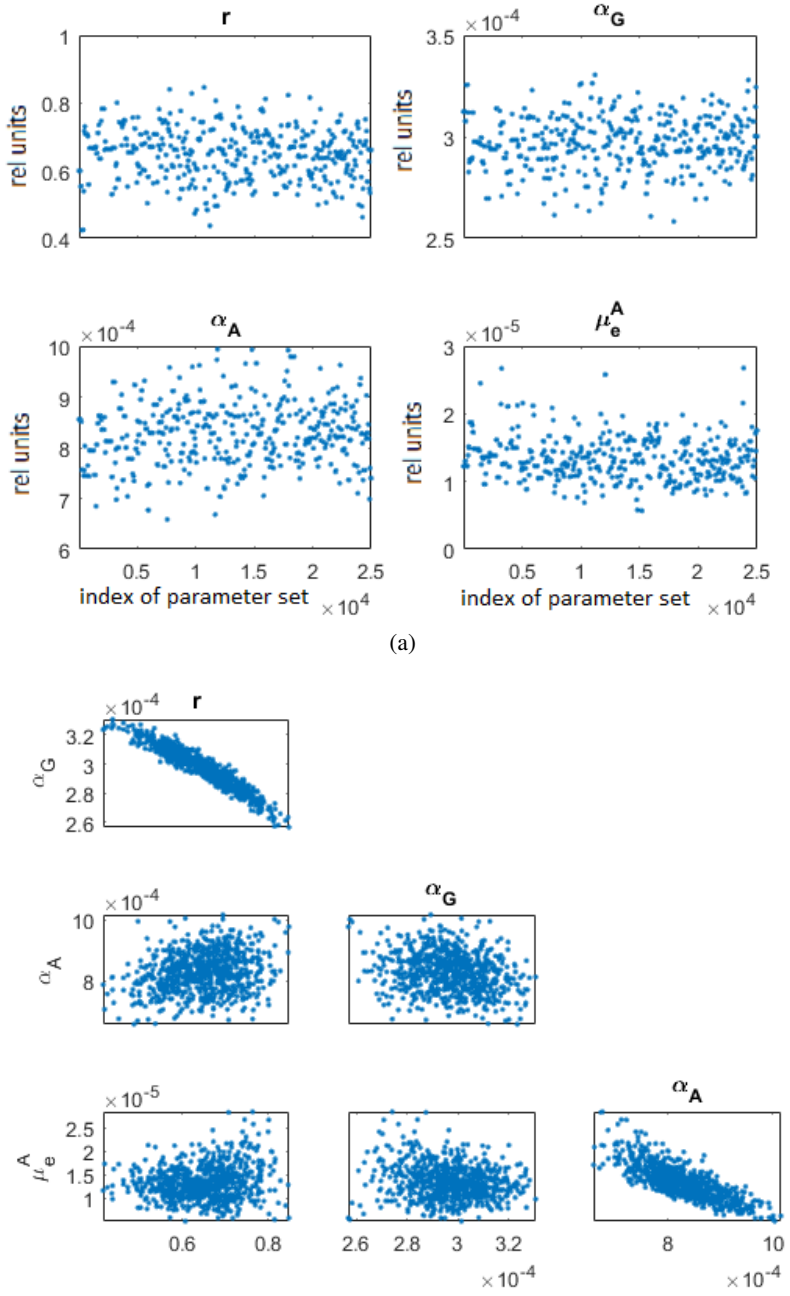

(a)

(b)

Figure 2.18: Results of the MCMC parameter estimation, where LLIN is impregnated with the long-lasting treatment kit (Alphacypermethrin). (a) Parameter chains and (b) pairwise distributions of model parameters summarized in Table 2.8.

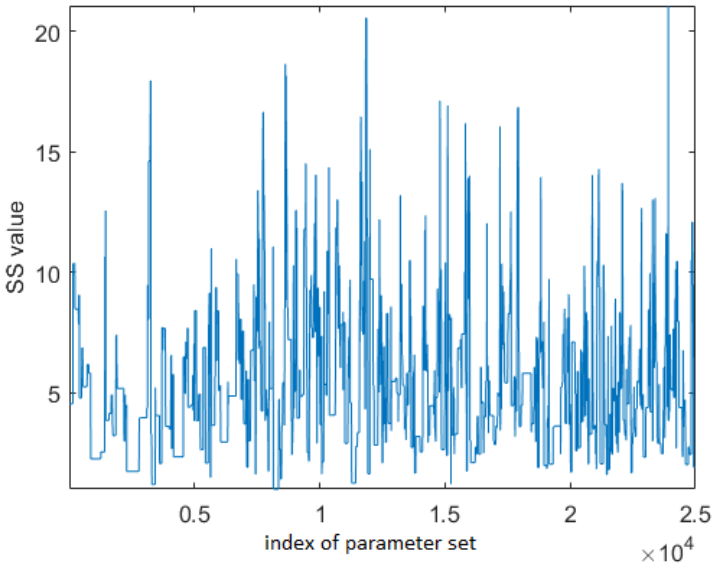

Figure 2.19: Results of the MCMC parameter estimation, where LLIN is impregnated with the long-lasting treatment kit (Alphacypermethrin). Sum of squared residuals for each of the sampled parameter combinations calculated by Equation 2.19.

It can be seen from the above results presented, that the model produces a fair fit to the responses, and the variabilities of the simulated model outputs match with the confidence limits reported for the data sets in Kitau et al. (2012). This is indicated by the Figures 2.11, 2.14 and 2.17, where the red dashed lines plot the error bounds of the real measurements; here, the mean value is depicted by the red constant line.

Moreover, all the estimated values of parameters that resulted in the outputs fitting the data sets are fairly restricted as indicated by the upper and lower limits, see Figures 2.12, 2.15 and 2.18 for the cases of Deltamethrin, Carbosulphan and Alphacypermethrin, correspondingly. Hence, after fixing the values of parameters that were not reasonably identified in the preliminary MCMC experiments (see the discussions for μ_p given above and r explained below), we obtained relatively low uncertainties in the sampled values of the remained parameters. The scatter correlation plots mostly do not indicate any significant correlation between the sampled parameters, with two exceptions. For Alphacypermethrin chemical repulsion parameter is strongly inversely proportional to the detoxification rate for *An. gambiae*, while no similar relation is revealed in the case of *An. arabiensis*. This must be due to the fact, that Alphacypermethrin features low blood-feeding rate with high exit for *An. Gambiae*, so that, given a fixed period before the exit (by fixing parameter μ_G), the chemical is either highly repulsive and moderately detoxified (high r and low α_G), or , alternatively, subject to intensive detoxification but lower repulsion (low r and high α_G), which results in a similar mortality rate, since the total accumulated dosage is also similar in these two cases. However, it should noted that the mortality rate for *An. gambiae* with Alphacypermethrin, produced with the sampled values of parameters, displays a high variation from the sampled mean of the model output, which is in some cases even comparable with that for *An. arabiensis*. However, the mean value of the model output is within the confidence bounds, see the Table 2.9. Additionally, in the case of Carbosulphan treatment, detoxification rate α_G and excito-repellency parameter μ_G displayed non-linear correlation. This chemical is almost 100% lethal for *An. gambiae* in hut experiment, simultaneously, the exit rate for this mosquito is low. Hence, there is a trade-off between the excito-repellency and detoxification: when the exit is earlier (larger value for μ_G), the rate of detoxification should be lower to maintain high mortality.
Finally, qualitative conclusion can be made on the basis of model calibration, comparing the properties of the chemicals under consideration. Due to the repellent effects (high values of r), it can be conjectured that IconMaxx is highly repulsive ($r = 0.88$), which can be conjectured from the low feeding rates it produces for the both mosquito species. This is followed by Carbosuphan and Alphacypermethrin that have a repulsive strength of approximately 0.8 and 0.61, correspondingly. Moreover, Deltamethrin features lower repulsion strength and this can be seen from the high feeding rates reported for the LLINs impregnated with this chemical. After preliminary estimation, the repulsive intensity for Deltamethrin r was found to be negligible and were set to a fixed value, $r = 0$ in the final process of the model calibration. Fixing $r = 0$ for Deltamethrin indicates that its probability of rejection in the case of this chemical will naturally be zero in all the simulations. The excito-repellency rates for all the chemicals are systematically higher in *An. gambiae* as compared to that of *An. arabiensis*, which is consistent with the observations of the exit rate for *An. gambiae* being systematically higher than that of *An. arabiensis*, except for the IconMaxx treatment, see the summary of experimental data in Figure 2.5.

Table 2.8: Model parameters for the extended model, together with the sampled mean of the chains. Note, that some of the parameters were fixed (denoted by the super-index F), while the other parameters were estimated (denoted by the super-index E).

Parameter symbols	Parameter description	Sampled mean value		
		Deltamethrin	Alpacypermethrin	Carbosulphan
r	Repulsive strength of the ITN/LLIN	0^F	0.61^E	0.8^E
α_G	Detoxification. rate for *An. gambiae*	$3.79e-4^E$	0.0003^E	0.0006^E
α_A	Detoxification. rate for *An. arabiensis*	$2.9e-5^E$	0.0008^E	$3.36e-5^E$
μ_e^G	The rate of increase of *Excito-repellency.* in *An. gambiae*	0.001^E	1^F	0.002^E
μ_e^A	The rate of increase of *Excito-repellency.* in *An. arabiensis*	$7.24e-6^E$	$1.4e-5^E$	$1.66e-5^E$

Table 2.9: Mean values of the death, exit and blood-feeding percentages produced with the posterior distribution of parameters obtained with the MCMC alongside the data sets from Kitau et al. (2012) (mean and 95% confidence intervals) for the experimental hut trials with the LLINs impregnated with Alphacypermethrin, Carbosulphan and Deltamethrin insecticidal treatments.

An. gambiae						
Chemicals/	**Simulated outputs, mean value**			**Experimental data, mean value/range**		
Responses	Deltamethrin	Alphacypermethrin	Carbosulphan	Deltamethrin	Alphacypermethrin	Carbosulphan
Percentage mortality	75.62	69.5	98.6	76 (73-79)	71(62-80)	99 (97-100)
Percentage exit	92.74	96.11	61.02	93 (89-96)	95(85-98)	60 (48-71)
Percentage fed	9.27	5.57	18.82	14 (9-20)	9 (4-19)	25 (19-45)

An. arabiensis						
Chemicals/	**Simulated outputs, mean value**			**Experimental data, mean value/range**		
Responses	Deltamethrin	Alphacypermethrin	Carbosulphan	Deltamethrin	Alphacypermethrin	Carbosulphan
Percentage mortality	28.70	36.8	66.01	29(23-44)	36(31-40)	67(63-71)
Percentage exit	84.71	84.63	53.47	85(78-90)	84(80-88)	45(35-57)
Percentage fed	17.33	17.94	24.60	18(13-25)	17(10-27)	25(21-30)

3 ABM extensions

Firstly, the ABM of mosquito host-seeking behaviour is extended to the household-level, with multiple individuals sleeping under the same roof. This is discussed in detail in Subsection 3.1. Next, a subsequent extension is developed for the community-level scenario with several households located in the landscape of interest, see Subsection 3.2 for further details. See the illustration of the workflow followed in the present thesis given in Figure 1.2.

3.1 Household-scale simulations

In this chapter, the factors that impact the contact rates and mortality at the household level are taken into account. Specifically, here we include the effect of household size and parasite ecology, as explained below. By so doing, the experiments were conducted separately when assuming no alterations in vector behaviour induced by parasites and when the alterations are taken into consideration. These simulations are conducted utilizing parameter values related to the action of chemicals (i.e., repellent properties, poisoning, detoxification and excito-repellency) previously estimated in the hut-level experiment for four different insecticidal treatments: Alphacypermethrin, Carbosulphan, Deltamethrin and IconMaxx.
In the household-level model, mosquitoes are assumed to choose one of the individuals upon entering the house by random selection. After that, the situation is reduced to the case of a single host in the hut. Additionally, the effect of mosquito switching to the neighbouring individual was included into the simulations, (see Shcherbacheva and Haario (2017)). This diversion to the other individuals occurs after a certain time spent in unsuccessful attempts to feed on the protected host. In the absence of more precise experimental evidence, we assume that the diversion to the neighbour happens after 10 minutes of the futile blood-feeding attempts. After abandoning the host, a new target individual is selected at random from the other individuals dwelling in the hut. This feature was also employed when simulating the impact of household size on mosquito-to-human contact rates, which is discussed below.
Unlike in the hut-level simulations conducted for model calibration, we account for more frequent exit from the hut in these cases, due to differences in the design of experimental huts and typical human dwellings, (see WHO (2006)). This is achieved by multiplying the probability of exiting the hut p_{hut} of the control case (see Section 2.5.3) by a value, which was taken to produce 90% exit rates per night in the absence of chemical treatment.
Household size effect Malaria is often regarded as a socio-economic disease associated with poverty and underdevelopment. The frequency of the disease tends to decline with economic development and associated improvement in domestic conditions, such as quality of housing and availability of medical aid, (see De Silva and Marshall (2012)). Studies have revealed a considerable correlation between malaria reduction and the decline of a typical household size, (see Huldén (2010), Huldén et al. (2013)). The more people live together in non-segregated quarters, the higher the probability of transmitting the infection to new uninfected human, (Huldén et al. (2013)). The probability of malaria disappear-

ance jumps abruptly, when the average number of individuals in the household declines below the threshold of four people, even when no specific control measures are applied Huldén et al. (2013).
Naturally, it should be noted that there are other household-related factors that can possibly influence the rate of transmission, apart from the household size. Such factors include household practices such as livestock/poultry rearing, as well as the rate of hygiene maintenance in a given household, (Semakula et al. (2015)). For simplicity, the latter factors are not considered in the present work. The situation is restricted to a given number of persons sleeping together in the same room, but the simulations can be extended in a similar manner to the case of people sleeping in separated quarters.
As a difference to the experimental hut considered in the model calibrations, it is assumed that mosquitoes can have several successful feeding attempts. In the absence of alterations in mosquito behaviour by parasite one successful blood-feeding is assumed to be sufficient for egg laying. Assumptions taken for the case of the alterations are discussed below. Similar to the hut-level experiment, mosquito is assumed to quit the host-seeking behaviour inside of the hut either after spending t_{max} inside, or after one successful feeding attempt. After quitting mosquito switches to the random walk with no influence of the attractive odour. However, the barriers created by the net and the repellent effect alongside the impact of chemical poisoning still impact on mosquito in the absence of directional orientation.
Behavioural alterations Infection with malaria parasites has been shown to alter the behaviour of mosquitoes, with varying effects depending on the life stage of the parasite, (see Cator et al. (2012)). The underlying mechanisms that engender these behavioural alterations are not fully explored but mostly result from a manipulation process. The parasite impairs the vector's ability to obtain a full blood meal upon a single bite, thereby inducing the vector to bite several times before it is fully engorged, (see Koella and Rieu (2002), Rossignol et al. (1984)). Another common alteration induces the increased attractiveness of infected hosts to mosquitoes, (Cornet et al. (2013), Lacroix et al. (2005)). As it was revealed, a human harbouring parasites at the stage transmissible to mosquitoes attracts twice more mosquitoes than uninfected host, (see Lacroix et al. (2005)). These behavioural changes associated with infection seem likely to be an evolutionary mechanism developed by malaria parasite that enhances the spread of infection, (see Schwartz and JC. (2001), Moore (2002)). More profound understanding of the behavioural tendencies of parasite-infected mosquitoes alongside the stage-specific changes in their host-seeking behaviour could provide a potential target for genetic manipulation of mosquitoes, as a preventive measure for the elimination of malaria infection, (see Cator et al. (2015)).
In this study, we evaluate the impact of the alterations. Thus, the mosquito-human contact rate is separately computed for populations of infected and uninfected mosquitoes.
We account for the impact of multiple biting, typical for infected mosquitoes, due to their damaged engorging system and we assume that an infected mosquito can take up to 5 bites per night at certain probability values associated with a given number of bites and tends to feed on multiple hosts, (see Vantaux et al. (2015)). Additionally, the statistics from Koella and Rieu (2002) is employed, which states that 10% of uninfected and 22% of infected mosquitoes obtain a blood meal on at least 2 hosts, depending on the accessi-

bility of the hosts. Herewith, the maximal number of successful feeding attempts can be up to 5. This property is randomized and sampled separately for each of the mosquito-agents. Here we assume that a dosage of blood sufficient for ovipositing is achieved after the maximal number of successful feeding attempts is reached.
The second behavioural alteration associated with the enhanced attractiveness of the infected humans to mosquitoes was preliminary tested and further omitted, since it had no significant impact on the simulation outcomes. In this work only multiple bites are included into the simulation.

3.2 Community-scale simulations

Next, the household-level model is extended to community-level scenarios, with a number of households randomly positioned inside of the spatial domain. These elaborations are particularly useful when accounting for heterogeneity inherent in local settings with partial coverage of the population with the nets, leading to higher exposure of humans in non-protected households.
Here, in community-level settings an additional component to simulate an enhancement in host-seeking is introduced when mosquito is approaching conspicuous features at a distance of less then 15 meters, (see Bidlingmayer and Hem (1980), van Breugel et al. (2015), Hawkes et al. (2017)). This is needed to model directional motion in the vicinity of human dwellings. Modelling mosquito attraction when navigating in between the huts in the village is conducted by the means explained below, with the aim of accounting for the fact that the bigger households attract more mosquitoes in comparison to the smaller ones.
Similar to the hut-level case, the movement of the mosquito outside of the hut is governed by the mechanism of *klinotaxis*. Due to the lack of data available for calibration of the parameters related to mosquito responses to the cues, a modelling approach for mosquito movement in-between the households is applied following the guidelines from the literature quoted above. The concentration which enables mosquito to sense the humans is computed similarly to the case of a single individual, see Equation 2.3, i.e., as a Gaussian with the argument given by a weighted sum of the individual distances from mosquito position $\mathbf{x}$ to the location of each of the hosts $\mathbf{x}_n^h$:

$$C_a^{tot}(\mathbf{x}) = C(W_n, \mathbf{x}, \mathbf{x}_n^h) = \exp\left(-\left[\frac{\sum_{j=1}^{N_h} W_n d(\mathbf{x}, \mathbf{x}_n^h)}{\sqrt{2}\sigma_a}\right]^2\right), \tag{3.1}$$

where N_h denotes the total number of individuals in the community, $d(\mathbf{x}, \mathbf{x}_n^h)$ stands for the distance from mosquito position $\mathbf{x}$ to the host location $\mathbf{x}_n^h$, and W_n is the weight attributed to the host n, as discussed next.
The total attracting concentration is modelled following the idea of the softmax function,

widely adopted in machine learning and neural networks, (see Bishop (2006), Montague (2018)). The weight W_n is introduced to account for the fact that mosquito's response to the cue emitted from the households increases at a short distance of 5-15 m, depending on the mosquito specie, due to the their enhanced orientation by odour in the presence of visual clues. While approaching the household, mosquito gradually gains the ability to discern the shape. Then, at a short distance, the concentration of carbon dioxide sensed by the mosquito is assumed to be that which is emitted from the closest household. Here, the main focus is placed on the nearest target concept, which practically means that at a short distance factors other than just the CO_2 alone also cause mosquito to localize the search, as reported in the literature referenced above. Following this reasoning, the non-normalized weights $\hat{W}_n$ are introduced, inversely proportional to the distance:

$$\hat{W}_n(\mathbf{x}, \mathbf{x}_n^h) = (1 - 1/(1 + exp(-(d(\mathbf{x}, \mathbf{x}_n^h) - d_{50}^h)/s^h)), \quad \mathbf{x}_n^h \in \mathbf{x}_n^h. \tag{3.2}$$

where $d_{50}^h = 10$ m stands for the distance at which the weight $\hat{W}_n(\mathbf{x}, \mathbf{x}_n^h)$ reaches 50% of the maximal value, and $s^h > 0$ governs the range of enhancement for mosquito sensitivity. Here, the value $s^h = 5$ m is used to account for a gradual boost of the mosquito's response to the cues. In the computational procedure, the weights $\hat{W}_n(\mathbf{x}, \mathbf{x}_n^h)$ are normalized, i.e., for each mosquito-agent the resulting weights are computed from non-normalized counterparts:

$$W_n(\mathbf{x}, \mathbf{x}_n^h) = \frac{\hat{W}_n(\mathbf{x}, \mathbf{x}_n^h)}{\sum_{j=1}^{N_h} \hat{W}_j(\mathbf{x}, \mathbf{x}_j^h)} \tag{3.3}$$

For a special example of two households with different number of individuals the total concentration that enables mosquito to sense the humans is plotted in Figure 3.1 in one and two-dimensional representation. Note that the form of Equation 3.1 implies that larger households are attributed with larger weights, which is consistent with the evidence, that larger agglomerates emit stronger odours, hence, attracting more mosquitoes, (see Cummins et al. (2012)).

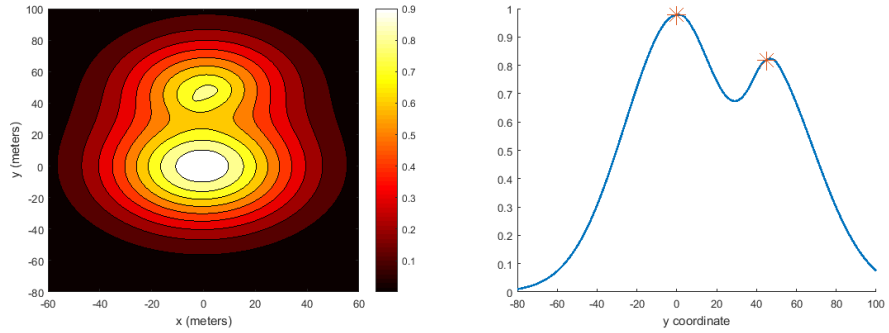

(a) (b)

Figure 3.1: Softmax function in a special case of two households,the first one is including 6 individuals (located (0,0)) and another one - 2 individuals (located at (0,45)) for $d_{50} = 10, s = 5$ in Equation 3.2, (a) 2D plot, (b) 1D plot along the y axis

Additionally, the scaling factor σ_{acc} (given by Equation 2.5) is calculated with distance to the closest hut, perceived as the nearest visible feature. This is conducted to imitate the pure random movement outside of the concentration plume created by the presence of the hosts. However, in the present study mosquitoes are considered only inside of the domain with households located at relatively close distances, such that this effect was not observed. Note that in the present study the environmental factors, such as wind and intermittency of the plume, are omitted for simplicity.
Note that to average the stochasticity originating from difference in spatial arrangement, households are randomly positioned at each successive repetition of the algorithm. In the case when insufficient amount of blood was consumed before the exit from household, mosquito starts the process of host-seeking (from the outset), except that the abandoned household is not accounted for when computing the total concentration of the CO_2. Additionally, it is assumed that after entering new household, the count of host-seeking time is reinitialized.
In this section the model is firstly described as introduced in Shcherbacheva et al. (2018) and the overall impact of parameter estimation is quantified on community-level results. Next, the additional model features included into the community-scale simulations are discussed, which enabled to account for several factors that impact malaria transmission.

3.3 Simulating different model versions

Here, the community-scale simulations are considered for LLINs treated with the IconMaxx using the model from Shcherbacheva et al. (2018). In this case, two modifications of the model with slightly different parametrization are simulated. Their outputs for multiple combinations of sampled parameters are compared with the aim of demonstrating that the model is capable of quantifying the overall impact of the LLINs. It turns out that both model versions produce statistically similar outcomes in community-level settings.

Next, several other chemical treatments are simulated in community-level settings with the extended model. Here Alphacypermethrin, Carbosulphan and Deltamethrin are considered, following model calibrations in the previous chapter. In this settings we compute the mortality and mosquito-to human contact rates for *An. gambiae* and *An. arabiensis* when confronted with each of the chemicals. Several scenarios are used to consider the impact of some of the key factors on outcomes of the ABM simulations. These factors include the partial coverage of the population with the LLINs, socio-economic factors (household size) and the effect of the malaria parasite on mosquito behaviour. Finally, response surfaces are fitted to the simulated mortality and feeding rate. Next, we compare the properties of the chemicals, such as lethality and repellency; and the efficiency of the chemicals in controlling to *An. gambiae* and *An. arabiensis* control.

3.3.1 The IconMaxx case

For the parametrization introduced in the previous chapter the estimated parameter distributions revealed a substantial uncertainty. However, we demonstrate here that regardless of parametrization and quality of the estimates, the model is capable of quantifying the overall impact of the LLINs in community-level situations: two model versions discussed in Subsection 2.4, simulated using parameter values randomly selected from the MCMC chains, produce essentially the same results when the simulations are extrapolated from the hut-level to community-scale scenario. Additionally, it appears that the LLINs are systematically less efficient in controlling *An. arabiensis* as compared to *An. gambiae*.
To demonstrate this, we simulate a community-level experiment with the two modifications of the model as given in the previous subsection. For the simulation example we select 20 persons in 4 households of the same size, 5 people in each. The households are located at a distance of no less than 10 meters from one another. The outcomes of the experimental runs evaluated under varying coverage with the LLINs, are averaged over three repetitions to decrease statistical uncertainty. The time period for the simulations was again one night, from 20:30â€“6:30. While in the hut-level experiment mosquitoes can only exit from the hut into the window traps, in the community-level experiment we assume realistic village conditions, where mosquitoes are able to move between huts, which also implies more frequent exit from the hut, due to the difference in design of experimental huts and real human dwellings. Note that although this particular experiment and its outcomes are discussed here, consistently similar results were obtained for a large variety of settings of households and people.
To estimate the impact of the LLINs, we perform the simulations with increasing levels of LLIN coverage of the hosts, with the percentage of protected individuals varying from 10% to 100%. In this way, we get respective increasing and decreasing values for the mosquito mortality and mosquito-human contact rates as shown in Figure 3.2. Moreover, we compute the reproductive number, defined as the number of secondary infection cases (see Smith et al. (2007)) given as

$$R_0 = ma^2bc\, e^{(-g\eta)}/g. \tag{3.4}$$

Here g stands for the mortality rate of mosquitoes, a denotes the mosquito-human contact rate, m gives the mosquito-to-human ratio, i.e., the number of female mosquitoes per human, η is the number of days required for parasite to reach fully developed stage (commonly 10 days for most of the species of mosquitoes), b is the probability of transmission of malaria parasite from infected mosquito to susceptible human, and c gives the probability of transmission of the parasite from infected human to uninfected mosquito. To isolate the effect of relative R_0 decrease in response to changes due to mosquito mortality g and contact rate a , we can set $m = b = c = 1$.
Multiple parameter combinations are randomly selected from the posterior distributions generated with the MCMC method. These combinations are further utilized in simulations of the community-level experiment for *An. gambiae* and *An. arabiensis* separately. The death and contact rates are calculated as the outcomes of the simulations. The results are plotted as the functions of the protection, see Figure 3.2.
In spite of the noisiness of the results, the main decreasing trend of R_0 as a function of the LLIN coverage is visible in the Figure 3.2. Additionally, it can be noted, that the variability between the Version 1 and Version 2 is similar to the variability of the outputs within the versions. As a result, we conclude that the two parametrizations produce statistically same results for the average effect of the LLIN control in the community-scale situation, in spite of the fact that the precise mechanism of the influence of the LLINs on mosquito short-distance attraction are not ideally identified. It should be noted that while the mosquito-to-human contact rates exhibit similar trends, the model produces systematically lower mortality rates for *An. arabiensis* in comparison to *An. gambiae*. This indicates lower efficiency of the LLIN protection in application to the former mosquito specie. Consequently, from the reproduction numbers R_0 for different LLIN coverage, it is observed that the minimal LLIN coverage sufficient for the disease elimination is higher in case of the *An. arabiensis*.

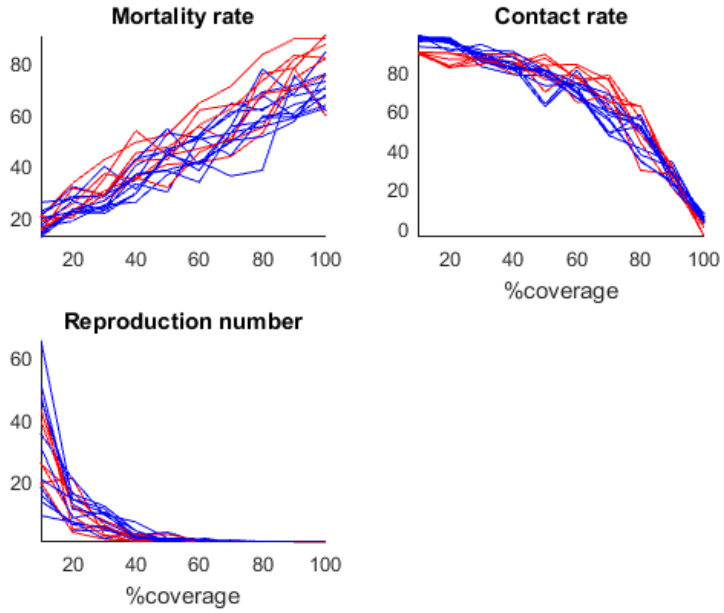

(a)

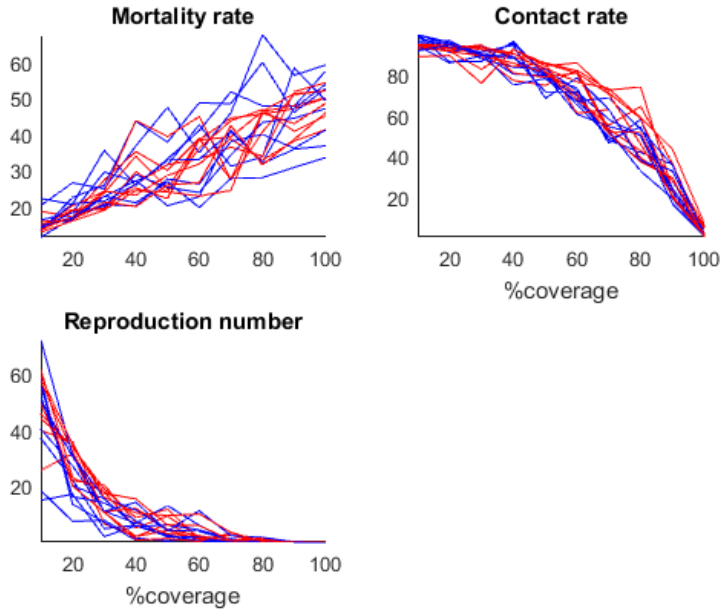

(b)

Figure 3.2: Mortality rate, contact rate and reproduction number R_0 conditioned on LLIN coverage percentage for (a) *An. gambiae* and (b) *An. arabiensis* simulated using two different modifications of the model: Version 1 (blue line) and Version 2 (red line) .

3.4 Regression of the ABM simulation results

Here, the results for community-scale simulations conducted for two case studies: assuming no behavioural alterations by parasite, and when the alterations are assumed as discussed in the previous subsection. In so doing, parameters previously estimated with the hut-level data for extended model parametrization are employed, separately for all the chemicals considered in the study.
In the present simulations mosquitoes are initially randomly placed inside of the experimental domain of 25600m^2 size with multiple households located at a distance not closer than 40m from one another, such that there is no competitive attraction induced by vision, (see Bidlingmayer and Hem (1980)). Within a single run all the households are of the same size. However, the household size varies between the runs. For example, see randomly generated experimental layout shown in Figure 3.3 below.

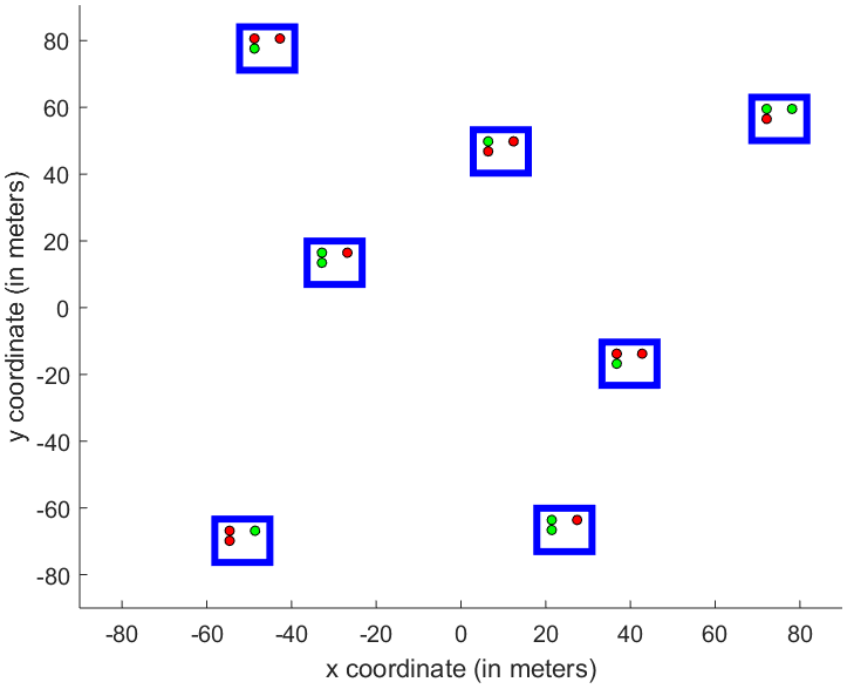

Figure 3.3: Randomly generated experimental layout with typical household size comprising 3 individuals. Here blue rectangles denote the houses, green/red circles mark individuals protected/non-protected with the impregnated nets, correspondingly.

The outputs of the ABM simulations are noisy, as it is revealed in the Figure 3.2. For clarity, we present only the outputs averaged over 7 repetitions of the experiment. A number of repetitions is larger than in the hut-level experiment to average the stochasticity attributed to the spatial arrangement of the households. Note that in these simulations parameter values are re-sampled from the estimated posteriors at each successive iteration

of the algorithm for uncertainty quantification.
Subsequently, after obtaining the relevant outputs of the ABM simulations, that are specifically the contact and mortality rates, a regression analysis is applied with respect to the household size and the coverage for outputs corresponding to Alphcypermethrin, Carbosulphan, Deltamethrin and IconMaxx insecticidal treatments, respectively. Given that one of the independent variables is discrete by definition, a uniform design is employed, while considering household sizes 2, 4, 6, 8 and 10, with the LLIN coverage varying from 0 to 100%. As revealed by the results, mortality rates exhibit an insignificant dependence on the household size, unlike the contact rates. However, both the mortality and contact rates strongly depend on the LLIN coverage. Hence, the mortality rate is fitted with second degree polynomial with respect to only the coverage, see Figure 3.4. Herewith, the regression analysis revealed fair fits for all the ABM results ($R_2 > 90$).
The regression is conducted in two cases: when assuming no behavioural alterations and when considering alterations by parasite, separately for *An. gambiae* and *An. arabiensis* when confronted with each of the chemical treatments considered in the present study.
As it is visible from Figure 3.6, the contact rates $\tilde{a}$ behave as the logistic functions with respect to the coverage x_2, with a certain threshold coverage required for the contact rate to start decreasing. Hence, the following parametrization was proposed:

$$\bar{a}(x_1, x_2) = N_b * (1 - 1./(1 + \exp(-(x_2 - b_1 - b_2 x_1)/b_3))) \tag{3.5}$$

$$\tilde{a}(x_1, x_2) = N_b * (1 - 1./(1 + \exp(-(x_2 - b_1 - b_2 x_1)/b_3))), \tag{3.6}$$

where x_1 stands for the household size, $N_b = 0.85$ denotes the average number of bites per mosquito when no control interventions are applied, which was obtained as the part of earlier fittings for the hut-level simulations, (see Shcherbacheva et al. (2018)). In the case of behavioural alterations, N_b is computed separately for uninfected and infected mosquitoes. In the latter case, the average number of bites taken by mosquito during the night is higher due to the fact that a higher percentage of infected mosquitoes take blood on more than one host as compared to the uninfected ones, see Subsection 2.3.
Comparing the lethality of the treatments, one can conclude that in the case of *An. gambiae*, Carbosulphan is the most efficient, while the other treatments display similar performances. Moreover, for *An. arabiensis* the foremost lethal effect is attained when confronted with IconMaxx, and this is seconded by Carbosulphan. Alphacypermethrin treatment induces the lowest mortality for *An. arabiensis* among all the chemicals, see Figure 3.4.
The trends fitted to the contact rates obtained from community-scale simulations suggest that Alphacypermethrin features the highest efficiency in reducing the contact rate when applied to *An. gambiae*, while all the other chemicals demonstrate similar reduction effects, which is consistent with the confidence intervals given in Kitau et al. (2012). Due to the latter fact, the results are presented only for Alphacypermethrin and Carbosuphan, see Figure 3.6. On the other hand, all the chemicals feature similar performance in reducing the contact rate in the case of *An. arabiensis*, with slightly better efficiency attributed to IconMaxx LN. Moreover, unlike the other treatments, Alphacypermethrin displays substantially better performance in reduction of the contact rates for *An. gam-*

biae as compared to *An. arabiensis*, as can be seen from Figure 3.6. The other chemicals demonstrate similar protection against both mosquito species with slightly lower contact rates when applied to *An. gambiae*.
The response surfaces are plotted for Alphacypermethrin in the case when assuming no behavioural alterations, see Figure 3.5. It should be noted that the response surfaces for the other chemical treatments considered in the present work are qualitatively similar. It can be seen that the impact of the household size on the contact rates is more significant at the medium percentage of LLIN coverage (comprising approximately 40-80%). Also the response surfaces of the contact rates for uninfected and infected *An. arabiensis* when confronted with the Alphacypermetrin treatment kit are illustrated, when assuming the alterations in behaviour caused by the parasite, see Figure 3.7. Note that in this case the contact rates of infectious mosquitoes are higher as compared to uninfected ones under the same level of LLIN coverage.
As a summary, after carrying out parameter estimation, the model is generalized to community-level scenario. The effects of the *in situ* behaviour, the settlement patterns and the parasite ecology are explored by fitting the response surfaces to the trends which are based on available experimental data. In all the above-mentioned cases the response surfaces generalize the trends. Note that all the results presented in this work are based on the data from Kitau et al. (2012). Additional experimental data would improve the reliability of the results, especially concerning the behaviour of mosquitoes in-between the households. Given that similar data are available elsewhere, the approach allows to produce general trends and response surfaces based on the data in an analogous way.

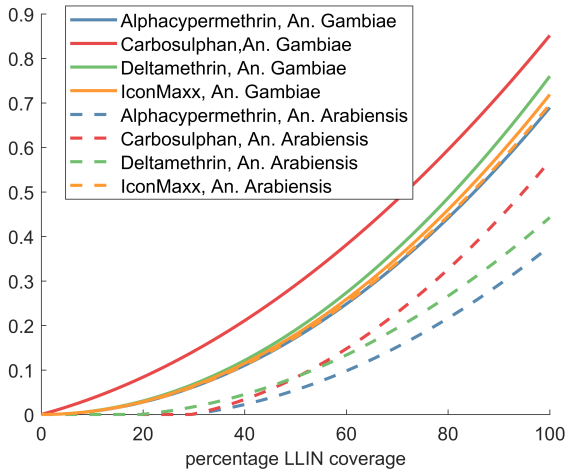

Figure 3.4: Mortality rates resulting from community-scale simulations (expressed in fractions of mosquito populations) for *An. gambiae* (solid lines) and *An. arabiensis* (dashed lines) fitted with respect to the LLIN coverage percentage for four LLIN treatment kits: Alphacypermethrin, Carbosulphan, Deltamethrin and IconMaxx LN, see the legend.

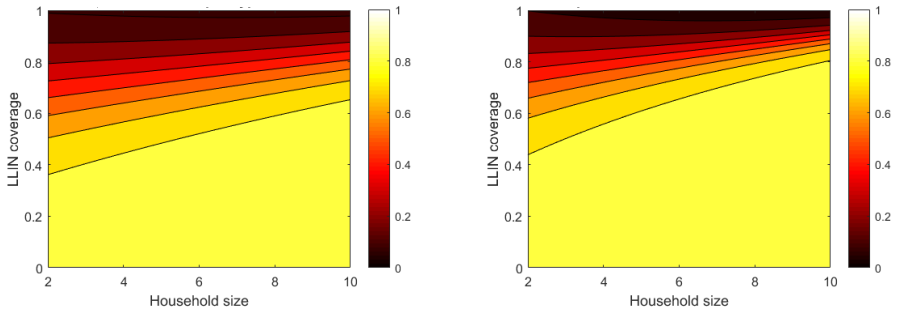

(a) (b)

Figure 3.5: Contact rates resulting from community-scale simulations (expressed in fractions of mosquito populations) for (a) *An. gambiae* and (b) *An. arabiensis* fitted with respect to the household size and the fraction of human population coverage with the LLINs when confronted with Alphacypermethrin treatment kit, assuming no behavioural alterations by parasite.

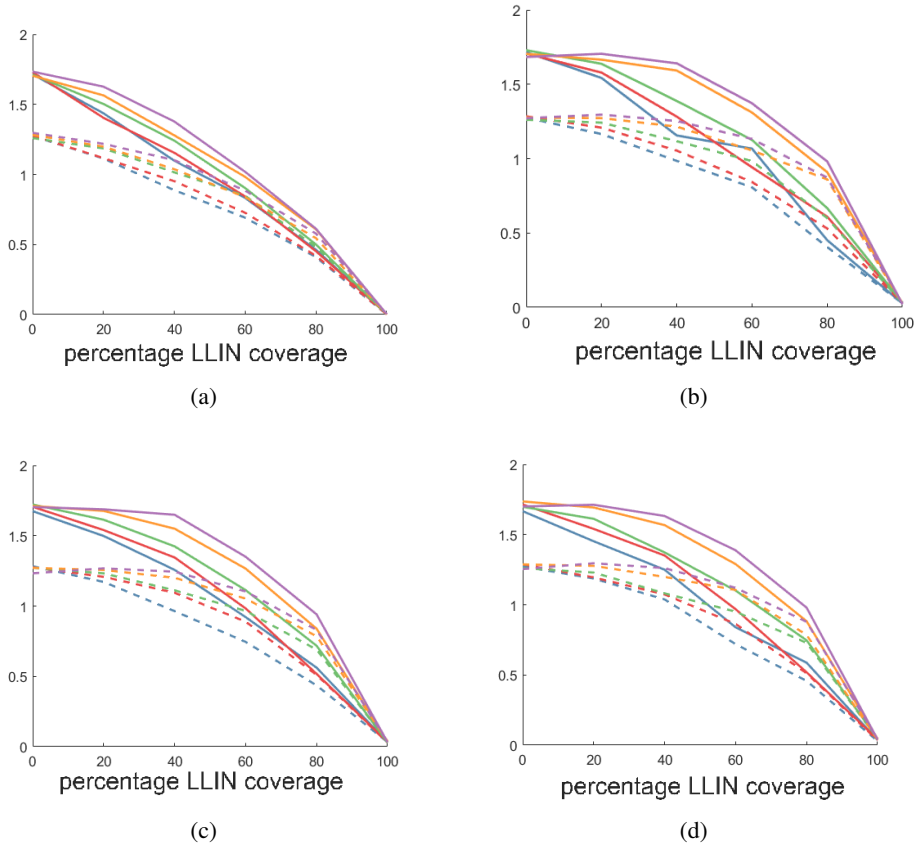

Figure 3.6: Contact rates for uninfected (dashed lines) and infectious (solid lines) mosquitoes resulting from community-scale simulations expressed in an average number of bites per mosquito per night when confronted with one of the four chemicals conditioned on the LLIN coverage percentage when assuming behavioural alterations by parasite, for different household sizes: 2 (blue) , 4 (red), 6 (green), 8 (yellow) and 10 (violet) people. Herewith, chemical treatments and mosquito species are grouped in the following order: a) *An. gambiae* and Alphacypermethrin b) *An. arabiensis* and Alphacypermethrin c) *An. gambiae* and Carbosulphan d) *An. arabiensis* and Carbosulphan.

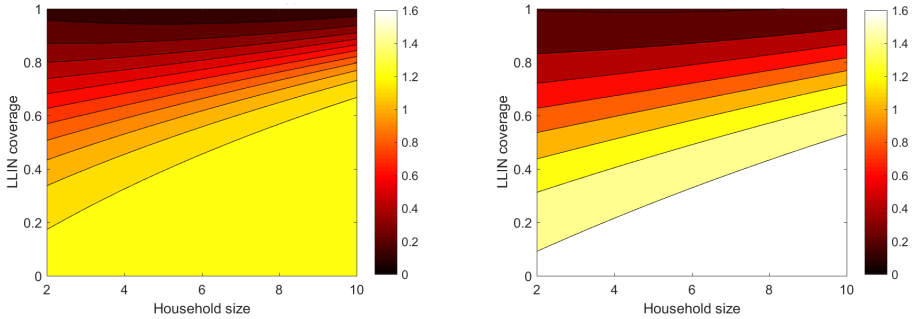

(a) (b)

Figure 3.7: Contact rates resulting from community-scale simulations (expressed in an average number of bites per mosquito per night) when confronted with Alphacypermethrin treatment kit fitted with respect to the household size and the fraction of human population coverage with the LLINs when assuming behavioural alterations by parasite for (a) infected *An. arabiensis* and (b) uninfected *An. arabiensis.*

4 Conclusion and future work

Here, an agent-based modelling (ABM) approach is developed with the aim of simulating the host-seeking behaviour of malaria mosquitoes. The model from Shcherbacheva et al. (2018) is calibrated with effects of the Long Lasting Insecticidal Nets (LLINs) by the means of experimental data from Kitau et al. (2012). Several model modifications were tested to achieve the most parsimonious version yet containing the basic factors: the movement towards host, the effects of the net and chemicals, and mortality. As a control case, the host-seeking is simulated in the absence of insecticidal treatment. In this situation no difference is assumed in the behavioural traits of *An. gambiae* and *An. arabiensis*, as was conjectured in Kitau et al. (2012). Thus, in the case of the absence of LLINs, the same host-seeking time is used for both mosquitoes, and the persistence of host-seeking attempts is assumed to be similar.

Next, the host-seeking is modelled in the presence of the LLIN. By introducing new features into the model and selecting different model parametrizations, various hypotheses can be tested explaining the difference in host-seeking behaviour of the species. In the first version of the basic model the maximal hosts-seeking time is estimated separately for both species to achieve close correspondence with the data. In the second version the same host-seeking time is used for both species, but a reduced host-seeking persistence in the presence of the LLINs is estimated for *An. arabiensis*. In both cases it is assumed that the rate of insecticide-induced poisoning and the deterrence parameters are the same for both mosquito species. The posterior distributions of model parameters were produced by applying extensive MCMC simulations.

The basic model version is found sufficient for calibration of the IconMaxx case. To make the model capable of fitting the other data sets from Kitau et al. (2012) three new features are added to the model: detoxification of the chemical in mosquitoes, delayed impact of the chemical and excito-repellency. As a result, three data sets are calibrated in addition to the IconMaxx: Alphacypermethrin, Deltamethrin and Carbosulphan.

It was revealed that the available data do not facilitate unambiguous identification of the factors that contribute to the host-seeking mechanism. But it turns out that overall trends can be captured utilizing the posterior distributions of parameters. For instance, regardless of the model parametrization, *An. arabiensis* is estimated to consistently abandon blood feeding attempts much earlier than *An. gambiae* when confronted with treated net.

Subsequently, the hut-level model is extended to the village-scale situation, where mosquito host-seeking behaviour is simulated in a domain with multiple households of typical size, inhabited by a number of individuals. As a result, it was found that the calibrated model can be used to evaluate the overall impact of the LLINs. It appeared that the fact that parameters are not uniquely identified has minor impact on the outcome of the community-scale simulations: the key factors such as the mosquito mortality and the mosquito-human contact rate under partial coverage of the population with the LLINS remain statistically the same when simulated using different parameter values from the sampled posterior distributions.

Next, the other factors that impact the mosquito behaviour at the *in situ* level are included into simulation, i.e., the household size and parasite ecology. The outputs of the ABM

simulations are obtained utilizing previously estimated parameters. Next, the results are fitted by regression with respect to two factors: household size and percentage of the LLIN coverage, separately for *An. gambiae* and *An. arabiensis* in the presence of each of the considered insecticidal treatments. In addition, the same simulations and regression are conducted when assuming behavioural alterations in mosquitoes induced by malaria parasite, which creates an enhanced activity of infected mosquitoes. In both cases, the results indicate that lower coverage is required to produce similar reduction in mosquito-human contact rates for smaller household sizes as compared to larger ones.

In the future work an extension of the ABM for a continuous time period will be developed by integrating the continuous model of malaria transmission. The community-level regression models enable to create the link from the *in situ* mechanism of mosquito host-seeking behaviour to the key parameters incorporated into continuous models of transmission, i.e., the mortality and contact rates.

Overall, the influence of the *in situ* behaviour, the settlement patterns and the parasite ecology can be explored by fitting the response surfaces to the trends calculated with parameter posteriors which are estimated by the means of the experimental data. Given more experimental data, the quality of the inference can be further improved. Generally, the approach suggested in the present work allows to produce the general trends and the response surfaces based on the limited *in situ* data.

In this study a constant mosquito density is assumed, although the interventions, such as LLINs and odour-baited traps can reduce the population of mosquitoes. Additionally, in the long-term, mosquito density exhibits inter-seasonal variations. It can also vary in space, depending on local disposition of breeding sites. In the future research, the influences of these factors can be investigated by including the mosquito life-cycle into the model either by the means of the ABM simulations, or following the procedure proposed for the continuous modelling, see Figure (1.2).

Also, the simulations and calibrations are conducted only for the cases of *An. gambiae* and *An. arabiensis* species. Given the necessary data for calibration of mosquito responses to the chemicals, the model is potentially capable of discriminating the transmission characteristics depending on local composition of mosquito species.

As a summary, a flexible approach was developed for modelling the behaviour of malaria vector mosquitoes, which enables to account for various factors that influence malaria transmission at the *in situ* level. Given that the proposed model is spatially explicit, it is especially suitable for taking into account spatial heterogeneities. Additionally, the simulations can be combined with continuous modelling, which enables to estimate the commonly measured quantifiers of malaria transmission, such as Epidemiological Inoculation Rate (EIR) and malaria incidence.

References

Abar, S., Theodoropoulos, G.K., Lemarinier, P., and O'Hare, G.M. (2017). Agent Based Modelling and Simulation tools: A review of the state-of-art software. *Computer Science Review*, 24, pp. 13–33. doi:10.1016/j.cosrev.2017.03.001, url: https://doi.org/10.1016%2Fj.cosrev.2017.03.001.

Abbott, C.A., et al. (1997). Parallel individual-based modeling of Everglades deer ecology. *IEEE Computational Science and Engineering*, 4(4), pp. 60–78. ISSN 1070-9924, doi:10.1109/99.641610.

Acevedo, M.A., et al. (2015). Spatial heterogeneity, host movement and mosquito-borne disease transmission. *PloS one*, 10, p. e0127552.

Alam, M.Z., et al. (2017). A spatial agent-based model of Anopheles vagus for malaria epidemiology: examining the impact of vector control interventions. *Malaria Journal*, 16(1), p. 432. ISSN 1475-2875, url: https://doi.org/10.1186/s12936-017-2075-6.

Albino, V., Carbonara, N., and Giannoccaro, I. (2003). Coordination Mechanisms Based on Cooperation and Competition Within Industrial Districts: an Agent-Based Computational Approach. *Journal of Artificial Societies and Social Simulation*, 6(4), pp. 1–3. url: https://ideas.repec.org/a/jas/jasssj/2003-4-2.html.

Allan, R.J. (2009). *Survey of Agent Based Modelling and Simulation Tools*.

Anderson, R.M., May, R.M., and Gupta, S. (1989). Non-linear phenomena in host-parasite interactions. *Parasitology*, 99 Suppl, pp. S59–79.

Arrignon, F. and et al. (2007). Modelling the overwintering strategy of a beneficial insect in a heterogeneous landscape using a multi-agent system. *Ecological Modelling*, 205, pp. 423–436.

Bedrossian, J. and Rodríguez, N. (2014). Inhomogeneous Patlak-Keller-Segel models and aggregation equations with nonlinear diffusion in Rd. *Discrete and Continuous Dynamical Systems - Series B*, 19(5), pp. 1279–1309. ISSN 1531-3492, doi:10.3934/dcdsb.2014.19.1279.

Bennett, D.A. and Tang, W. (2006). Modelling adaptive, spatially aware, and mobile agents: Elk migration in Yellowstone. *International Journal of Geographical Information Science*, 20(9), pp. 1039–1066. ISSN 1365-8816, doi:10.1080/13658810600830806, url: http://dx.doi.org/10.1080/13658810600830806.

Bidlingmayer, W.L. and Hem, D.G. (1980). The range of visual attraction and the effect of competitive visual attractants upon mosquito (Diptera: Culicidae) flight. *Bulletin of Entomological Research*, 70(2), pp. 321–342. doi:10.1017/S0007485300007604.

Bishop, C.M. (2006). *Pattern Recognition and Machine Learning (Information Science and Statistics)*. Berlin, Heidelberg: Springer-Verlag. ISBN 0387310738.

Blower, S.M. and Dowlatabadi, H. (1994). Sensitivity and Uncertainty Analysis of Complex Models of Disease Transmission: An HIV Model, as an Example. *International Statistical Review / Revue Internationale de Statistique*, 62(2), pp. 229–243. ISSN 03067734, 17515823, url: http://www.jstor.org/stable/1403510.

Boero, R. and Castellani, M.and Squazzoni, F. (2004). Micro Behavioural Attitudes and Macro Technological Adaptation in Industrial Districts: an Agent-Based Prototype. *Journal of Artificial Societies and Social Simulation*.

Bomblies, A., Duchemin, J.B., and Eltahir, E.A.B. (2008). Hydrology of malaria: Model development and application to a Sahelian village. *Water Resources Research*, 44(12). ISSN 0043-1397, doi:10.1029/2008wr006917, url: https://doi.org/10.1029/2008WR006917.

Bomblies, A. and Eltahir, E.A.B. (2009). Assessment of the impact of climate shifts on malaria transmission in the Sahel. *Ecology & Health*, 6, pp. 426–37.

Borrelli, F., Ponsiglione, C.and Iandoli, L., and Zollo, G. (2005). Inter-Organizational Learning and Collective Memory in Small Firms Clusters: an Agent-Based Approach. *Journal of Artificial Societies and Social Simulation*, 8.

Bowen, M.F. (1991). The sensory physiology of host-seeking behavior in mosquitoes. *Annual review of entomology*, 36, pp. 139–58.

Bowler, D.E. and Benton, T.G. (2005). Causes and consequences of animal dispersal strategies: relating individual behaviour to spatial dynamics. *Biological reviews of the Cambridge Philosophical Society*, 80, pp. 205–25.

Box, G.E.P., Hunter, W.G., and Hunter, J.S. (1978). *Box, G. E. P., Hunter, W. G., & Hunter, J. S. (1978)*, 6th edn. New York.

van Breugel, F., Riffell, J., Fairhall, A., and Dickinson, M.H. (2015). Mosquitoes use vision to associate odor plumes with thermal targets. *Current biology : CB*, 25(16), pp. 2123–2129. ISSN 1879-0445, url: http://www.ncbi.nlm.nih.gov/pmc/articles/PMC4546539/.

Broek, I. and Otter, C.J. (1999). *Olfactory sensitivities of mosquitoes with different host preferences (Anopheles gambiae s.s., An. arabiensis, An. quadriannulatus, An. m. atroparvus) to synthetic host odours*, vol. 45. 1001–1010 p.

Brooks, G.T. (1985). Comprehensive insect physiology, biochemistry and pharmacology: Edited by G. A. Kerkut and L. I. Gilbert. Pergamon Press, Oxford. 1985. 13 Volumes. 8200 pp approx. £1700.00/$2750.00. ISBN 0 08 026850 1. *Insect Biochemistry*, 15(5), pp. i–xiv. ISSN 0020-1790, url: http://www.sciencedirect.com/science/article/pii/0020179085901313.

Brown, D.G., et al. (2005). Spatial process and data models: Toward integration of agent-based models and GIS. *Journal of Geographical Systems*, 7(1), pp. 25–47. ISSN 1435-5949, url: http://dx.doi.org/10.1007/s10109-005-0148-5.

Buhl, J., et al. (2006). From disorder to order in marching locusts. *Science (New York, N.Y.)*, 312, pp. 1402–6.

Burger, M., Capasso, V., and Morale, D. (2007). On an aggregation model with long and short range interactions. 8(3), pp. 939–958. ISSN 1468-1218, url: http://www.sciencedirect.com/science/article/pii/S1468121806000514.

Cardé, R. (1996). Odour plumes and odour-mediate flight in insects. *Ciba Found Symp*, 200, pp. 54–66.

Cator, L.J., Lynch, P.A., Read, A.F., and Thomas, M.B. (2012). Do malaria parasites manipulate mosquitoes? *Trends in parasitology*, 28, pp. 466–70.

Cator, L.J., et al. (2015). Immune response and insulin signalling alter mosquito feeding behaviour to enhance malaria transmission potential. *Scientific Reports*, 5, p. 11947. url: http://dx.doi.org/10.1038/srep11947.

Chamchod, F. and Britton, N.F. (2011). Analysis of a Vector-Bias Model on Malaria Transmission. *Bulletin of Mathematical Biology*, 73(3), pp. 639–657. ISSN 1522-9602, url: https://doi.org/10.1007/s11538-010-9545-0.

Chitnis, N., Hardy, D., and Smith, T. (2012). A periodically-forced mathematical model for the seasonal dynamics of malaria in mosquitoes. *Bulletin of mathematical biology*, 74, pp. 1098–124.

Churcher, T.S., et al. (2010). Population biology of malaria within the mosquito: density-dependent processes and potential implications for transmission-blocking interventions. *Malaria journal*, 9, p. 311.

Clements, A. and Paterson, G. (1981). The analysis of mortality and survival rates in wild populations of mosquitoes. *J Appl Ecol*, 18, pp. 373–399.

Comiskey, E. and et al. (1997). A spatially-explicit individual-based simulation model for Florida panther and whitetailed deer in the Everglades and Big Cypress landscapes. In: Ft. Myers, F., ed., *Jordan, D.* U.S. Fish and Wildlife Service.

Conti, S. and OHagan, A. (2010). Bayesian emulation of complex multi-output and dynamic computer models. *Journal of Statistical Planning and Inference*, 140(3), pp. 640–651. ISSN 0378-3758, url: http://www.sciencedirect.com/science/article/pii/S0378375809002559.

Cornet, S., Nicot, A., Rivero, A., and Gandon, S. (2013). Both infected and uninfected mosquitoes are attracted toward malaria infected birds. *Malaria Journal 2013, 12:179*, 12(179).

Creech, T., et al. (2017). *Simulating the spread of selection-driven genotypes using landscape resistance models for desert bighorn sheep*, vol. 12. e0176960 p.

Cummins, B., et al. (2012). A Spatial Model of Mosquito Host-Seeking Behavior. *PLoS Comput Biol*, 8(5), p. e1002500.

Czirók, A. and Vicsek, T. (2007). Collective motion. vol. 527, pp. 152–164.

Dagorn, L., Menczer, F., Bach, P., and Olson, R. (2000). Co-evolution of movement behaviours by tropical pelagic predatory fishes in response to prey environment : a simulation model. *Ecological Modelling*, 134, pp. 325–341. ISSN 0304-3800, doi: 10.1016/{S}0304-3800(00)00374-4, url: http://www.documentation.ird.fr/hor/fdi:010024419.

Dale, K. and Collett, T.S. (2001). Using artificial evolution and selection to model insect navigation. *Current Biology*, 11(17), pp. 1305–1316. ISSN 0960-9822, url: http://www.sciencedirect.com/science/article/pii/S0960982201004183.

Day, C., et al. (2018). *Using simulation modeling to inform management of invasive species: A case study of eastern brook trout suppression and eradication*, vol. 221. 10–22 p.

De Silva, P.M. and Marshall, J.M. (2012). Factors contributing to urban malaria transmission in sub-saharan Africa: a systematic review. *Journal of tropical medicine*, 2012, p. 819563.

Deffuant, G., Amblard, F., G., W., and Faure, F. (2002). How can extremism prevail? A study based on the relative agreement interaction model. *Journal of Artificial Societies and Social Simulation*, 5. 2.

Deffuant, G., Amblard, F., and Weisbuch, G. (2004). Modelling Group Opinion Shift to Extreme: the Smooth Bounded Confidence Model. *Journal of Artificial Societies and Social Simulation*, 9.

Dekker, T. and Carde, R.T. (2011). Moment-to-moment flight manoeuvres of the female yellow fever mosquito (Aedes aegypti L.) in response to plumes of carbon dioxide and human skin odour. *The Journal of experimental biology*, 214, pp. 3480–94.

Dekker, T., Geier, M., and Carde, R.T. (2005). Carbon dioxide instantly sensitizes female yellow fever mosquitoes to human skin odours. *The Journal of experimental biology*, 208, pp. 2963–72.

Depinay, J.M.O., et al. (2004). A simulation model of African Anopheles ecology and population dynamics for the analysis of malaria transmission. *Malaria Journal*, 3(1), p. 29. ISSN 1475-2875, url: https://doi.org/10.1186/1475-2875-3-29.

Dietz, K., Raddatz, G., and Molineaux, L. (2006). Mathematical model of the first wave of Plasmodium falciparum asexual parasitemia in non-immune and vaccinated individuals. *The American journal of tropical medicine and hygiene*, 75, pp. 46–55.

Dumont, B. and Hill, D.R.C. (2001). Multi-agent simulation of group foraging in sheep: effects of spatial memory, conspecific attraction and plot size. *Ecological Modelling*, 141(1), pp. 201–215. ISSN 0304-3800, url: http://www.sciencedirect.com/science/article/pii/S0304380001002745.

Eckhoff, P.A. (2011). A malaria transmission-directed model of mosquito life cycle and ecology. *Malaria Journal*, 10(1), p. 303. ISSN 1475-2875, url: https://doi.org/10.1186/1475-2875-10-303.

Eckhoff, P.A., Wenger, E.A., Godfray, H.C.J., and Burt, A. (2016). Impact of mosquito gene drive on malaria elimination in a computational model with explicit spatial and temporal dynamics. *Proceedings of the National Academy of Sciences of the United States of America*, 114(2), pp. E255–E264. ISSN 1091-6490, url: http://www.ncbi.nlm.nih.gov/pmc/articles/PMC5240713/.

Edelstein-Keshet, L., Watmough, J., and Grunbaum, D. (1998). Do travelling band solutions describe cohesive swarms? An investigation for migratory locusts. *Journal of Mathematical Biology*, 36(6), pp. 515–549. ISSN 1432-1416, url: http://dx.doi.org/10.1007/s002850050112.

Feachem, R.G.A., Phillips, A.A., Targett, G.A., and Snow, R.W. (2010). Call to action: priorities for malaria elimination. *Lancet (London, England)*, 376, pp. 1517–21.

Fetecau, R.C., Sun, W., and Tan, C. (2016). First-order aggregation models with alignment. *Physica D Nonlinear Phenomena*, 325, pp. 146–163. doi:10.1016/j.physd.2016.03.011.

Fievet, L. and Sornette, D. (2018). Calibrating emergent phenomena in stock markets with agent based models. *PLOS ONE*, 13(3), p. e0193290. doi:10.1371/journal.pone.0193290, url: https://doi.org/10.1371/journal.pone.0193290.

Figueredo, G.P., et al. (2014). Comparing Stochastic Differential Equations and Agent-Based Modelling and Simulation for Early-Stage Cancer. *PLOS ONE*, 9(4), pp. 1–18. doi:10.1371/journal.pone.0095150, url: https://doi.org/10.1371/journal.pone.0095150.

Forester, B., Landguth, E., K. Hand, B., and Balkenhol, N. (2018). *Landscape Genomics for Wildlife Research*.

Forman, R.T. (1995). *Land Mosaics: the ecology of landscapes and regions: Land Mosaics: the ecology of landscapes and regions*. Cambridge: Cambridge University Press.

Franke, R. (2009). *Applying the method of simulated moments to estimate a small agent-based asset pricing model*, vol. 16. 804–815 p.

Gatton, M.L. and Cheng, Q. (2004). Modeling the development of acquired clinical immunity to Plasmodium falciparum malaria. *Infection and immunity*, 72, pp. 6538–45.

Giardina, I. (2008). Collective behavior in animal groups: Theoretical models and empirical studies. *HFSP Journal*, 2(4), pp. 205–219. ISSN 1955-2068, doi:10.2976/1.2961038, url: http://www.tandfonline.com/doi/abs/10.2976/1.2961038.

Gilbert, N. and Troitzsch, K. (2005). *Simulation for the social scientist*. McGraw-Hill Education (UK).

Gillespie, D.T. (1976). A general method for numerically simulating the stochastic time evolution of coupled chemical reactions. *Journal of Computational Physics*, 22(4), pp. 403–434. ISSN 0021-9991, url: http://www.sciencedirect.com/science/article/pii/0021999176900413.

Gillespie, D.T. (2007). Stochastic Simulation of Chemical Kinetics. *Annu. Rev. Phys. Chem.*, 58(1), pp. 35–55. ISSN 0066-426X, doi:10.1146/annurev.physchem.58.032806.104637, url: https://doi.org/10.1146/annurev.physchem.58.032806.104637.

Gillies, M. (1957). Age-groups and the Biting Cycle in *Anopheles gambiae*. A preliminary Investigation. *Bull Entomol Res*, 48(03), pp. 553–559.

Gillies, M. and Wilkes, T. (1968). A comparison of the range of attraction of animal baits and of carbon dioxide for some West African mosquitoes. *Bull Entomol Res*, 59(3), p. 441â€“456.

Griffin, J.T., et al. (2010). Reducing Plasmodium falciparum Malaria Transmission in Africa: A Model-Based Evaluation of Intervention Strategies. *PLOS Medicine*, 7(8), p. e1000324. doi:10.1371/journal.pmed.1000324, url: https://doi.org/10.1371/journal.pmed.1000324.

Grimm, V., et al. (2005). Pattern-oriented modeling of agent-based complex systems: lessons from ecology. *science*, 310(5750), pp. 987–991.

Gu, W. and Novak, R.J. (2009). Predicting the impact of insecticide-treated bed nets on malaria transmission: the devil is in the detail. *Malaria Journal*, 8(1), p. 256. ISSN 1475-2875, url: https://doi.org/10.1186/1475-2875-8-256.

Gueron, S., A. Levin, S., and Rubenstein, D. (1996). *The Dynamics of Herds: From Individuals to Aggregations*, vol. 182. 85–98 p.

Gurarie, D. and McKenzie, F.E. (2006). Dynamics of immune response and drug resistance in malaria infection. *Malaria Journal*, 5(PMC1629019), pp. 86–86. ISSN 1475-2875, url: http://www.ncbi.nlm.nih.gov/pmc/articles/PMC1629019/.

Gurarie, D. and McKenzie, F.E. (2007). A stochastic model of immune-modulated malaria infection and disease in children. *Mathematical biosciences*, 210(2), pp. 576–597. ISSN 0025-5564, url: http://www.ncbi.nlm.nih.gov/pmc/articles/PMC2173879/.

Haario, H., Laine, M., Mira, A., and Saksman, E. (2006). DRAM: Efficient adaptive MCMC. *Statistics and Computing*, 16(4), pp. 339–354. ISSN 1573-1375, url: https://doi.org/10.1007/s11222-006-9438-0.

Haario, H., Saksman, E., and Tamminen, J. (2001). An adaptive Metropolis algorithm. *Bernoulli*, 7(2), pp. 223–242. url: https://projecteuclid.org:443/euclid.bj/1080222083.

Harris, K.J. and Blackwell, P.G. (2013). Flexible continuous-time modelling for heterogeneous animal movement. *Ecological Modelling*, 255, pp. 29–37. ISSN 0304-3800, url: http://www.sciencedirect.com/science/article/pii/S0304380013000471.

Hawkes, F.M., et al. (2017). Exploiting Anopheles responses to thermal, odour and visual stimuli to improve surveillance and control of malaria. *Scientific Reports*, 7(1), p. 17283. ISSN 2045-2322, url: https://doi.org/10.1038/s41598-017-17632-3.

Hemelrijk, C.K. (1999). An individual-orientated model of the emergence of despotic and egalitarian societies. *Proceedings of the Royal Society B: Biological Sciences*, 266(1417), pp. 361–361. ISSN 1471-2954, url: http://www.ncbi.nlm.nih.gov/pmc/articles/PMC1689690/.

Hölker, F. and Breckling, B. (2005). A spatiotemporal individual-based fish model to investigate emergent properties at the organismal and the population level. *Ecological Modelling*, 186, pp. 406–426.

Hooten, M.B., Johnson, D.S., Hanks, E.M., and Lowry, J.H. (2010). Agent-Based Inference for Animal Movement and Selection. *Journal of Agricultural, Biological and Environmental Statistics*, 15(4), pp. 523–538. ISSN 1537-2693, url: http://dx.doi.org/10.1007/s13253-010-0038-2.

Huldén, L. (2010). Household size explains successful malaria eradication. *Malaria Journal*, 9.

Huldén, L., McKitrick, R., and Huldén, L. (2013). Average household size and eradication of malaria. *Journal of the Royal Statistical Society Series A*, DOI: 10.1111/rssa.12036.

Huse, G., Strand, E., and Giske, J. (1999). Implementing behaviour in individual-based models using neural networks and genetic algorithms. *Evolutionary Ecology*, 13(5), pp. 469–483. ISSN 1573-8477, doi:10.1023/A:1006746727151, url: http://dx.doi.org/10.1023/A:1006746727151.

Kalman, R.E. (1960). A New Approach to Linear Filtering and Prediction Problems. *Journal of Basic Engineering*, 82(1), pp. 35–45. ISSN 0098-2202, doi:10.1115/1.3662552, url: http://dx.doi.org/10.1115/1.3662552.

Kareiva, P. and Shigesada, N. (1983). Analyzing insect movement as a correlated random walk. *Oecol*, 56, pp. 234–238.

Kawada, H., et al. (2014). Preventive effect of permethrin-impregnated long-lasting insecticidal nets on the blood feeding of three major pyrethroid-resistant malaria vectors in western Kenya. *Parasit Vectors*, 7, p. 383.

Killeen, G. and Chitnis, N. (2014). *Potential causes and consequences of behavioural resilience and resistance in malaria vector populations: A mathematical modelling analysis*, vol. 13. 97 p.

Killeen, G., Chitnis, N., Moore, S., and Okumu, F. (2011). Target product profile choices for intradomiciliary malaria vector control pesticide products: repel or kill? *Malar J*, 10, p. 207.

Kirkpatrick, S., Gelatt, C., and Vecchi, M. (1983). Optimization by Simulated Annealing. *Science*, 220(4598), pp. 671–680.

Kitau, J., et al. (2012). Species Shifts in the Anopheles gambiae Complex: Do LLINs Successfully Control Anopheles arabiensis? *PLOS ONE*, 7(3), pp. 1–7. doi: 10.1371/journal.pone.0031481, url: https://doi.org/10.1371/journal.pone.0031481.

Koella, J. and Rieu, L. (2002). Stage-specific manipulation of a mosquito's host-seeking behavior by the malaria parasite Plasmodium gallinaceum. *Behavioral Ecology*, 13: doi:10.1093/beheco/13.6.816.

Kristensen, T., et al. (2018). *Spatial genetic structure in American black bears (Ursus americanus): female philopatry is variable and related to population history*, vol. 120. 329–341 p.

Kukacka, J. and Barunik, J. (2017). Estimation of financial agent-based models with simulated maximum likelihood. *Journal of Economic Dynamics and Control*, 85, pp. 21–45. ISSN 0165-1889, url: http://www.sciencedirect.com/science/article/pii/S0165188917302014.

Lacroix, R., Mukabana, W., Gouagna, L., and Koella, J. (2005). Malaria Infection Increases Attractiveness of Humans to Mosquitoes. *PLoS Biology*, 3(9): e298.

Lamperti, F., Roventini, A., and Sani, A. (2018). Agent-based model calibration using machine learning surrogates. *Journal of Economic Dynamics and Control*, 90, pp. 366–389. ISSN 0165-1889, url: http://www.sciencedirect.com/science/article/pii/S0165188918301088.

Lehane, M. (2005). *The Biology of Blood-Sucking in Insects, Second Edition.*, 2nd edn. NY: Cambridge University Press.

Linard, C., Poncon, N., Fontenille, D., and Lambin, E. (2009). A multi-agent simulation to assess the risk of malaria re-emergence in southern France. *Ecological Modelling*, 220(2), pp. 160–174. ISSN 03043800, doi:10.1016/j.ecolmodel.2008.09.001, url: http://dx.doi.org/10.1016/j.ecolmodel.2008.09.001.

Lorenz, L.M., et al. (2013). Taxis assays measure directional movement of mosquitoes to olfactory cues. *Parasites & Vectors*, 6(PMC3652730), pp. 131–131. ISSN 1756-3305, url: http://www.ncbi.nlm.nih.gov/pmc/articles/PMC3652730/.

Macal, C.M. (2010). To agent-based simulation from System Dynamics. In: *Proceedings of the 2010 Winter Simulation Conference*, pp. 371–382. ISSN 1558-4305.

Macal, C.M. (2016). Everything you need to know about agent-based modelling and simulation. *Journal of Simulation*, 10(2), pp. 144–156. ISSN 1747-7778, doi:10.1057/jos.2016.7, url: https://doi.org/10.1057/jos.2016.7.

MacDonald, G. (2003). *Biogeography: Space, Time, and Life*. John Wiley & Sons Australia, Limited. ISBN 9780471452607.

Maire, N., et al. (2006). A model for natural immunity to asexual blood stages of Plasmodium falciparum malaria in endemic areas. *The American journal of tropical medicine and hygiene*, 75, pp. 19–31.

Mann, R.P. (2011). Bayesian Inference for Identifying Interaction Rules in Moving Animal Groups. *PLOS ONE*, 6(8), p. e22827. doi:10.1371/journal.pone.0022827, url: https://doi.org/10.1371/journal.pone.0022827.

Marino, S., Hogue, I.B., Ray, C.J., and Kirschner, D.E. (2008). A Methodology For Performing Global Uncertainty And Sensitivity Analysis In Systems Biology. *Journal of theoretical biology*, 254(PMC2570191), pp. 178–196. ISSN 1095-8541, url: http://www.ncbi.nlm.nih.gov/pmc/articles/PMC2570191/.

Marvuglia, A., et al. (2016). *A return on experience from the application of agent-based simulations coupled with life cycle assessment to model agricultural processes*, vol. 142.

Maude, R.J., et al. (2009). The last man standing is the most resistant: eliminating artemisinin-resistant malaria in Cambodia. *Malaria journal*, 8, p. 31.

McKay, M.D., Beckman, R.J., and Conover, W.J. (1979). A Comparison of Three Methods for Selecting Values of Input Variables in the Analysis of Output from a Computer Code. *Technometrics*, 21(2), pp. 239–245. ISSN 00401706, url: http://www.jstor.org/stable/1268522.

McKenzie, F.E. and Samba, E.M. (2004). The role of mathematical modeling in evidence-based malaria control. *The American journal of tropical medicine and hygiene*, 71, pp. 94–6.

McKenzie, F.E., Wong, R.C., and Bossert, W.H. (1999). Discrete-Event Models of Mixed-Phenotype Plasmodium falciparum Malaria. *Simulation*, 73, pp. 213–217.

Metropolis, N., et al. (1953). Equations of State Calculations by Fast Computing Machines. *J Chem Phys*, 21(6), pp. 1087–1092.

Milewski, P.A. and Yang, X. (2008). A simple model for biological aggregation with asymmetric sensing. *Commun. Math. Sci.*, 6(2), pp. 397–416. url: http://projecteuclid.org/euclid.cms/1214949929.

Mogilner, A. and Edelstein-Keshet, L. (1999). A non-local model for a swarm. *Journal of Mathematical Biology*, 38(6), pp. 534–570. ISSN 1432-1416, url: http://dx.doi.org/10.1007/s002850050158.

Montague, P.R. (2018). Reinforcement Learning: An Introduction, by Sutton, R.S. and Barto, A.G. *Trends in Cognitive Sciences*, 3(9), p. 360. ISSN 1364-6613, doi:10.1016/s1364-6613(99)01331-5, url: https://doi.org/10.1016/S1364-6613(99)01331-5.

Moore, J. (2002). *Parasites and the Behavior of Animals*. Oxford University Press, USA.

Morale, D., Capasso, V., and Oelschläger, K. (2005). An interacting particle system modelling aggregation behavior: from individuals to populations. *Journal of Mathematical Biology*, 50(1), pp. 49–66. ISSN 1432-1416, url: http://dx.doi.org/10.1007/s00285-004-0279-1.

Morales, J., Fortin, D., Frair, J., and Merrill, E. (2005). Adaptive models for large herbivore movements in heterogeneous landscapes. *Landscape Ecology*, 20, pp. 301–316.

Muiños-Landin, S., Ghazi-Zahedi, K., and Cichos, F. (2018). Reinforcement Learning of Artificial Microswimmers.

Murray, J.D. (2002). *Mathematical Biology I. An Introduction*, 3rd edn, vol. 17, Interdisciplinary Applied Mathematics. New York: Springer.

Nagai, T. and Mimura, M. (1983). Some nonlinear degenerate diffusion equations related to population dynamics. *J. Math. Soc. Japan*, 35(3), pp. 539–562. doi:10.2969/jmsj/03530539, url: http://dx.doi.org/10.2969/jmsj/03530539.

Nardini, L., et al. (2012). Detoxification enzymes associated with insecticide resistance in laboratory strains of Anopheles arabiensis of different geographic origin. *Parasites & Vectors*, 5(PMC3430573), pp. 113–113. ISSN 1756-3305, url: http://www.ncbi.nlm.nih.gov/pmc/articles/PMC3430573/.

Nathan, R. (2008). An emerging movement ecology paradigm. *Proceedings of the National Academy of Sciences*, 105(49), pp. 19050–19051. doi:10.1073/pnas.0808918105, url: http://www.pnas.org/content/105/49/19050.short.

Nguyen, T.D., et al. (2015). Optimum population-level use of artemisinin combination therapies: a modelling study. *The Lancet. Global health*, 3, pp. e758–66.

Okumu, F.O., et al. (2013). Comparative field evaluation of combinations of long-lasting insecticide treated nets and indoor residual spraying, relative to either method alone, for malaria prevention in an area where the main vector is Anopheles arabiensis. *Parasit Vectors*, 6: 10.1186/1756-3305-6-46.

Okumu, F. (2012). *Combining insecticide treated bed nets and indoor residual spraying for malaria vector control in Africa*. Ph.D. thesis. London School of Hygiene & Tropical Medicine.

Olsson, A., Sandberg, G., and Dahlblom, O. (2003). On Latin hypercube sampling for structural reliability analysis. *Structural Safety*, 25(1), pp. 47–68. ISSN 0167-4730, doi:10.1016/S0167-4730(02)00039-5.

Patterson, T.A., et al. (2008). State-space models of individual animal movement. *Trends in Ecology & Evolution*, 23(2), pp. 87 – 94. ISSN 0169-5347, doi:http://dx.doi.org/10.1016/j.tree.2007.10.009, url: http://www.sciencedirect.com/science/article/pii/S0169534707003588.

Pizzitutti, F., et al. (2015). A validated agent-based model to study the spatial and temporal heterogeneities of malaria incidence in the rainforest environment. *Malaria Journal*, 14, p. 514. ISSN 1475-2875, url: http://www.ncbi.nlm.nih.gov/pmc/articles/PMC4688926/.

Pizzitutti, F., et al. (2018). Out of the net: An agent-based model to study human movements influence on local-scale malaria transmission. *PLOS ONE*, 13(3), p. e0193493. doi:10.1371/journal.pone.0193493, url: https://doi.org/10.1371/journal.pone.0193493.

Quammen, D. (1996). *Song of the dodo: island biogeography in an age of extinction.* New York: Simon and Schuster.

Railsback, S.F., Lytinen, S.L., and Jackson, S.K. (2006). Agent-based Simulation Platforms: Review and Development Recommendations. *SIMULATION*, 82(9), pp. 609–623. doi:10.1177/0037549706073695, url: http://dx.doi.org/10.1177/0037549706073695.

Rasmussen, C.E. (2006). Gaussian processes for machine learning. MIT Press.

Reddy, M., et al. (2011). Outdoor host seeking behaviour of *Anopheles gambiae* mosquitoes following initiation of malaria vector control on Bioko Island, Equatorial Guinea. *Malaria Journal*, 10(184).

Reuter, H. and Breckling, B. (1999). Emerging properties on the individual level: modelling the reproduction phase of the European robin *Erithacus rubecula*: Ecological Modelling. *Ecological Modelling*, 121, pp. 199–219.

Risken, H. and Haken, H. (1989). *The Fokker-Planck Equation: Methods of Solution and Applications Second Edition*. Springer.

Roshanbin, A., Collette, C., and Preumont, A. (2009). *Mathematical Modelling of Insect–Like Flapping Wings for Application to MAVs*. 11–13 p.

Ross, A., Killeen, G., and Smith, T. (2006). Relationships between host infectivity to mosquitoes and asexual parasite density in Plasmodium falciparum. *The American journal of tropical medicine and hygiene*, 75, pp. 32–7.

Ross, R. (1903). *Report and the Prevention of Malaria in Mauritius*. Waterlow and Sons Limited, London Wall.

Rossignol, P.A., Ribeiro, J.M.C., and Spielman, A. (1984). Increased Intradermal Probing Time in Sporozoite-Infected Mosquitoes. *The American Journal of Tropical Medicine and Hygiene*, 33(1), pp. 17–20. doi:https://doi.org/10.4269/ajtmh.1984.33.17, url: http://www.ajtmh.org/content/journals/10.4269/ajtmh.1984.33.17.

Russell, S.J. and Norvig, P. (1995). *Artificial Intelligence: A Modern Approach*. Upper Saddle River, NJ, USA: Prentice-Hall, Inc. ISBN 0-13-103805-2.

Schick, R.S., et al. (2008). Understanding movement data and movement processes: current and emerging directions. *Ecology letters*, 11, pp. 1338–50.

Schwartz, A. and JC., K. (2001). Trade-offs, conflicts of interest and manipulation in Plasmodium-mosquito interactions. *Trends in Parasitology*, 6(17), p. 285.

Sean, C., Smith, J., Joshi, A., and Ding, J. (2001). TIGMOD: an individual-based spatially explicit model for simulating tiger/human interaction in multiple use forests. *Ecological Modelling*, 140(1), pp. 81 – 97. ISSN 0304-3800, doi:http://dx.doi.org/10.1016/S0304-3800(01)00258-7, url: http://www.sciencedirect.com/science/article/pii/S0304380001002587.

Sellers, W.I., Hill, R.A., and Logan, B.S. (2007). An agent-based model of group decision making in baboons. *Philosophical Transactions of the Royal Society B: Biological Sciences*, 362(1485), pp. 1699–1710. ISSN 1471-2970, url: http://www.ncbi.nlm.nih.gov/pmc/articles/PMC2440783/.

Semakula, H.M., Song, G., Zhang, S., and Achuu, S.P. (2015). Potential of household environmental resources and practices in eliminating residual malaria transmission: a case study of Tanzania, Burundi, Malawi and Liberia. *African health sciences*, 15, pp. 819–27.

Senda, K., et al. (2012). Aerodynamic forces and vortical structures in flapping butterfly's forward flight. *Phys Fluids*, 7(2): 021902 DOI: 10.1063/1.4790882.

Shaman, J. (2007). Amplification due to spatial clustering in an individual-based model of mosquito-avian arbovirus transmission. *Transactions of The Royal Society of Tropical Medicine and Hygiene*, 101(5), pp. 469–483. ISSN 0035-9203, doi:10.1016/j.trstmh.2006.11.007, url: http://dx.doi.org/10.1016/j.trstmh.2006.11.007.

Shcherbacheva, A. and Haario, H. (2017). The Impact of Household Size on Malaria Reduction in Relation with Alterations in Mosquito Behavior by Malaria Parasite. *Multiple-Valued Logic and Soft Computing*, 29, pp. 455–468.

Shcherbacheva, A., Haario, H., and Killeen, G.F. (2018). Modeling host-seeking behavior of African malaria vector mosquitoes in the presence of long-lasting insecticidal nets. *Mathematical biosciences*, 295, pp. 36–47.

Shcherbacheva, A. and Kauranne, T. (2013). Population dynamics with limited perception establish global swarm topology. In: *ECAL*.

Shettleworth, S.J. (2001). Animal cognition and animal behaviour. 61(2), pp. 277–286. ISSN 0003-3472, url: http://www.sciencedirect.com/science/article/pii/S0003347200916063.

Shimizu, N., Ogino, C., Kawanishi, T., and Hayashi, Y. (2002). Fractal analysis of Daphnia motion for acute toxicity bioassay. *Environ Toxicol*, 17(2), p. 441â€“448.

Smallegange, R.C., Verhulst, N.O., and Takken, W. (2011). Sweaty skin: an invitation to bite? *Trends in parasitology*, 27, pp. 143–8.

Smith, D., McKenzie, F., Snow, R., and Hay, S. (2007). Revisiting the Basic Reproductive Number for Malaria and Its Implications for Malaria Control. *PloS Biology*, 5(3).

Smith, N.R., et al. (2018). Agent-based models of malaria transmission: a systematic review. *Malaria Journal*, 17(1), p. 299. ISSN 1475-2875, url: https://doi.org/10.1186/s12936-018-2442-y.

Smith, T., et al. (2006). Mathematical modeling of the impact of malaria vaccines on the clinical epidemiology and natural history of Plasmodium falciparum malaria: Overview. *The American journal of tropical medicine and hygiene*, 75, pp. 1–10.

Snow, W. (1980). Field estimates of the flight speed of some West African mosquitoes. *Ann Trop Med Parasitol*, 74(2), pp. 239–242.

Spitzen, J., et al. (2013). A 3D Analysis of Flight Behavior of *Anopheles gambiae* sensu stricto Malaria Mosquito in Response to Human Odor and Heat. *PLoS One*, 8(5), p. e62995.

Strader, T., Lin, F., and Shaw, M. (1998). Simulation of Order Fulfillment in Divergent Assembly Supply Chains. *Journal of Artificial Societies and Social Simulation*, 1.

Strombom, D. (2011). Collective motion from local attraction. *Journal of theoretical biology*, 283, pp. 145–51.

Stucki, S., et al. (2017). *High performance computation of landscape genomic models including local indicators of spatial association*, vol. 17. 1072–1089 p.

Syed, Z. and Leal, W. (2009). Acute olfactory response of *Culex* mosquitoes to a human-and bird-derived attractant. *Proc Natl Acad Sci U S A*, 106(44): 10.1073/pnas.0906932106.

Tang, W. and Bennett, D. (2010). Agent-based Modeling of Animal Movement: A Review. *Geography Compass*, 4, pp. 682–700.

Tang, W. (2008). Simulating Complex Adaptive Geographic Systems: A Geographically Aware Intelligent Agent Approach. *Cartography and Geographic Information Science*, 35(4), pp. 239–263. ISSN 1523-0406, doi:10.1559/152304008786140551, url: `http://dx.doi.org/10.1559/152304008786140551`.

T.C., S. (1971). Dynamic models of segregation. *Journal of Mathematical Sociology*, 1, pp. 143+186.

Thatte, P., et al. (2017). *Maintaining tiger connectivity and minimizing extinction into the next century: Insights from landscape genetics and spatially-explicit simulations*, vol. 218. 181–191 p.

Thiele, J.C., Kurth, W., and Grimm, V. (2014). Facilitating Parameter Estimation and Sensitivity Analysis of Agent-Based Models: A Cookbook Using NetLogo and 'R'. *Journal of Artificial Societies and Social Simulation*, 17(3), p. 11. ISSN 1460-7425, doi:10.18564/jasss.2503, url: `http://jasss.soc.surrey.ac.uk/17/3/11.html`.

Turchin, P.B. (2003). *Complex population dynamics: A theoretical/empirical synthesis*, vol. 35.

Turner, M. (1989). Landscape ecology: the effect of pattern on process. *Annual Review of Ecology and Systematics*, 20, pp. 171–197.

Turner, M.G., et al. (1994). Simulating Winter Interactions Among Ungulates, Vegetation, and Fire in Northern Yellowstone Park. *Ecological Applications*, 4(3), pp. 472–496. ISSN 10510761, url: `http://www.jstor.org/stable/1941951`.

Vantaux, A., et al. (2015). Host-seeking behaviors of mosquitoes experimentally infected with sympatric field isolates of the human malaria parasite Plasmodium falciparum: no evidence for host manipulation. *Frontiers in Ecology and Evolution*, 3(86): doi: 10.3389/fevo.2015.00086.

Vaughan, J.A., Noden, B.H., and Beier, J.C. (1991). Concentrations of human erythrocytes by anopheline mosquitoes (Diptera: Culicidae) during feeding. *Journal of medical entomology*, 28, pp. 780–6.

Verhulst, N.O., et al. (2013). Relation between HLA genes, human skin volatiles and attractiveness of humans to malaria mosquitoes. *Infection, Genetics and Evolution*, 18, pp. 87–93. ISSN 1567-1348, url: `http://www.sciencedirect.com/science/article/pii/S1567134813001986`.

Vickers, N.J. (2000). Mechanisms of animal navigation in odor plumes. *The Biological bulletin*, 198, pp. 203–12.

WHO (2006). *Guidelines for testing mosquito adulticides for indoor residual spraying and treatment of mosquito nets*. Technical report. Geneva: WHO.

(WHO), W.H.O. (2015). *World Malaria Report 2015*. Technical report. Geneva, Switzerland: World Health Organization (WHO).

Wolff, W.F. (1994). An individual-oriented model of a wading bird nesting colony. *Ecological Modelling*, 72, pp. 75–114.

Wu, T.Y. (2011). Fish Swimming and Bird/Insect Flight. *Annu. Rev. Fluid Mech.*, 43(1), pp. 25–58. ISSN 0066-4189, doi:10.1146/annurev-fluid-122109-160648, url: `https://doi.org/10.1146/annurev-fluid-122109-160648`.

Yahouódo, G.A., et al. (2017). Contributions of cuticle permeability and enzyme detoxification to pyrethroid resistance in the major malaria vector Anopheles gambiae. *Scientific Reports*, 7(1), p. 11091. ISSN 2045-2322, url: `https://doi.org/10.1038/s41598-017-11357-z`.

Yamana, T.K., et al. (2013). Linking environmental variability to village-scale malaria transmission using a simple immunity model. *Parasites & vectors*, 6, p. 226.

Zbikowski, R., Ansari, S.A., and Knowles, K. (2006). On mathematical modelling of insect flight dynamics in the context of micro air vehicles. *Bioinspiration & biomimetics*, 1, pp. R26–37.

Zhu, L., et al. (2015a). Modelling optimum use of attractive toxic sugar bait stations for effective malaria vector control in Africa. *Malaria Journal*, 14, p. 492. ISSN 1475-2875, url: `http://www.ncbi.nlm.nih.gov/pmc/articles/PMC4672472/`.

Zhu, L., et al. (2015b). A spatial individual-based model predicting a great impact of copious sugar sources and resting sites on survival of Anopheles gambiae and malaria parasite transmission. *Malaria Journal*, 14(1), p. 59. ISSN 1475-2875, url: https://doi.org/10.1186/s12936-015-0555-0.

Zitzler, E., Deb, K., and Thiele, L. (2000). Comparison of Multiobjective Evolutionary Algorithms: Empirical Results. *Evol. Comput.*, 8(2), pp. 173–195. ISSN 1063-6560, doi:10.1162/106365600568202, url: http://dx.doi.org/10.1162/106365600568202.

ACTA UNIVERSITATIS LAPPEENRANTAENSIS

806. PROSKURINA, SVETLANA. International trade in biomass for energy production: The local and global context. 2018. Diss.

807. DABIRI, MOHAMMAD. The low-cycle fatigue of S960 MC direct-quenched high-strength steel. 2018. Diss.

808. KOSKELA, VIRPI. Tapping experiences of presence to connect people and organizational creativity. 2018. Diss.

809. HERALA, ANTTI. Benefits from Open Data: barriers to supply and demand of Open Data in private organizations. 2018. Diss.

810. KÄYHKÖ, JORMA. Erityisen tuen toimintaprosessien nykytila ja kehittäminen suomalaisessa oppisopimuskoulutuksessa. 2018. Diss.

811. HAJIKHANI, ARASH. Understanding and leveraging the social network services in innovation ecosystems. 2018. Diss.

812. SKRIKO, TUOMAS. Dependence of manufacturing parameters on the performance quality of welded joints made of direct quenched ultra-high-strength steel. 2018. Diss.

813. KARTTUNEN, ELINA. Management of technological resource dependencies in interorganizational networks. 2018. Diss.

814. CHILD, MICHAEL. Transition towards long-term sustainability of the Finnish energy system. 2018. Diss.

815. NUTAKOR, CHARLES. An experimental and theoretical investigation of power losses in planetary gearboxes. 2018. Diss.

816. KONSTI-LAAKSO, SUVI. Co-creation, brokering and innovation networks: A model for innovating with users. 2018. Diss.

817. HURSKAINEN, VESA-VILLE. Dynamic analysis of flexible multibody systems using finite elements based on the absolute nodal coordinate formulation. 2018. Diss.

818. VASILYEV, FEDOR. Model-based design and optimisation of hydrometallurgical liquid-liquid extraction processes. 2018. Diss.

819. DEMESA, ABAYNEH. Towards sustainable production of value-added chemicals and materials from lignocellulosic biomass: carboxylic acids and cellulose nanocrystals. 2018. Diss.

820. SIKANEN, EERIK. Dynamic analysis of rotating systems including contact and thermal-induced effects. 2018. Diss.

821. LIND, LOTTA. Identifying working capital models in value chains: Towards a generic framework. 2018. Diss.

822. IMMONEN, KIRSI. Ligno-cellulose fibre poly(lactic acid) interfaces in biocomposites. 2018. Diss.

823. YLÄ-KUJALA, ANTTI. Inter-organizational mediums: current state and underlying potential. 2018. Diss.

824. ZAFARI, SAHAR. Segmentation of partially overlapping convex objects in silhouette images. 2018. Diss.

825. MALKKI, HELENA. Identifying needs and ways to integrate sustainability into energy degree programmes. 2018. Diss.

826. JUNTUNEN, RAIMO. LCL filter designs for paraller-connected grid inverters. 2018. Diss.

827. RANAEI, SAMIRA. Quantitative approaches for detecting emerging technologies. 2018. Diss.

828. METSO, LASSE. Information-based industrial maintenance - an ecosystem perspective. 2018. Diss.

829. SAREN, ANDREY. Twin boundary dynamics in magnetic shape memory alloy Ni-Mn-Ga five-layered modulated martensite. 2018. Diss.

830. BELONOGOVA, NADEZDA. Active residential customer in a flexible energy system - a methodology to determine the customer behaviour in a multi-objective environment. 2018. Diss.

831. KALLIOLA, SIMO. Modified chitosan nanoparticles at liquid-liquid interface for applications in oil-spill treatment. 2018. Diss.

832. GEYDT, PAVEL. Atomic Force Microscopy of electrical, mechanical and piezo properties of nanowires. 2018. Diss.

833. KARELL, VILLE. Essays on stock market anomalies. 2018. Diss.

834. KURONEN, TONI. Moving object analysis and trajectory processing with applications in human-computer interaction and chemical processes. 2018. Diss.

835. UNT, ANNA. Fiber laser and hybrid welding of T-joint in structural steels. 2018. Diss.

836. KHAKUREL, JAYDEN. Enhancing the adoption of quantified self-tracking wearable devices. 2018. Diss.

837. SOININEN, HANNE. Improving the environmental safety of ash from bioenergy production plants. 2018. Diss.

838. GOLMAEI, SEYEDMOHAMMAD. Novel treatment methods for green liquor dregs and enhancing circular economy in kraft pulp mills. 2018. Diss.

839. GERAMI TEHRANI, MOHAMMAD. Mechanical design guidelines of an electric vehicle powertrain. 2019. Diss.

840. MUSIIENKO, DENYS. Ni-Mn-Ga magnetic shape memory alloy for precise high-speed actuation in micro-magneto-mechanical systems. 2019. Diss.

841. BELIAEVA, TATIANA. Complementarity and contextualization of firm-level strategic orientations. 2019. Diss.

842. EFIMOV-SOINI, NIKOLAI. Ideation stage in computer-aided design. 2019. Diss.

843. BUZUKU, SHQIPE. Enhancement of decision-making in complex organizations: A systems engineering approach. 2019. Diss.

ISBN 978-952-335-344-2
ISBN 978-952-335-345-9 (PDF)
ISSN-L 1456-4491
ISSN 1456-4491
Lappeenranta 2019